

CHAPTER 3

Global Ozone: Past and Present

Lead Authors:

M.P. Chipperfield
V.E. Fioletov

Coauthors:

B. Bregman
J. Burrows
B.J. Connor
J.D. Haigh
N.R.P. Harris
A. Hauchecorne
L.L. Hood
S.R. Kawa
J.W. Krzyścin
J.A. Logan
N.J. Muthama
L. Polvani
W.J. Randel
T. Sasaki
J. Stähelin
R.S. Stolarski
L.W. Thomason
J.M. Zawodny

Contributors:

G. Bodeker
P. Demoulin
W. Feng
L. Flynn
S. Frith
S. Guillas
M. Ilyas
B. Knudsen
B. Liley
R. McPeters
A.J. Miller
R. Müller
S. Oltmans
Y. Orsolini
I. Petropavlovskikh
W. Steinbrecht
H. Struthers
D. Tarasick
Y. Terao

Final Release: February 2007

From *Scientific Assessment of Ozone Depletion: 2006*

CHAPTER 3

GLOBAL OZONE: PAST AND PRESENT

Contents

SCIENTIFIC SUMMARY	3.1
3.1 INTRODUCTION	3.5
3.2 UPDATE OF OZONE CHANGES	3.5
3.2.1 Statistical Methods	3.5
3.2.2 Changes in Total Ozone	3.7
3.2.3 Changes in the Vertical Distribution of Ozone	3.8
3.2.3.1 Upper Stratosphere	3.10
3.2.3.2 Lower Stratosphere	3.13
3.2.3.3 Consistency of Column and Profile Trends	3.17
3.2.4 Tropospheric Ozone	3.18
3.3 SUMMARY OF OTHER OBSERVATIONS	3.19
3.3.1 Stratospheric Aerosol and Its Precursors	3.19
3.3.2 Nitrogen Dioxide (NO ₂)	3.20
3.4 UNDERSTANDING AND INTERPRETATION OF OZONE CHANGES	3.21
3.4.1 Models	3.21
3.4.2 Dynamical Processes	3.22
3.4.3 Chemical Processes	3.25
3.4.3.1 Update of Relevant Kinetics	3.25
3.4.3.2 Lower Stratosphere	3.26
3.4.3.3 Upper Stratosphere	3.30
3.4.4 Solar Cycle Variations	3.30
3.4.5 Assessment Model Simulations	3.32
REFERENCES	3.41
APPENDIX 3A: DESCRIPTION OF THE OZONE DATASETS	3.55
3A.1 Column Ozone Data	3.55
3A.2 Ozone Profile Measurements	3.57

SCIENTIFIC SUMMARY

Total Column Ozone

- **Global mean total column ozone values for 2002-2005 were approximately 3.5% below 1964-1980 average values.** The 2002-2005 values are similar to the 1998-2001 values and this indicates that ozone is no longer decreasing. These changes are evident in all available global datasets, although differences of up to 1% between annual averages exist between some individual sets.
- **Averaged for the period 2002-2005, total column ozone for the Northern Hemisphere (NH) and Southern Hemisphere (SH) midlatitudes (35°-60°) are about 3% and 5.5%, respectively, below their 1964-1980 average values and are similar to their 1998-2001 values.** However, as noted in previous Assessments, the behavior of column ozone in the two hemispheres during the 1990s was different. The NH shows a minimum around 1993, followed by an increase. The SH shows an ongoing decrease through the late 1990s, followed by the recent leveling off.
- **There are seasonal differences in ozone changes over midlatitudes between the NH and the SH.** Changes since the pre-1980 period over northern midlatitudes (35°N-60°N) are larger in spring, while those over southern midlatitudes (35°S-60°S) are nearly the same throughout the year.
- **Total column ozone over the tropics (25°S-25°N) remains essentially unchanged.** Total ozone trends in this region for the period 1980-2004 are not statistically significant. These findings are consistent with the findings of the previous Assessments.

Vertical Ozone Distribution

- **Upper stratospheric ozone declined during 1979-1995, but has been relatively constant during the last decade.** Measurements from the Stratospheric Aerosol and Gas Experiment (SAGE I+II) and Solar Backscatter Ultraviolet (SBUV(2)) satellite instruments show significant declines through 1995 when averaged over 60°N-60°S and altitudes of 35 to 50 kilometers (km). The net ozone decrease was ~10-15% over midlatitudes; smaller but significant changes occurred over the tropics. Available independent Umkehr, lidar, and microwave ozone measurements confirm these findings.
- **Lower stratospheric ozone declined over the period 1979-1995, but has been relatively constant with significant variability over the last decade.** At midlatitudes of both the Northern and Southern Hemispheres, measurements by SAGE I+II and SBUV(2) showed declines of up to 10% by 1995 between 20 and 25 km altitude. These decreases did not continue in the last decade.
- **In the lowermost stratosphere, between 12 and 15 km in the Northern Hemisphere, a strong decrease in ozone was observed from ozonesonde data between 1979 and 1995, followed by an overall increase from 1996 to 2004, leading to no net long-term decrease at this level.** These changes in the lowermost stratosphere have a substantial influence on the column. The Southern Hemisphere midlatitude data do not show a similar increase since 1995 at these altitudes.
- **Significant ozone decreases of ~3% between the tropopause and 25 km are found in the SAGE satellite measurements between 1979 and 2004 at 25°S-25°N.** Since no change is found in total ozone over the tropics, this could be explained by significant increases in tropospheric ozone in the tropics. While regional increases in tropical tropospheric ozone have been seen, not all tropical regions or datasets show an increase.

GLOBAL OZONE

Understanding Past Changes in Ozone

- **There has been no change in our basic understanding that, analyzed over all latitudes and seasons, halogen increases have been the principal driver of ozone depletion over the past few decades.** There is good overall agreement between observed long-term changes in extrapolar ozone and model simulations that include the effects of increasing halogens. The models generally reproduce the observed ozone changes as a function of altitude, latitude, and season, confirming our understanding that halogen changes are the main driver of global ozone changes. This link is supported by the statistical fit of globally averaged ozone observations with Equivalent Effective Stratospheric Chlorine (EESC).
- **Empirical and model studies have shown that changes in tropospheric and stratospheric dynamics have been partially responsible for the observed NH midlatitude winter ozone decline from 1979 to the mid-1990s and ozone increase thereafter.** Whether this is due to dynamical variability or results from a long-term trend in stratospheric circulation is not yet clear. Estimates of these dynamical effects on long-term trends range from ~20% up to 50% for the winter period.
- **The impact of aerosols (dynamical and chemical) on midlatitude ozone was greatest in the early 1990s after the eruption of Mt. Pinatubo in 1991.** The observed decrease in NH column ozone in 1993 agrees with chemical-dynamical models that include these effects. An outstanding issue is the absence of an effect of the Mt. Pinatubo eruption on the observed SH ozone column, which contrasts with model predictions.
- **Several independent modeling studies covering periods in the 1990s confirm that dilution of ozone-depleted polar air makes a substantial contribution to midlatitude ozone depletion, especially in the Southern Hemisphere (due to the much larger polar ozone loss there).** Long-term annually averaged model-based estimates indicate that dilution by polar air contributes about one-third of the midlatitude ozone depletion in the Northern Hemisphere, with large interannual variation; in the Southern Hemisphere midlatitudes, the contribution is estimated to be about one-half.
- **The inclusion of additional inorganic bromine (Br_y) from very short-lived substances (VSLS) in models leads to larger ozone destruction at midlatitudes, compared with studies including only long-lived bromine source gases.** The enhanced ozone loss occurs in the lower stratosphere via interactions of this bromine with anthropogenic chlorine. Midlatitude ozone loss is most enhanced during periods of high aerosol loading. Ozone loss through cycles involving bromine and odd-hydrogen (HO_x) is also enhanced at midlatitudes under all conditions. The impact on long-term midlatitude ozone trends (1980-2004), assuming constant VSLS Br_y , is calculated to be small because aerosol loading was low at the start and end of this time period.
- **The profile shape of upper stratospheric ozone trends from 1980-2004 is generally consistent with our understanding of gas-phase chlorine chemistry as the cause, modulated by changes in temperature and other gases such as methane (CH_4).** However, global dynamical-chemical models have not demonstrated that they can simultaneously reproduce realistic trends in all relevant parameters, although observations over the full time period are limited. Non-interactive models obtain ozone change that peak at about 14% for 1980-2004 (in altitude coordinates), consistent with SAGE observations. Interactive models, which calculate their own temperatures, obtain ozone trends that are nearly half in magnitude.
- **Both two-dimensional (2-D) and three-dimensional (3-D) models perform better in reproducing observed past changes in the NH than in the SH.** Consistent with results presented in the previous Assessment, 2-D models show large model-model differences in the SH due to different treatments of the Antarctic ozone loss. Off-line 3-D chemical transport models (CTMs) are now also routinely available to study past changes. These models are inherently better in simulating the polar regions and this leads to relatively small model-model differences, especially in the SH. CTMs also clearly perform better at reproducing long-term changes in the NH than in the SH. The ongoing disagreement between model-observation comparisons in the NH versus the SH indicates that we do not yet have a full understanding of the processes controlling ozone changes at midlatitudes.

Solar Cycle

- **Identification of the solar cycle signal in observed ozone has been improved due to the absence of major volcanic eruptions over the past 15 years.** The deduced solar cycle variation in column ozone has a mean amplitude of 2-3% (from minimum to maximum) in low to midlatitudes from the extended data series.
- **Model estimates and measurements suggest that the amplitude of the solar cycle in ozone concentration is less than 4% throughout the stratosphere, although there are apparent differences between the models and observations at some altitudes.** The vertical structure of the ozone solar cycle variation is subject to observational uncertainties (e.g., short record lengths, instrument intercalibration problems) that make it difficult to test models critically.

3.1 INTRODUCTION

The abundance of stratospheric ozone is determined by a combination of chemical and dynamical processes. The importance of these processes changes with location (particularly altitude and latitude) and with time. These processes also act on different time scales. For example, the influence of the solar cycle on total column ozone varies over its 11-year cycle, the quasi-biennial oscillation (QBO) over an approximately 27-month cycle, and strong volcanic eruptions have an effect lasting a few years.

The long-term changes in global ozone were last reviewed in Chapter 4 of WMO (2003). At that time, global total ozone values were about 3% below the pre-1980 levels. This reduction had occurred primarily in the mid- to high latitudes of both hemispheres, with no significant trends reported in the tropics. Clear differences between the two hemispheres were noted. Annually averaged total ozone over the northern midlatitudes was 3% lower than pre-1980 levels, with twice as much decline in winter than in summer. Over the southern midlatitudes, by contrast, a long-term decrease of 6% had occurred, roughly constant through the year.

WMO (2003) concluded that models including observed changes in halocarbons, other source gases, and aerosols captured the long-term behavior in midlatitudes. At that time, the differences between the Northern and Southern Hemispheres were not explained. However, the report did conclude that there was increased evidence that the observed changes in atmospheric dynamics had a significant influence on ozone over northern midlatitudes on decadal time scales. It also noted that the magnitude of these influences, largest in the lower stratosphere, had not been quantified unambiguously. At higher altitudes (35–50 kilometers (km)), ozone trends were up to 8%/decade over midlatitudes in both hemispheres, consistent with expectation due to the observed changes in chlorine concentrations.

In this chapter, the same issues are examined with the benefit of an additional four years of measurements and a number of new analyses and interpretations. Equivalent effective stratospheric chlorine (EESC) peaked in the late 1990s to early 2000s, and so there are now several years of observations since that peak. There is an encouraging consistency between the observations of ozone and the behavior expected from EESC changes. Major emphases of this chapter are whether the gradual reduction in EESC, described in Chapter 1, can be found in the observational record when broken down by latitude and altitude, and whether the observational record can be reproduced by models. The decadal influence of the changes in dynamical processes is again an important issue

for Northern Hemisphere midlatitudes, and one that is critical for a complete understanding of total ozone changes over the last decades.

Both dynamical and chemical processes may contribute to decadal ozone (O_3) changes in the lower stratosphere. There is no single cause and the relative contributions of different processes will change with time period considered and between the hemispheres. Chemical changes in midlatitudes may result from changes in O_3 loss processes occurring locally or those at polar latitudes (see Chapter 4), whose effects are subsequently transported to midlatitudes. Both gas-phase and heterogeneous chemical processes are important in these processes. A major chemical driver for long-term lower stratospheric ozone changes is increases in chlorine and bromine.

Previous Assessments described long-term ozone changes in terms of linear trends, estimated using regression analysis. The decision to fit a linear trend was based on the expected response to the approximately linear increase in ozone-depleting substances (ODSs). However, it has become clear that the change of ODSs after the mid-1990s is no longer linear with time. In addition, ozone data in the late 1990s to early 2000s do not follow the trend line drawn by fitting the past data to a linear function. Recent studies of long-term changes in ozone are focused on detection of the ODS-related signal in the available data. Typically this is done by including a term in statistical models that is proportional to the stratospheric burden of ODSs, such as EESC or a similar function.

In this chapter, Section 3.2 presents the basic observations of ozone, with particular emphasis on behavior over the past 4 years and a statistical interpretation. Section 3.3 presents observations of long-term changes in aerosols and nitrogen dioxide (NO_2) that are relevant to stratospheric ozone. Finally, Section 3.4 discusses the dynamical and chemical processes that lead to ozone changes and summarizes the use of “physical” models for quantifying the contributions of the key processes to these changes.

3.2 UPDATE OF OZONE CHANGES

3.2.1 Statistical Methods

The general purpose of the use of statistical models is to characterize and quantify the relationship between “predictor” or “explanatory” variables and ozone. Some of the explanatory variables describe natural variations in ozone, while others are included in the model to reflect possible anthropogenic changes in ozone. Multiple linear regression is typically used to estimate statistical model

GLOBAL OZONE

parameters (e.g., SPARC, 1998; Weatherhead et al., 1998, 2000; Reinsel et al., 2002, 2005; Svenby and Dahlback, 2004; Krzyścin, 2006).

Seasonal cycle, solar flux (see Section 3.4.4), and quasi biennial oscillation (QBO) indices are commonly used as proxies for natural ozone variability. Characteristics of volcanic aerosols, such as aerosol optical depth, are used in some models to account for effects of volcanic eruptions, particularly for the El Chichón and Mt. Pinatubo eruptions (see Section 3.3.1).

The way proxies are included in a regression model can be an issue. Steinbrecht et al. (2004a) used harmonic oscillations to describe ozone variations related to the 11-year solar cycle, while Newchurch et al. (2003) assume strict proportionality to the 10.7-cm solar radio flux with no seasonal variation. Debate over the accuracy, robustness, and physical meaning of such choices of proxies is found in Steinbrecht et al. (2004b) and Cunnold et al. (2004). Stolarski et al. (2006) used the 10.7-cm solar radio flux proxy and allowed for possible seasonal variations. Harris et al. (2003) and Malanca et al. (2005) used a polynomial fit to separate long-term ozone changes from natural variability.

A linear function was used in earlier ozone Assessments (WMO, 1995; 1999) to describe long-term changes in ozone due to ODSs. As noted above, the increase of ODSs is not approximated well by a linear function over the time period from the late 1970s through the 1990s and beyond. The piecewise linear trend concept, in which different linear fits are used before and after a turning point, has been incorporated in several recent trend analyses (e.g., Newchurch et al., 2003; Reinsel et al., 2005; Miller et al., 2006). The turnaround date has been chosen to be January 1996 (Reinsel et al., 2002; 2005) or 1994 (Krzyścin et al., 2005).

Instead of fitting a linear (or piecewise) trend to the ozone time series, the changes in ozone can be analyzed using the EESC function (Chapter 1). The EESC is an index reflecting the amount of ozone-depleting chlorine and bromine in the stratosphere (Chapter 8). Daniel et al. (1995) suggested that a change in total column ozone can be assumed to be generally proportional to the EESC. The EESC trend model has been used in several recent statistical analyses of ozone (e.g., Newman et al., 2004; Guillas et al., 2004; Yang et al., 2005; Fioletov and Shepherd, 2005; Dhomse et al., 2006; Stolarski et al., 2006). This chapter is focused on detection of the EESC-related signals in available ozone records and so we use this method. Piecewise trends and other methods used for the detection of ozone recovery are discussed further in Chapter 6.

The contribution of different explanatory variables to ozone fluctuations is illustrated in Figure 3-1 (upper

panel). It shows area-weighted seasonal mean total ozone values for the region 60°S-60°N estimated from ground-based data, and the contribution (in Dobson units, DU) of major components of the ozone variability to the total integral: the seasonal cycle, solar cycle-related signal, QBO, and an estimated volcanic-related component. The EESC-related term included in the regression model allows for possible seasonal variations. The residuals are also shown. Possible anthropogenic changes in ozone are isolated by removing known natural components of ozone variability. Total ozone for the region 60°S-60°N, with seasonal components and volcanic-, solar cycle-, and QBO-related components removed, are shown in Figure 3-1 (lower panel). The seasonal component of the EESC-related signal is also removed from the data to reduce seasonal variations of the residuals. The plot illustrates the good agreement between the long-term changes in ozone and the EESC.

For trends derived as a regression onto the EESC time series as shown in Figure 3-1, the results can be expressed in several ways:

- (a) The results can be simply expressed as ozone change per unit of EESC (e.g., % per 0.1 parts per billion by volume (ppbv) EESC).
- (b) The EESC time series is nearly linear for 1979-1989 (see Figure 3-1), with a net change of approximately 1.0 ppbv of chlorine. Thus the EESC fit to ozone can be expressed in terms of linear changes for this time period, with results reported in ozone changes (% or DU) per decade (as in Stolarski et al., 2006).
- (c) Ozone changes associated with EESC can also be expressed as simple differences between two time periods.

Here we follow (b) and show results expressed as percent per decade for 1979-1989. The net change in ozone between 1979 and 2005 is approximately 1.4 times these linear trend values (i.e., a -5% per decade trend corresponds to approximately a -7% net change for 1979-2005). Approach (b) also makes it easier to compare EESC-related trends discussed here with linear ozone trends reported in the earlier Assessments.

There are certain issues related to the use of EESC as a regressor. The EESC calculation depends on the age of air spectrum, which varies with altitude and latitude (see Newman et al. (2006) and Box 8-1 of Chapter 8 for details). The age of air is about 3 years in the midlatitude lower stratosphere. It is longer, about 6 years, over the poles and in the upper stratosphere. Ozone dilution from the Antarctic, and to a lesser degree from the Arctic, affects lower stratospheric ozone over midlatitudes (Section 3.4.3) and, strictly speaking, the “polar” EESC should also

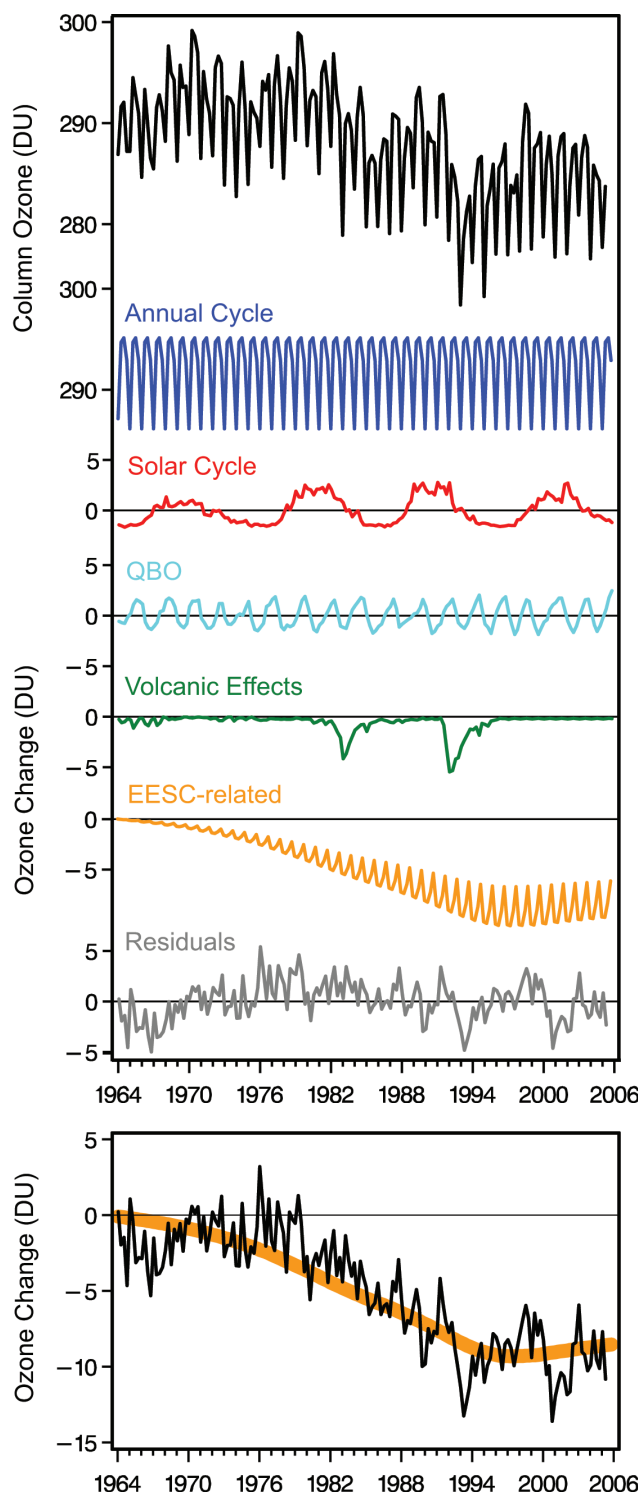


Figure 3-1. Top: Ozone variations for 60°S-60°N estimated from ground-based data and individual components that comprise ozone variations. Bottom: Deseasonalized, area-weighted total ozone deviations estimated from ground-based adjusted for solar, volcanic, and QBO effects, for 60°S-60°N. The thick yellow line represents the EESC curve scaled to fit the data from 1964-2005.

be used as a contributing factor when midlatitude trends are considered. However, due to the shape of the EESC curve, a 3-year difference in the age of air has limited effect on the estimated EESC-related regression coefficient. For example, the annual trend for 60°S-60°N is $-1.6\% \pm 0.17\%$ and $-1.3\% \pm 0.15\%$ per decade (2σ uncertainties here and elsewhere in this chapter) for EESC calculated with an age of air of 3 and 6 years, respectively. However, the age of air plays a major role when ozone recovery is considered (see Chapter 8).

Care must be used when comparing trends derived from data in different vertical coordinate systems. In the presence of a temperature trend, the various representations of the changes in ozone profiles will give different trends because of the changing altitudes of pressure surfaces and the changing air density on pressure surfaces with time. These trend differences will depend on the magnitude of the temperature trend and are important only in the upper stratosphere. Rosenfield et al. (2005) demonstrated that between 1979 and 1997, ozone trend differences at 3 hectoPascals (hPa) are as large as 1-2%/decade depending on how ozone changes are reported, with the largest differences in the southern high latitudes. The most negative trend is computed when ozone profiles are given as number densities on geometric altitude, while the least negative trend is computed for number densities on pressure levels. The Stratospheric Aerosol and Gas Experiment (SAGE) instrument measures ozone profiles as number densities on geometric altitude, while Solar Backscatter Ultraviolet (SBUV) data are provided as mixing ratios on a pressure grid. Thus, upper stratospheric ozone trends computed from SAGE data will be larger than those computed from SBUV data when the trends are computed in the natural vertical coordinate for each instrument. For comparison with SBUV, SAGE data are typically converted from number density on altitude levels to mixing ratio on pressure levels (e.g., Wang et al., 1996; McPeters et al., 1994). However, errors in the temperature data used to carry out this conversion can then affect the computed trends. Li et al. (2002) estimated that adjustment for the temperature trends would reduce differences in SBUV trends relative to SAGE by about 1%/decade, in agreement with Rosenfield et al. (2005).

3.2.2 Changes in Total Ozone

Since the previous Assessment (WMO, 2003), satellite data from Total Ozone Mapping Spectrometer (TOMS) and SBUV(2) instruments have been reprocessed with the new version 8 algorithm (Bhartia et al., 2004). This has resulted in better agreement between satellite and ground-based datasets, particularly in the 1980s and early 1990s. The version 8 algorithm was also

GLOBAL OZONE

applied to 1970-1977 measurements from the Nimbus 4 Backscatter Ultraviolet (BUV) instrument, and these data are shown in figures below. A new version of Global Ozone Monitoring Experiment (GOME) data was also used here. Details of the instruments and datasets can be found in Appendix 3A.

The approach used in WMO (2003) is again used here (Fioletov et al., 2002). Five datasets of 5°-wide zonal averages of total ozone values are analyzed in this Assessment and described in the Appendix. Area-weighted seasonal (3-month) averages are calculated for different latitude belts and for the globe. Each dataset has been deseasonalized with respect to the period 1979-1987, followed by subtraction of the average of the monthly mean anomalies for 1964-1980, estimated from ground-based data. Deviations are expressed as percentages of the ground-based time average for the period 1964-1980.

As a part of the deseasonalizing process, the long-term trends for individual seasons have been removed and replaced by the average of seasonal trends, as was previously done in WMO (1999). Unlike WMO (1999), where the trend was approximated by a straight line, the EESC curve is used here as a proxy for the trend function. For regions with missing data, ozone deviations are assumed to be identical to the surrounding latitude belts where data are available.

The total ozone deviations for the 90°S-90°N, 60°S-60°N, 35°-60°N, and 35°-60°S latitude belts are shown in Figures 3-2 and 3-3. These plots differ slightly from those of WMO (2003) because the satellite data processing algorithms have changed. The ozone deviations in the most recent years are similar to those in the late 1990s-early 2000s, with no clear change in magnitude. A decadal periodic component related to the 11-year solar cycle is discussed in Section 3.4.4. Another distinct feature seen in the unsmoothed data plot is a periodic structure with a period of 2-3 years that is likely associated with the QBO. These components are estimated and removed using statistical models as described above. Furthermore, to remove short-term fluctuations, annual averages were calculated (Figure 3-2 and 3-3, bottom). Comparing hemispheres, midlatitude ozone values in 2002-2005 are about 3% lower than the pre-1980 level in the Northern Hemisphere (NH) and about 5.5% lower in the Southern Hemisphere (SH) (Figure 3-3), i.e., they are similar to those reported in WMO (2003).

Figure 3-4 shows the total ozone deviations in the tropics (25°S-25°N), where about 40% of global ozone is located. No long-term changes in total column ozone have been observed over the equator (e.g., Reinsel et al., 2005). Outside the equatorial region, total ozone at 10°-25°S and 10°-25°N shows some signs of decline, but the trends are

not statistically significant. As discussed in Section 3.4.4, there is a strong decadal periodic component in tropical total ozone variations, probably related to the solar cycle. The solar flux at 10.7 cm is shown at the top of Figure 3-4. Pre-1980 ozone deviation estimates from ground-based data for the tropics are less reliable because the number of stations in that region was very limited and there were no regular Dobson instrument intercomparisons prior to 1974 (Bojkov and Fioletov, 1996). Ground-based data do seem to agree with Nimbus 4 BUV measurements; however, BUV measurements were very sparse after 1972 (Stolarski et al., 1997).

Total ozone changes in different seasons (DJF, MAM, JJA, and SON) from 35°-60°S and 35°-60°N are shown in Figure 3-5 for the period 1979-2005. The variability is high during the seasonal ozone buildup period in winter and spring and is less through summer and autumn. Long-term ozone declines in winter and spring seasons are similar between hemispheres; ozone values are 5-6% lower than the pre-1980 values. Summertime ozone deviations from the pre-1980 level are smaller in the NH (about 2%) than in the SH (about 5%).

Figure 3-5 shows that there is a clear difference in long-term ozone variations over NH and SH midlatitudes. Ozone variations over northern midlatitudes have a minimum in 1992-1995 (see also Figure 3-3 for annual averages). The large anomalies in winter-spring of 1992 and 1993 have been associated with the Mt. Pinatubo volcanic eruption in June 1991 (Gleason et al., 1993; Bojkov et al., 1993; Kerr et al., 1993; Hofmann et al., 1994). Low values in the mid-1990s were followed by increases in the late 1990s-early 2000s (Reinsel et al., 2005; Yang et al., 2006). This increase in column ozone is associated with the rise in ozone content in the lower stratosphere below 18 km, as described in Section 3.2.3 and further discussed in Section 3.4.5. Similar features are not seen over southern midlatitudes, where strong ozone minima occurred in 1985 and 1997 (Brinksma et al., 1998; Connor et al., 1999; Cordero and Nathan, 2002). Differences in the seasonal cycle of long-term ozone loss between NH and SH midlatitudes are partly caused by the export of ozone-depleted air from the polar vortex (see Section 3.4.3.2). This effect exists in both hemispheres, but its effect on spring- and summertime ozone is stronger in the SH due to the larger and more regular springtime ozone depletion over the Antarctic.

3.2.3 Changes in the Vertical Distribution of Ozone

There are a number of sources of vertically resolved ozone data. Ozonesondes make in-situ measurements up

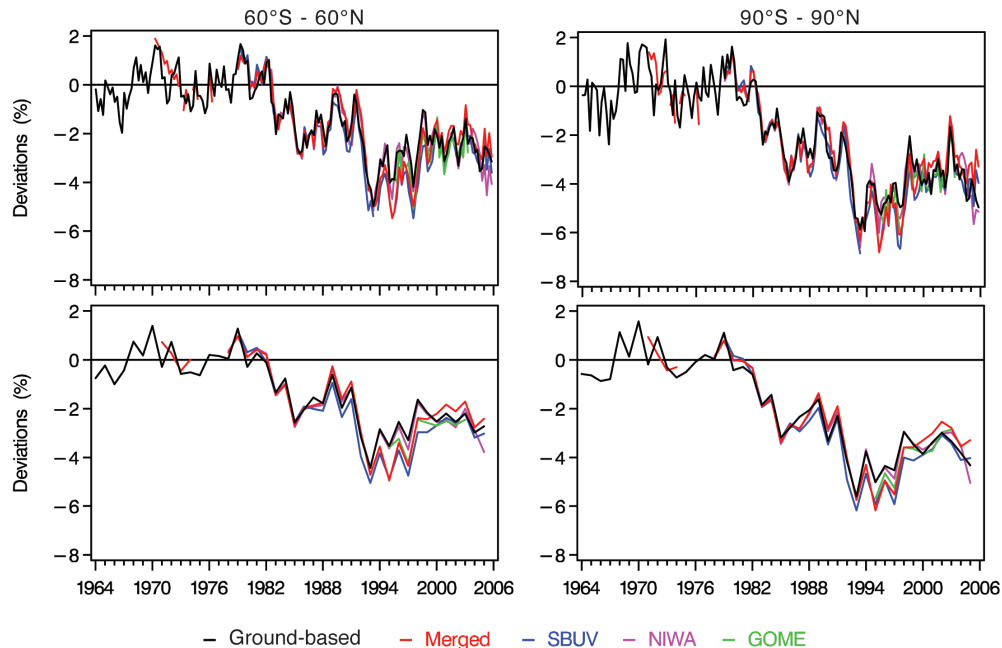


Figure 3-2. Top: Deseasonalized, area-weighted seasonal (3-month average) total ozone deviations, estimated from different global datasets: ground-based, merged satellite dataset, National Institute of Water and Atmospheric Research (NIWA) assimilated dataset, SBUV(/2), and GOME total ozone data. See Appendix 3A for details. Each dataset was deseasonalized with respect to the period 1979-1987, the average of the monthly mean anomalies for 1964-1980 estimated from ground-based data was then subtracted from each anomaly time series, and deviations are expressed as percentages of the ground-based time average for the period 1964-1980. Results are shown for the region 60°S-60°N (left) and the entire globe (90°S-90°N) (right). Updated from Fioletov et al. (2002) and WMO (2003). Bottom: The same plot, but for annual averages.

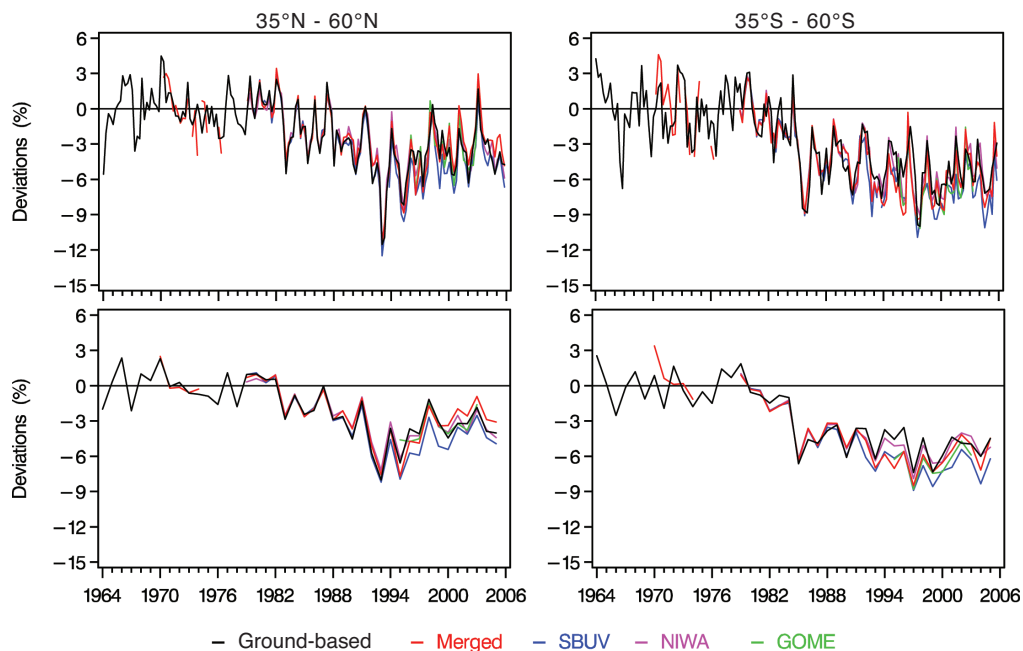


Figure 3-3. Top: Deseasonalized, area-weighted total ozone deviations from datasets for the latitude bands 35°N-60°N (left) and 35°S-60°S (right). Anomalies were calculated with respect to the time average for the period 1964-1980. Updated from Fioletov et al. (2002) and WMO (2003). Bottom: The same plot, but for annual averages.

GLOBAL OZONE

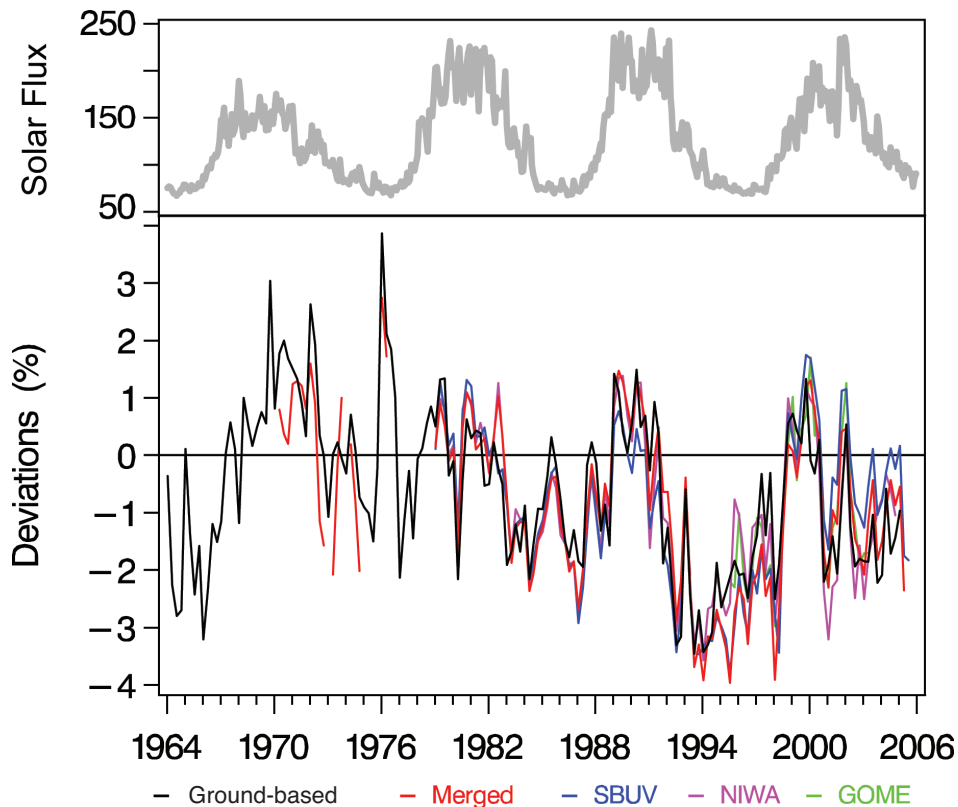


Figure 3-4. Deseasonalized, area-weighted total ozone deviations from five datasets for the latitude bands 25°S-25°N. The solar flux at 10.7 cm is shown as a proxy for solar variability.

to 30-35 km. Lidar and microwave instruments measure ozone vertical profiles from the lower stratosphere to about 50 km (higher for microwave) and their records are now long enough to assess long-term ozone changes (e.g., Schneider et al., 2003; Hartogh et al., 2004; Steinbrecht et al., 2006). The Umkehr method provides profile data to about 50 km from ground-based observations by Dobson and Brewer instruments. A new version of the Umkehr algorithm, UMK04, has been developed recently (Petrovavlovskikh et al., 2005a, b). Long records of ozone profile retrieval from satellite observations are available from the SAGE and SBUV and SBUV/2 series of instruments, although there are also satellite instruments with shorter records, such as the Halogen Occultation Experiment (HALOE) (e.g., Nazaryan et al., 2005). The SBUV and SBUV/2 instruments have been in operation since 1978, with six SBUV(2) instruments having flown since then. A new version 8 of SBUV(2) data has recently been released (Bhartia et al., 2004). First results have demonstrated a significant improvement of the SBUV(2) data quality (McPeters et al., 2004). While there are some differences between the SBUV and SAGE time series, they both demonstrate similar features of long-term changes in the vertical distribution of ozone. The biases between the SAGE II and the SBUV record vary with time, according to which of the individual SBUV(2) sensors are used in

the long-term record (Nazaryan and McCormick, 2005; Fioletov et al., 2006; Terao and Logan, 2006). These biases, of several percent, are largest in the upper stratosphere and will contribute to differences in trends derived from SAGE II and SBUV data. Data sources are discussed in detail in the Appendix.

3.2.3.1 UPPER STRATOSPHERE

Figure 3-6 shows the evolution of upper stratospheric ozone relative anomalies, averaged between 35 and 45 km altitude, from lidar and microwave measurements, for five stations (Steinbrecht et al., 2006). The corresponding zonal averages from satellite data (SAGE, SBUV, and HALOE) are also plotted. Anomalies are defined as the deviation of individual monthly means from the average climatological annual cycle. All records starting before 1990 clearly show the long-term decline of ozone in the upper stratosphere. Steinbrecht et al. (2006) estimated that ozone in the upper stratosphere shows a long-term decline of 10 to 15% since 1980. Upper stratospheric ozone trends before 1997 were about $-6\%/decade$ at the northern midlatitude stations, almost $-8\%/decade$ at Lauder in southern midlatitudes, and only $-4.5\%/decade$ at subtropical Hawaii (Steinbrecht et al., 2006). This confirms similar findings of interhemispheric and latitudinal

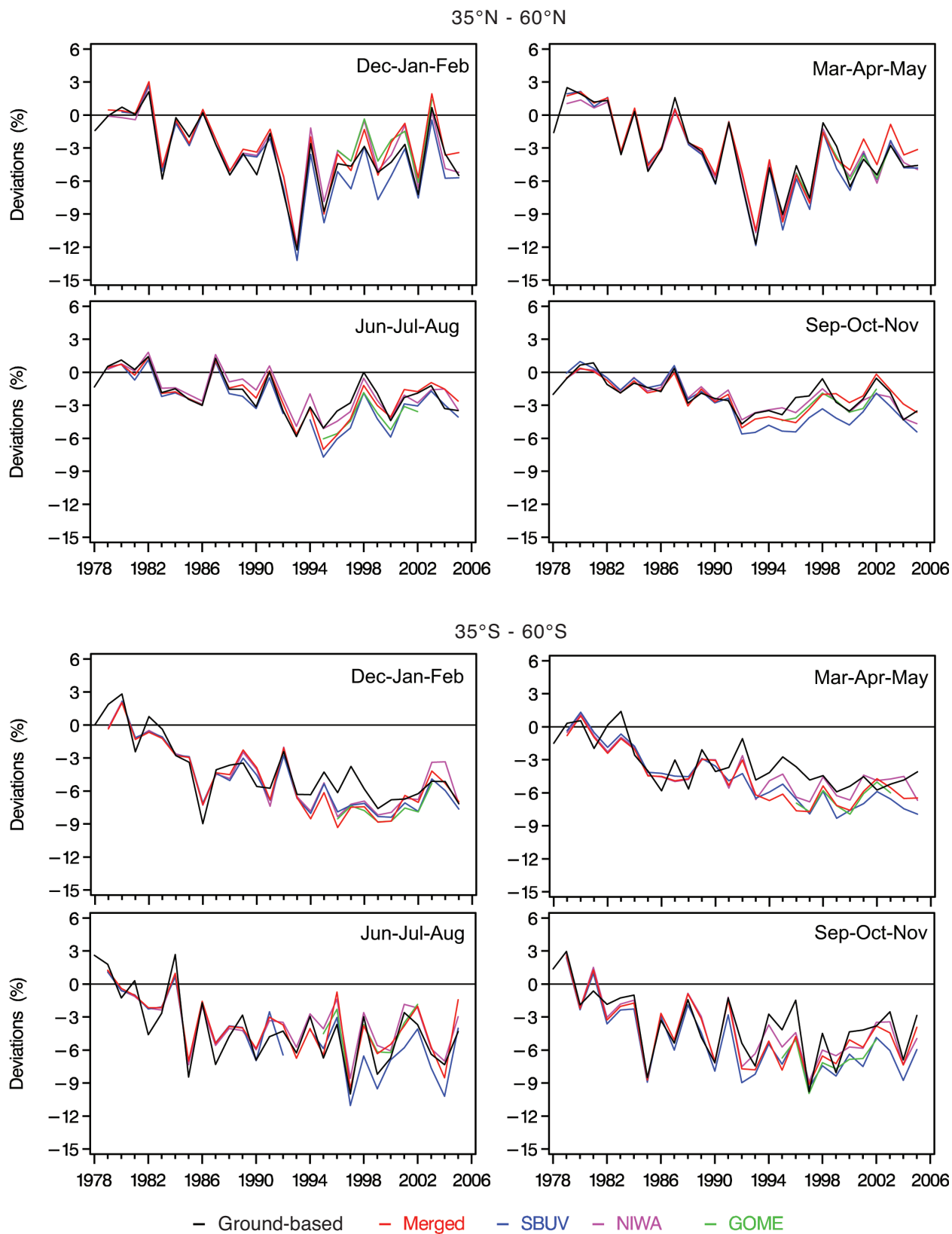


Figure 3-5. Seasonal area-weighted total ozone deviations from the 1964-1980 means, calculated for four seasonal averages, for the latitude bands 35°N-60°N (top) and 35°S-60°S (bottom). Updated from WMO (2003).

GLOBAL OZONE

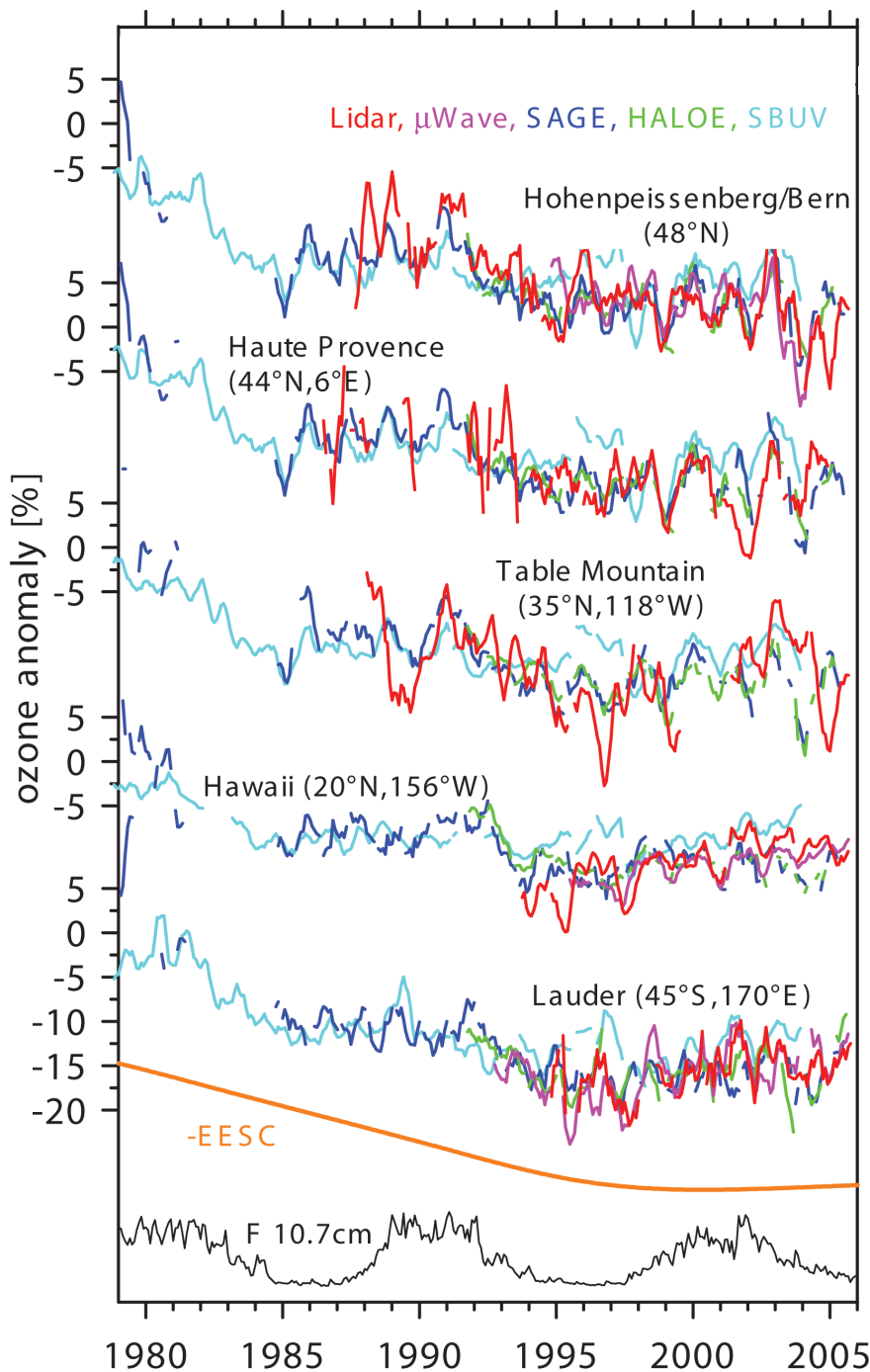


Figure 3-6. Upper stratospheric ozone anomalies as measured by ground-based lidars and microwave radiometers at selected stations of the Network for the Detection of Atmospheric Composition Change (NDACC), and by the corresponding zonal means from the satellite-borne Stratospheric Aerosol and Gas Experiments (SAGE, v6.20), Halogen Occultation Experiment (HALOE, v19), and Solar Backscatter Ultraviolet instruments (SBUV). Anomalies are averaged over the altitude range from 35 to 45 km, or the pressure range from 6.4 to 1.6 hPa for SBUV (V8-merged dataset). For clarity, 5-month running means are plotted. The EESC in the figure is for the age of air spectrum with mean age of 6 years and width of 3 years, and zero bromine (see Box 8-1 of Chapter 8). Thin black curve at the bottom shows the solar flux at 10.7 cm. Adapted from Steinbrecht et al. (2006).

differences reported from SAGE data by Li et al. (2002) and from SBUV(2) data by Rosenfield et al. (2005). Figure 3-6 also shows that ozone levels seem to be inversely following the chlorine curve, and at many stations the previously steep ozone decline has not continued in the last five years. Newchurch et al. (2003), using SAGE data, also emphasized the lack of decline of ozone in the upper stratosphere since 1997.

The vertical structure of ozone trends has been derived from SAGE data (Wang et al., 2002; Li et al., 2002; Randel and Wu, 2006) and SBUV data (Rosenfield et al., 2005). Updated ozone trend estimates attributed to the changes in the EESC as a function of latitude and altitude estimated using SAGE I+II data and SBUV(2) data for 1979-2004 are shown in Figure 3-7. Values are given in % per decade for the period of linear change of the EESC, and were calculated in the native units of each instrument.

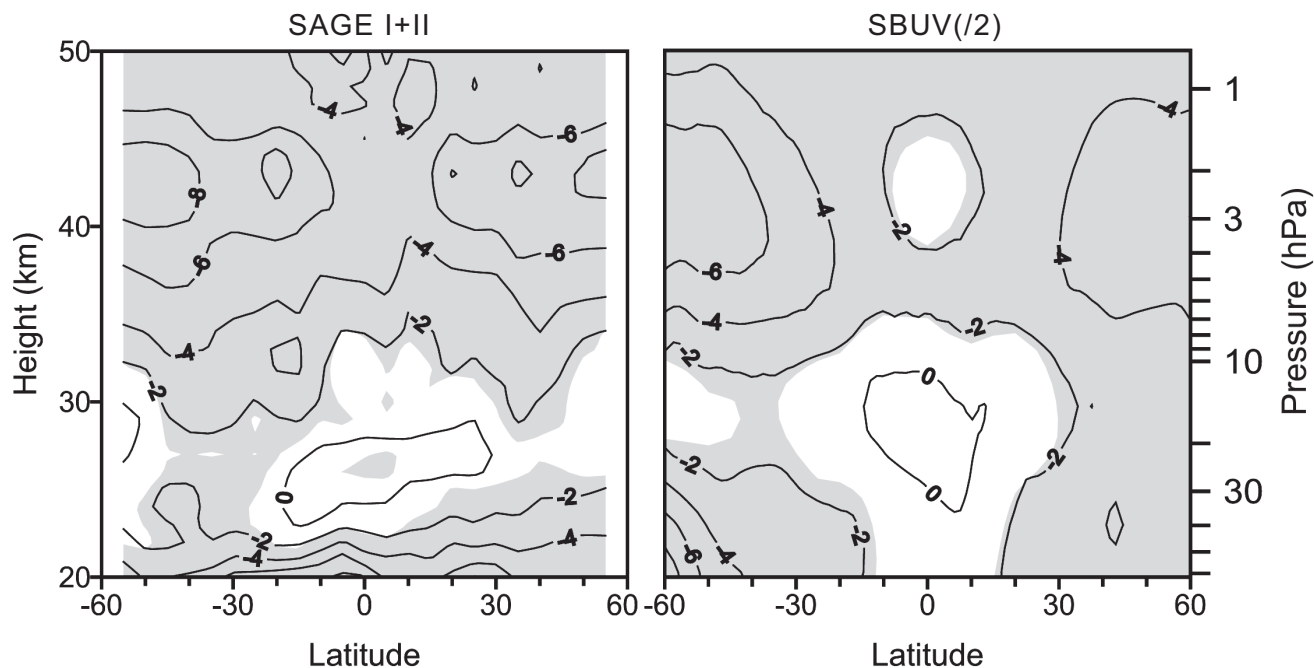


Figure 3-7. SAGE I+II and SBUV(/2) annual trends in percent per decade as a function of latitude and altitude for the period 1979-2004. The trends were estimated using regression to an EESC curve and converted to %/decade using the variation of EESC with time in the 1980s. The SAGE trends were calculated in geometric altitude coordinates, and the SBUV(/2) trends were calculated in pressure coordinates. Shadings indicate that the changes are statistically significant at the 2σ level.

Also, as noted in Section 3.2.1, the SAGE data give larger trends than SBUV data in the upper stratosphere due to the temperature trend and the use of pressure (SBUV) rather than geometric altitude (SAGE) coordinates. Some of the differences are also likely caused by different biases between ozone measured by SAGE and by the different SBUV(/2) instruments. The strongest decline (7-9% per decade, or 10-15% since 1979) occurred at 40-45 km over midlatitudes. The overall pattern of upper stratosphere ozone trends shown in Figure 3-7 is similar to that reported in WMO (2003) from SAGE data for a shorter period and using a linear trend function.

The vertical profiles of trends in ozone over northern midlatitudes (35° - 60° N) derived from SAGE, SBUV, and Umkehr instruments are very similar for 30-38 km. SAGE trends are larger than the SBUV and Umkehr trends above 40 km (Figure 3-8). Similarly, over 35° - 60° S, SAGE and SBUV trends are essentially the same for 30-38 km and the SAGE trends are larger above 40 km. Despite the difference in the magnitude of the trend, both SAGE and SBUV show that the decline at 40 km over SH midlatitudes is slightly larger than that over NH midlatitudes, but the difference is within the error bars. A slightly stronger decline over the SH was previously reported from SAGE data in WMO (2003).

Upper stratospheric negative trends are generally largest in winter and smallest in summer (Hood et al., 1993; Hollandsworth et al., 1995). Ozone trends for four seasons estimated using the EESC from version 8 SBUV data for 1979-1997 are shown in Figure 3-9 (Rosenfield et al., 2005). In both hemispheres the winter decline is larger (maximum of $-5.7 \pm 2.8\%$ /decade in the NH and $-6.9 \pm 2.8\%$ /decade in the SH) than the summer decline ($-3.1 \pm 1.5\%$ /decade and $-4.9 \pm 1.6\%$ /decade, respectively). Spring and autumn negative trends are also larger in the SH than in the NH. The spring and autumn upper stratospheric trends lie in between the winter and summer trends.

3.2.3.2 LOWER STRATOSPHERE

Ozone values in the lower stratosphere from the late 1970s to the present from measurements made by sondes, SAGE, SBUV(/2), and HALOE are shown over Europe (Figure 3-10a) and over Lauder, New Zealand (Figure 3-10b) (updated from WMO, 2003 for sondes; Terao and Logan, 2006). There is good agreement among the various datasets. Ozone reached minimum values in 1993 in the NH from 13 to 25 km (158-25 hPa) in the NH. Since then, from 13 to 16 km (158-100 hPa), ozone values have increased and are about the same as in the early 1980s,

GLOBAL OZONE

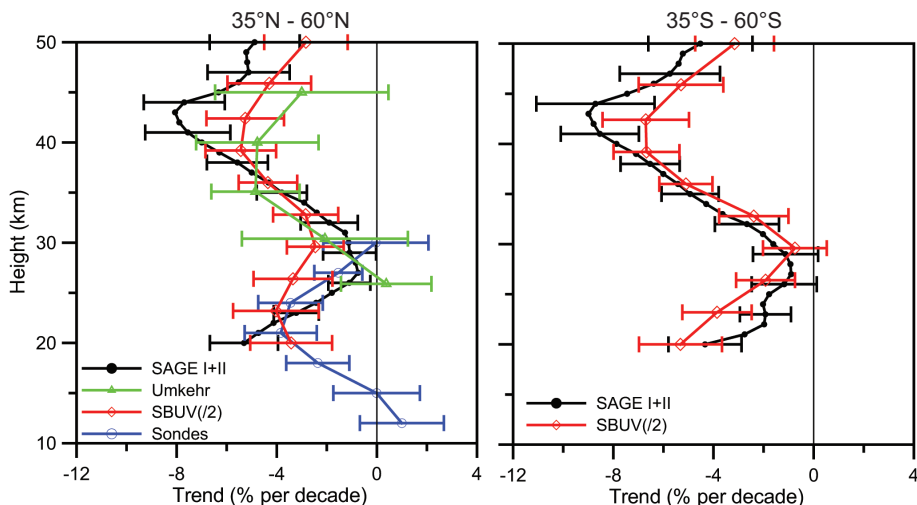
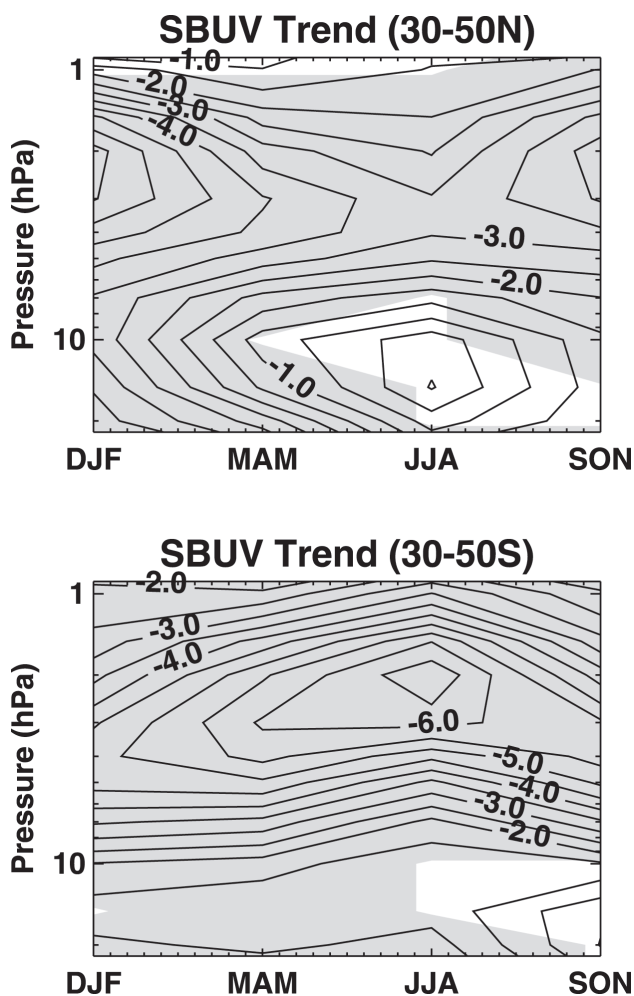


Figure 3-8. Vertical profile of ozone trends over northern and southern midlatitudes estimated from ozonesondes, Umkehr, SAGE I+II, and SBUV(/2) for the period 1979-2004. The trends were estimated using regression to an EESC curve and converted to %/decade using the variation of EESC with time in the 1980s. The trends were calculated in geometric altitude coordinates for SAGE and in pressure coordinates for SBUV(/2), sondes, and Umkehr data, and then converted to altitude coordinates using the standard atmosphere. The 2σ error bars are shown.



while from 22 to 25 km (40-25 hPa), they are about 5-8% lower than in the early 1980s.

Estimating long-term ozone changes below 20 km from satellite data is still a challenge. SBUV(/2) version 8 Layer 1 data represent the partial ozone column from approximately 7 to 19 km. However, it is a fairly new data product and more validation is required. The use of SAGE data is limited in this altitude range because the present version of SAGE I data is not reliable below 20 km. The ozone amount below a certain level in the lower stratosphere can be estimated by subtracting SAGE I and II partial column ozone above that level from total column measured by TOMS. Figure 3-11 shows estimates of partial column ozone below 19 km from satellite data for northern and southern midlatitudes from SBUV(/2) and SAGE/TOMS data. (The SAGE partial column above 19 km is derived from a regression analysis of the SAGE profile measurements, as described in Randel and Wu, 2006.) Figure 3-11 demonstrates that ozone levels below 19 km in the NH in the 2000s are similar to these from the early 1980s but are ~10% lower in 1992-1995. In the SH, the data also show a decline between 1980 and the mid-1990s; however levels in the 2000s remain ~10% lower than the levels of the late 1970s to early 1980s.

Figure 3-9. Season-pressure sections of SBUV mid-latitude linear ozone trends for (top) Northern Hemisphere and (bottom) Southern Hemisphere for 1979-1997 in % per decade (Rosenfield et al., 2005). Shaded areas are significant at the 2σ level.

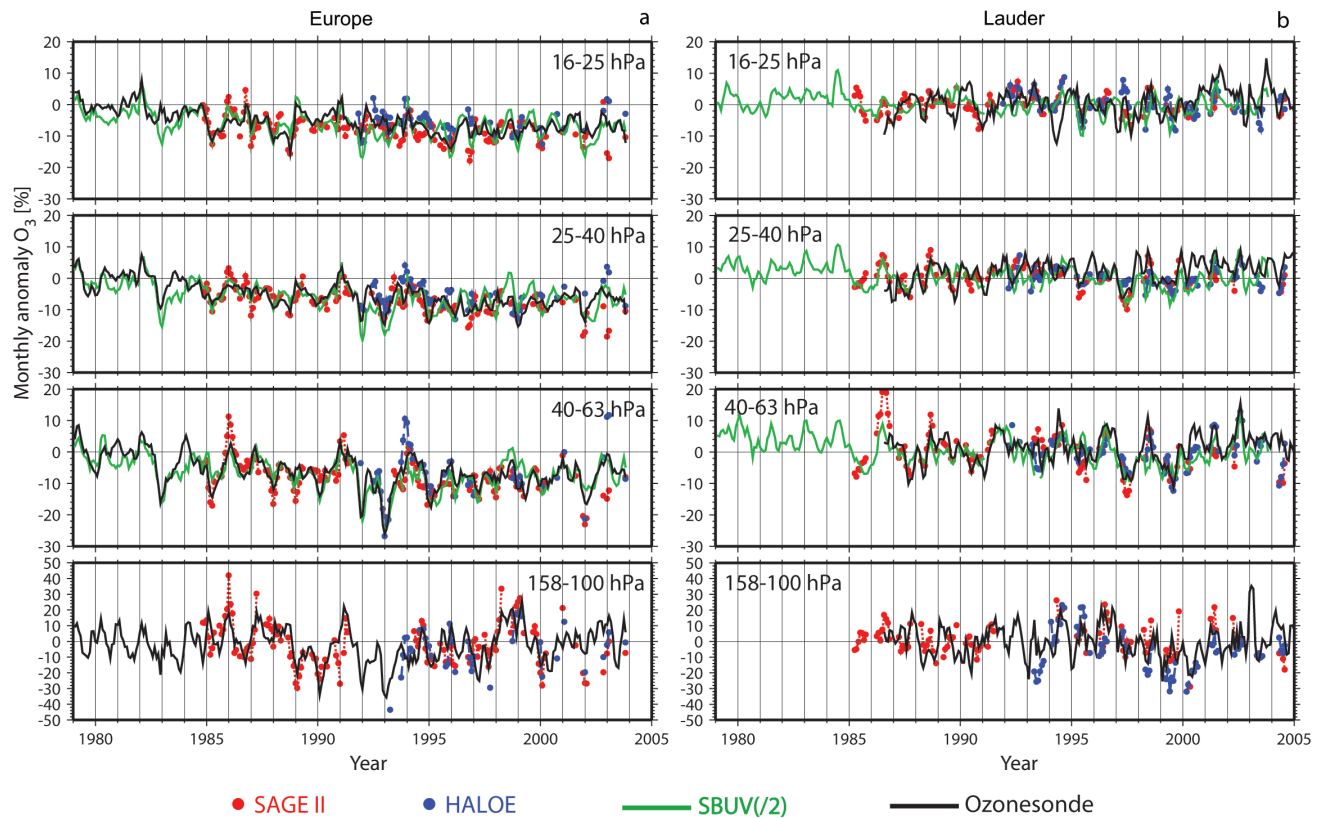


Figure 3-10. (a) Monthly ozone anomalies for Europe as measured by ozonesondes (black line), SAGE II (red circles), HALOE (blue circles), and SBUV(2) (green line) at four pressure layers. The monthly anomalies were calculated as the difference between a given monthly mean and the average of monthly means for 1985–1990 for each dataset, except for HALOE where 1994–1999 was used; the average of the monthly mean ozonesonde anomalies for 1979–1981 was then subtracted from each anomaly time series. The ozonesonde data are the average of measurements at three European stations: Hohenpeissenberg, Payerne, and Uccle. The satellite data were selected within a grid box of 45°N–55°N and 10°W–30°E. A 3-month running mean was applied to the data. For SAGE II and HALOE, results are shown when the number of observations is larger than 4 per month. (b) Same as (a), but for Lauder, New Zealand. The monthly anomalies were calculated using the 1987–1991 monthly means for each dataset, except for HALOE where 1994–1999 was used. The satellite data were selected within a grid box of 40°S–50°S and 150°E–170°W. Adapted from Terao and Logan (2006).

Earlier Assessments reported a large negative trend (more than 5%/decade) in the lower stratosphere below 18 km (WMO, 1992, 1999; SPARC, 1998; Logan et al., 1999) over northern midlatitudes for the period up to the mid-1990s. A maximum decline of about –10% per decade was reported at 15 km (see Figure 3-12). However, the ozonesonde trends reported by WMO (2003) for 1980–2000 at 12–18 km (200–63 hPa) are half as large as those for 1980–1996. A similar reduction of the trend magnitude is shown by Umkehr data analysis (Bojkov et al., 2002). Recent trend estimates over northern midlatitudes for the period up to 2004 show no decline at 15 km (Figures 3-8, 3-12) and ozone values at 13–16 km are similar to those in the early 1980s (Figure 3-10).

The dramatic change in ozone trend estimates at 12–18 km results from a decline in ozone during the 1980s and early 1990s followed by a rapid increase thereafter (see Figure 3-10). This behavior can be partially attributed to low ozone values in the lower stratosphere in 1992 and 1993 (Figure 3-10) when the stratosphere was influenced by the Mt. Pinatubo eruption. Miller et al. (2006) fit the sonde data from 13 NH stations for 1970–2003 with a piecewise linear trend, with the change in trend specified at January 1996. They removed two years of data after June 1991 to reduce the influence of the Mt. Pinatubo eruption. Nevertheless, they found that the trend is about –3 to –4%/decade at 15–18 km for 1970–1995, with a statistically significant change in trend of +9 to +13%/decade

GLOBAL OZONE

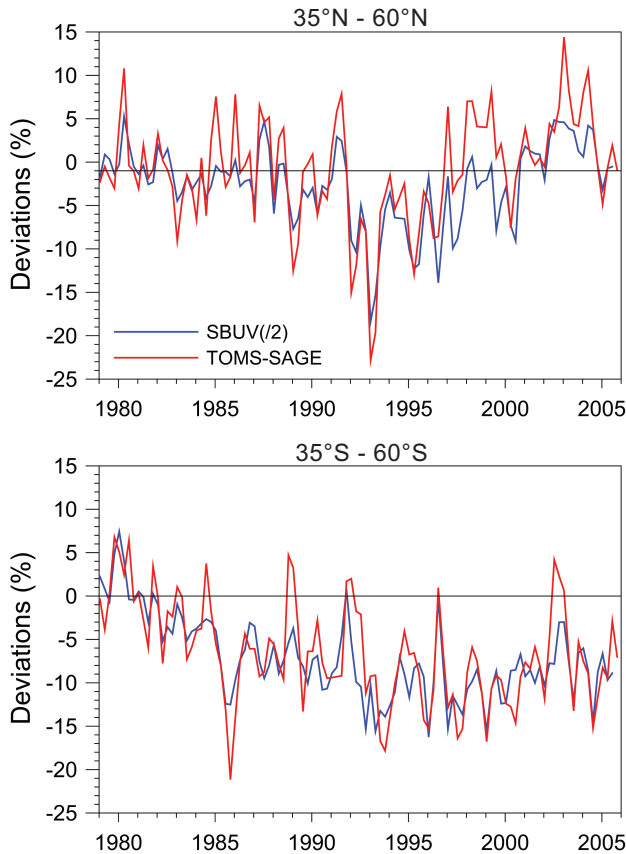


Figure 3-11. Deseasonalized, seasonal (3-month average) ozone deviations from SBUV and SAGE II data for the latitude bands 35°N-60°N (top) and 35°S-60°S (bottom) below 19 km. Anomalies were calculated with respect to the time average during 1979-1982. The blue line represents SBUV(/2) Layer 1 data (1000-63 hPa). The red line represents the difference between TOMS column ozone and SAGE I+II data vertically integrated above 19 km. The SAGE partial column above 19 km is derived from a regression analysis of the SAGE profile measurements, as described in Randel and Wu (2006).

after January 1996, i.e., there was a positive trend of 6 to 11% per decade in 1996-2003. Similar results are reported by Yang et al. (2006) and their study is discussed in detail in Chapter 6. The piecewise method gives an increase in ozone after 1996 because of the low ozone values in the first half of the 1990s and the higher values in the early 2000s (Figure 3-10a). The pre-1996 trends for 12-18 km are largest in spring, as in earlier studies (Logan et al., 1999), and the trend change is also largest in spring (Miller et al., 2006).

Ozonesonde data from Lauder, New Zealand (45°S), show no significant trends at 12-19 km (Figure 3-

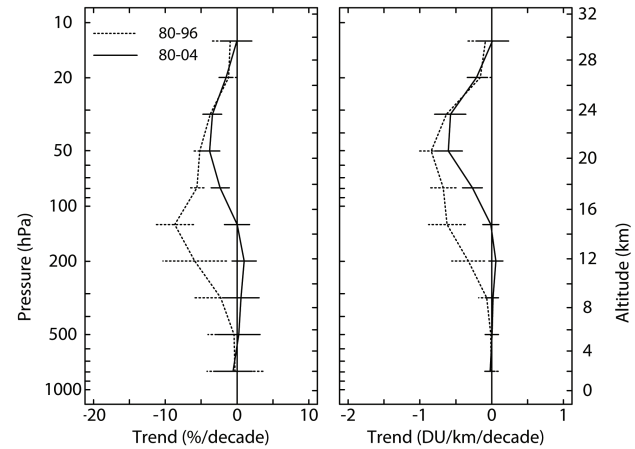


Figure 3-12. Ozone trends over northern midlatitudes (36°N-59°N) as a function of altitude in %/decade and DU/km/decade estimated from ozonesonde data for 1980-1996 (dotted line) and 1980-2004 (solid line). The trends were estimated using regression to an EESC curve and converted to %/decade and DU/decade using the variation of EESC with time in the 1980s. The error bars represent the 95% confidence limits. Updated from Logan et al. (1999).

10b). The lack of trend in the Lauder record, which begins in late 1986, is not inconsistent with the satellite data in Figure 3-11, because much of the ozone decline over southern midlatitudes occurred before 1986. An ozonesonde record from earlier years is available from Melbourne, Australia. It demonstrates a significant decline of about 10% per decade at 100 hPa (~16 km) for 1970-1990 (Logan, 1994; WMO, 1995). However, the record is affected by infrequent measurements for many years, as well as changes in sonde type and site location, and further analysis is required for trend studies.

At 18-25 km, ozone values have been relatively flat in the NH since the late 1990s, as shown in Figure 3-10. According to Miller et al. (2006), at 20-22 km, the trend is -4.5%/decade for 1970-1995, with a change in trend of 2-4%/decade after January 1996. Yang et al. (2006) suggested that the cessation of ozone depletion at 18-25 km is consistent with a leveling of the EESC curve. The ozone trend estimated using the EESC curve is about -3 to -4%/decade at 18-24 km (Figures 3-7 and 3-8) in the both hemispheres. In the past five years, ozone values at 22-25 km (40-25 hPa) were about 5% below those in the early 1980s. As shown by the ozone time series discussed above and the EESC curve, this decrease occurred prior to about 1996.

As was previously reported by SPARC (1998) and WMO (1999, 2003), the trend magnitude over midlati-

tudes has its minimum near 30 km. The SAGE I+II data and the ozonesonde data give almost no trend related to EESC at 30 km in northern midlatitudes, while the SBUV data give a small negative trend (-2 to -3% /decade) (Figures 3-7 and 3-8).

In the tropics, the SAGE data in Figure 3-7 show negative trends in the lower stratosphere, while the SBUV data show no significant trends in tropical ozone from 22 to 30 km. WMO (2003) showed significant negative trends in the tropical lower stratosphere below 22 km based on SAGE I+II data, and these changes have been accentuated by several recent years of low ozone (Figure 3-7; Randel et al., 2006). However, these results should be viewed with caution as there are no other long-term records for ozone in the tropical lower stratosphere. This is a region of small ozone concentrations and large vertical gradients, which present challenges for satellite observations. On the other hand, interannual changes in SAGE II data show good agreement with tropical ozonesonde data from the SHADOZ (Southern Hemisphere Additional Ozonesondes) network (Thompson et al., 2003) for 1998-2004 (Randel et al., 2006).

3.2.3.3 CONSISTENCY OF COLUMN AND PROFILE TRENDS

The vertical profile trends over midlatitudes discussed in Section 3.2.3 are in general consistent with column ozone trends there. Less than 10% of the midlatitude total column ozone is located above 35 km, and a 10-15% decline there accounts for a total column decline of about 1%. The lower stratosphere between 20 and 25 km contains 20-25% of the total column ozone, and an 8-10% decline in this layer contributes a total column decline of about 2%. Ozone located below 18 km contributes about 30% to the total column. As shown in Figure 3-11, there is no ozone decline below 19 km over northern midlatitudes and about a 10% decline at southern midlatitudes, yielding a total column decline of about 3%. Thus, the overall total column decline from the vertically integrated profiles is about 3% over northern midlatitudes and about 6% over southern midlatitudes; these are similar to the declines in column ozone described in Section 3.2.2.

As mentioned in Appendix 3A, SBUV(2) total ozone used in Section 3.2.2 is the vertically integrated SBUV(2) ozone profiles. Therefore, SBUV(2) column ozone and integrated profile trends are necessarily consistent. Section 3.2.2 shows that SBUV(2) column ozone data agree with total ozone data from the other sources.

Figure 3-13 shows a latitudinal profile of the vertically integrated SAGE I+II ozone changes for 1979-2005 compared with corresponding changes in column ozone,

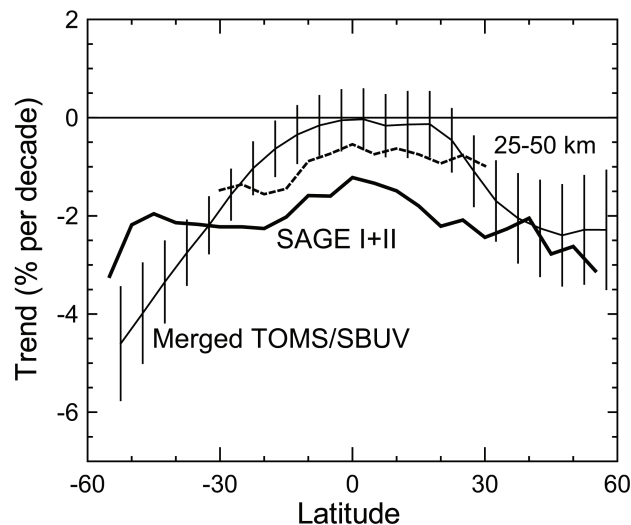


Figure 3-13. Latitudinal profile of ozone trends derived from the vertically integrated SAGE I+II data, compared with results from the merged TOMS/SBUV column ozone dataset. The trends were estimated using regression to an EESC curve and converted to $\%/decade$ using the variation of EESC with time in the 1980s. The SAGE I+II results are a vertical integral of the changes in Figure 3-7, integrated between the tropopause and 50 km. For comparison, the dashed line shows the SAGE results integrated over a limited range of 25-50 km (for 30°N - 30°S). Adapted from Randel and Wu (2006).

derived from the merged satellite ozone data. The SAGE results represent a vertical integral of the profile trends from the tropopause to 50 km. Results from both datasets show reasonable agreement for net ozone decreases over the extratropics. There are significant differences, however, in the magnitude of changes in the tropics, with the integrated SAGE results giving larger changes than the column measurements (which are near zero in the equatorial region). This difference could have several implications. There could be compensating positive trends in tropical tropospheric column ozone, with increases of ~ 6 DU over 1979-2005 ($\sim 15\%$ of background levels). Tropical tropospheric ozone trends for this period are not well known. Lelieveld et al. (2004) have reported substantial increases in near-surface ozone in the tropical Atlantic ocean for 1972-2002, and Bortz et al. (2006) suggest a 20% increase in tropical upper tropospheric ozone during 1994-2003, based on aircraft measurements. On the other hand, Ziemke et al. (2005) suggested that there have not been significant trends in tropical tropospheric ozone for this period based on satellite observations. An alternative explanation of the tropical differences in

GLOBAL OZONE

Figure 3-13 is that the ozone changes derived from SAGE data are simply too large, particularly the lower stratospheric maximum (as discussed above). For comparison, Figure 3-13 also includes the SAGE I+II changes integrated over the limited altitude range of 25-50 km (for 30°N-30°S), and this produces smaller trends that border on the statistical uncertainty levels for the tropical column trends.

3.2.4 Tropospheric Ozone

A recent analysis of long-term changes in tropospheric ozone emphasizes that trends vary regionally and that within a given region, trends have changed over the past 25-35 years (Oltmans et al., 2006). This section updates the discussion in WMO (2003) and focuses on ozonesonde data and surface data at remote, or relatively remote, sites.

Tarasick et al. (2005) showed that tropospheric ozone over Canada (53°-75°N) decreased from 1980 to around 1994 and then increased up to the present, with ozone values in the early 2000s similar to those in the early 1980s. They also found that annual average ozone anomalies in the troposphere at the Canadian sites are correlated with those in the lower stratosphere ($r \sim 0.65$). Ozone over the eastern U.S.A. (Wallops Island) shows relatively small changes from 1970 to the present (<5%), with highest ozone in the late 1980s (Oltmans et al., 2006). An analysis of short-term trends in MOZAIC (Measurements of Ozone and Water Vapor by In-service Airbus Aircraft) aircraft data finds an increase of 12%/decade in the middle troposphere over New York from mid-1994 to 2001; the increase is much larger in winter (20%/decade) than summer (6%/decade). Ozone was particularly high in 1998 and 1999 (Zbinden et al., 2006).

Over Europe, the sonde data from Hohenpeissenberg (the longest self-consistent record) show a steady increase from 1966 to the mid- to late 1980s, followed by a slow decrease and considerable interannual variability. Values in the past few years are similar to those in the early 1980s (Oltmans et al., 2006). Sonde data from Payerne and Uccle show little change in ozone in the mid-troposphere in the last decade. Oltmans et al. (2006) compare mean values for 1995-2004 to those for 1985-1994 for Hohenpeissenberg and the nearby mountain station of Zugspitze (~3000 m). The sonde data show little change except a small decrease in May-July, while the Zugspitze data show a small increase in summer, and a larger increase in winter. Simmonds et al. (2004) report an increase in ozone of 13%/decade in background air at Mace Head (Ireland) from 1987 to 2003, with highest values in 1998 and 1999. The MOZAIC data over Frankfurt and Paris also give an increase in ozone, 7 and

15%/decade, for 1994 to 2001, with the largest trend in winter and spring and almost no trend in summer (Zbinden et al., 2006).

Jonson et al. (2006) recently summarized reports on trends over Europe and noted that the differences between the trends given by sondes, and those from MOZAIC, mountain sites, and Mace Head cannot easily be reconciled. They also note that surface sites within Europe generally show substantial downward trends in high ozone (95th or 98th percentiles) over the past 10-15 years, as well as increases in ozone at polluted surface sites. Both these features are caused by substantial decreases in emissions of ozone precursors in Europe, leading to less ozone formation in summer, and a reduction in titration of ozone by nitric oxide (NO) in winter (e.g., Jonson et al., 2006).

Long-term ozonesonde measurements over Japan (32°-43°N) show an overall increase since 1970, but most of this occurs early in the record, and the last few years show a downturn in ozone (Oltmans et al., 2006). Naja and Akimoto (2004) find that ozone below 3 km in regionally polluted air over Japan increased by 11-22% from the 1970s to the 1990s. The MOZAIC data over Japan give an increase of 8%/decade for 1994-2001, with no trend in summer and an increase of ~10%/decade in other seasons (Zbinden et al., 2006).

In summary, the sonde data for northern midlatitudes for the last decade show increases in ozone over Canada and slight decreases over Europe and Japan. The average trend for the sonde data for 1980 to 2004 is zero (Figure 3-12).

There has been a long-term increase in ozone over Hawaii of $3.5 \pm 1.5\%$ /decade during autumn and winter, in both surface data at 3.4 km and sonde data at 3-6 km, that appears to be related to shifts in transport patterns (Oltmans et al., 2006). There is little change in ozone since 1985 in spring, when transport events from Asia occur.

Indian ozonesonde data demonstrate a statistically significant increase of tropospheric ozone ($43\% \pm 25\%$ per decade at 800-1000 hPa and more than 50% per decade at 200-500 hPa) over Delhi for the period 1972-2001 (Saraf and Beig, 2004). However, Indian sondes have demonstrated large, more than 30%, uncertainties in the troposphere during international ozonesonde intercomparisons (Attmanspacher and Dutsch, 1970; SPARC, 1998) and these trend results should be interpreted with caution.

Analysis of MOZAIC data indicates that that tropical ozone at cruise altitudes (7.7-11.3 km) has increased by ~1 ppb/year, or by ~20%/decade, from 1994 to 2003 (Bortz et al., 2006). This is twice as large as the increase reported for surface ozone over the tropical Atlantic from shipboard data by Lelieveld et al. (2004). Surface and

sonde data up to the mid-troposphere from Samoa (14°S) show a small decrease from the late 1980s to the most recent decade in austral winter, and no change the rest of the year (Oltmans et al., 2006). Unfortunately, the longest tropical sonde record from Natal (Brazil) suffers from changes in sonde types and procedures, as well as data gaps, and the record is not suitable at present for deriving reliable trends.

The Samoa sonde data since 1995 do not show the increase seen in the MOZAIC data for the southern tropics. The MOZAIC data are from South America, the Atlantic, and Africa, while the sonde data are from the Pacific. Ziemke et al. (2005) found no trend in the tropospheric column of ozone derived from TOMS data in the tropics from 1979 to 2003. There appear to be inconsistencies among the various data records for tropospheric ozone.

In southern midlatitudes, ozone at Lauder (45°S) increased from 1986 to present by ~5%/decade below 3 km, with a marginally significant increase of 2%/decade at 3-6 km, and no trend at 6-9 km (Oltmans et al., 2006). Sonde data from the South Pole show a small increase in ozone of 0.5%/decade since 1986 in the mid-troposphere, primarily in spring and summer. No such increase is seen at Syowa (69°S) (Oltmans et al., 2006).

It appears that the short-term trends from MOZAIC data for both the midlatitudes and the tropics may be inconsistent with sonde data, but more analysis is needed.

3.3 SUMMARY OF OTHER OBSERVATIONS

The observed long-term changes in temperature and water vapor are discussed in Chapter 5. In addition, observations of past changes in long-lived source gases and halogen-containing species are discussed in Chapter 1. In this subsection we therefore focus on the remaining parameters that are important for long-term changes in ozone and for which there are relevant data records.

3.3.1 Stratospheric Aerosol and Its Precursors

The source of stratospheric aerosol observed since the late 1970s has been dominated by the injection of sulfur dioxide (SO₂) from a few major volcanic events including El Chichón in 1982 and Mt. Pinatubo in 1991. The inference of a nonvolcanic stratospheric background is hampered by very limited periods without volcanic influence since systematic measurements began; however, the best indications are that there is no long-term trend in the background aerosol level (Deshler et al., 2006). For background periods, observed since the late 1990s, the dominant stratospheric aerosol precursor gases

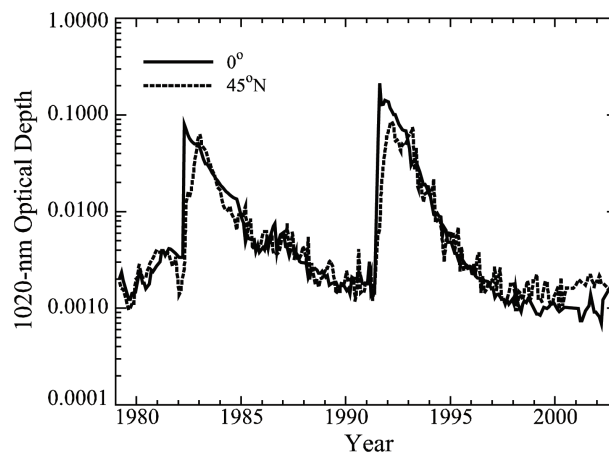


Figure 3-14. The Assessment of Stratospheric Aerosol Particles (ASAP) reconstruction of the tropical (solid line) and northern midlatitude (dotted) 1020-nm aerosol optical depth from 1979 through 2002 based on a combination of SAGE, SAGE II, and ground-based and airborne lidar data. From SPARC, 2006.

are carbonyl sulfide (OCS) and SO₂. Through SO₂, human-related activities may influence the observed background stratospheric aerosol. There is general agreement between measured OCS and modeling of its transformation to sulfate aerosol, and observed aerosols. However, there is a significant dearth of SO₂ measurements, and the role of tropospheric SO₂ in the stratospheric aerosol budget, while significant, remains a matter of some guesswork. In addition, it is not well understood whether global human-derived SO₂ emissions, which are decreasing, or emissions in low latitude developing countries, such as China, which are increasing, dominate the human component of SO₂ transport across the tropical tropopause (e.g., Notholt et al., 2005).

As shown in Figure 3-14, aerosol loading during the past 20 years has varied by as much as 2 orders of magnitude. As a result, the quality of the measurements and the agreement among diverse measure systems varies strongly as a function of the level of aerosol loading. For instance, results from the SPARC *Assessment of Stratospheric Aerosol Properties* (ASAP) (SPARC, 2006) demonstrate that space-based and in situ measurements of aerosol parameters, in particular surface area density (SAD), tend to be consistent following significant volcanic events like El Chichón and Mt. Pinatubo. However, during periods of very low aerosol loading, this consistency breaks down and significant differences exist between systems for inferred parameters like SAD and directly measured parameters like aerosol extinction coefficient (SPARC, 2006). Although integrated aerosol

GLOBAL OZONE

quantities such as surface area density and effective radius can be calculated without approximation from a known size distribution, the satellite and in situ observational bases for size distributions are controlled by a priori assumptions regarding the distribution itself or by having coarse size resolution, respectively. ASAP showed that during volcanically quiescent periods, models and observations disagree significantly mainly because of the modeled fraction of the surface area density that resides in particles too small to be measured, especially near nucleation regions. While there are some model shortcomings relative to observations, particularly in the lower stratosphere, it seems likely that space-based datasets underestimate, perhaps significantly, aerosol surface area density in the lower stratosphere during low loading periods.

In the past, the effect on ozone variability of stratospheric aerosol driven by sporadic volcanic events (primarily the El Chichón and Mt. Pinatubo eruptions) has given concern that it could mimic the effects of the 11-year solar cycle. However, since stratospheric aerosol has remained near nonvolcanic background levels since the late 1990s through much of the recent solar maximum, such concerns have been greatly mitigated (see Section 3.4.4).

3.3.2 Nitrogen Dioxide (NO₂)

Long-term ground-based observations of column NO₂ have been made at Lauder, New Zealand (45°S), since late 1980, by UV/visible observations of sunlight scattered from the zenith. Trends in the observations were discussed in Liley et al. (2000) and WMO (2003). Here the observations and analysis are updated through early 2006. A statistical analysis of geophysical cycles (solar cycle, QBO, El Niño-Southern Oscillation), trends, and volcanic eruptions was done to assess correlations with the observed NO₂. Linear increases of $6.2 \pm 1.8\%$ per decade (am) and $5.7 \pm 1.1\%$ per decade (pm) are inferred. These are not significantly different from those reported in Liley et al. (2000). Figure 3-15 shows the time series for monthly averages of morning and afternoon column NO₂ at Lauder, after subtraction of the seasonal cycle.

NO₂ columns have also been measured at the Jungfraujoch (47°N) since 1985 (Mahieu et al., 2000). The Jungfraujoch measurements are made by Fourier transform spectroscopy (FTS) in solar absorption in the infrared. The monthly averaged vertical column densities from 1985-2005 are also shown in Figure 3-15. Analysis of these data using the same algorithm applied to the Lauder data produces a linear trend of $1.5 \pm 1.0\%$ per decade. The trend reported by Mahieu et al. for 1986-1998 ($7 \pm 3\%$ per decade) may have been significantly affected

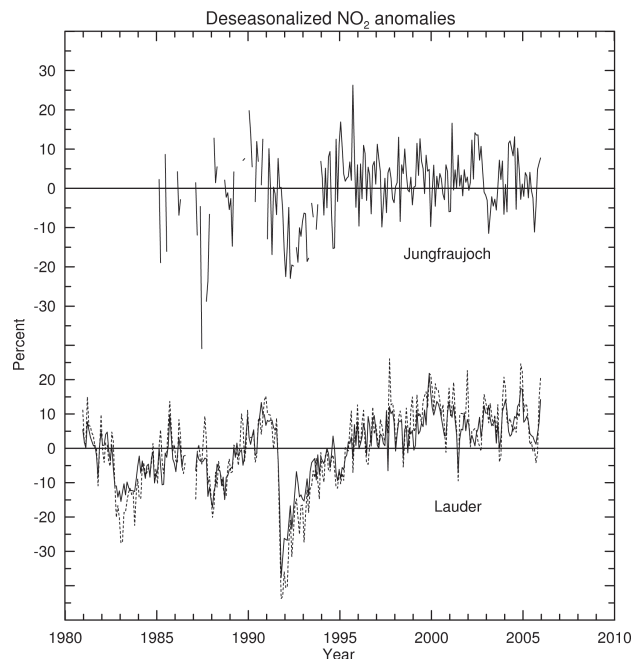


Figure 3-15. Deseasonalized anomalies of the NO₂ slant column measured at two sites, the Jungfraujoch, Switzerland (47°N), and Lauder, New Zealand (45°S). The Jungfraujoch data are measured in direct, solar absorption in the infrared, at a wide range of zenith angles, while the Lauder data are UV/visible absorption of sunlight scattered from the zenith at solar zenith angles of 90°. Sunrise measurements are shown as dashed lines, and sunset measurements as solid lines.

by not explicitly accounting for the effect of the Mt. Pinatubo eruption from 1992-1994. SAGE II satellite observations of profile NO₂ (Cunnold et al., 1991) are consistent with the Lauder data and show that the bulk of the increase occurs in the lower stratosphere. The SAGE II data also show a large hemispheric asymmetry, with no significant trend at Northern Hemisphere midlatitudes.

Thus, the available evidence suggests that the trend of NO₂ in the Southern Hemisphere is significantly larger than that in the Northern Hemisphere. The trend at the Jungfraujoch is consistent with the 2.4%/decade increase in tropospheric N₂O reported in WMO (2003). Other factors may be required to explain the larger increase at Lauder. WMO (2003) concluded that observed nitrous oxide (N₂O) increases and decreases in ozone explained a trend in NO₂ of $5 \pm 1\%$ /decade. The origin of the apparent hemispheric difference in trend remains unexplained, although uncertainties in the analysis due to the relatively short data records should be noted.

3.4 UNDERSTANDING AND INTERPRETATION OF OZONE CHANGES

3.4.1 Models

In order to quantify the effect of certain processes on long-term ozone changes, we need to describe these processes by numerical models. These models can either be “physical” models, which solve the governing equations of the physics/chemistry of the atmosphere, or “statistical” models, in which changes in the long-term ozone time series are linked with forcing terms, typically by multiple regression (see Section 3.2.1).

In this chapter, we use the term “physical model” to describe a numerical model that integrates the relevant equations of the chemistry and dynamics of the atmosphere to predict the evolution of the atmosphere with time. These models are a mathematical representation of our current understanding of the chemistry and physics of the atmosphere. These models can be 0-D (box), 1-D (column), 2-D (latitude-height), or 3-D models. The 3-D models can be classified as “off-line” chemical transport models (CTMs), which are forced by specified winds, or general circulation models (GCMs), which calculate their own winds and temperatures. The components of such models were described in Chapter 4 of WMO (2003). GCMs that contain interactive, detailed chemistry schemes are called coupled Chemistry-Climate Models (CCMs). The various types of models are also described in more detail in Chapter 5 (Box 5-1).

Aside from increased computer power allowing more 3-D simulations, and therefore a better understanding of the performance of these models, a major development in these tools over the past four years for understanding past ozone changes has been the new availability of long-term, whole-stratosphere meteorological reanalyses that can be used to force CTMs.

The European Centre for Medium-range Weather Forecasts (ECMWF) and the National Centers for Environmental Prediction (NCEP) have extended the upper boundary of their operational meteorological analyses to the lower mesosphere (0.1 hPa, more recently 0.01 hPa) and upper stratosphere (1 hPa), respectively. The United Kingdom Met Office (UKMO) has provided meteorological analyses extending to 0.3 hPa since 1991 (Swinbank et al., 2002). The Global Modeling and Assimilation Office (GMAO) of the National Aeronautics and Space Administration (NASA) also produces meteorological analyses for the troposphere and stratosphere. The Goddard Earth Observing System, version 4 (GEOS-4) data assimilation system (Bloom et al., 2005) has an upper

boundary near 80 km (0.01 hPa), with data constraints up to about 55 km. Furthermore, both ECMWF and NCEP have performed 40- and 50-year reanalyses labeled ERA-40 (Simmons et al., 2005; Uppala et al., 2005) and REAN or NCEP-50 (Kanamitsu et al., 2002), respectively. ERA-40 extends to 0.1 hPa, although REAN only extends up to 10 hPa. These reanalyses have been performed with a 3-D variational analysis (3D-VAR), while the operational analyses are performed with the computationally more expensive 4-D variational analysis (4D-VAR), which is regarded as more accurate, due to the re-integration in time.

Some general issues relating to the quality of wind datasets used to force CTMs have been identified. Schoeberl et al. (2003), Strahan and Douglass (2004), and Tan et al. (2004) showed that GMAO and UKMO winds are too dispersive as a result of the assimilation procedure. The procedure causes excessive mixing in the tropical lower stratosphere, forcing large-scale meridional tracer circulation in the stratosphere. The consequence is that the mean residence time of air in the stratosphere becomes too short, which has a negative impact on long-term tracer integrations. Schoeberl et al. (2003) showed that winds from GCMs are much less dispersive and contain a weaker residual circulation, leading to a mean age of air closer to observations.

The ERA-40 reanalyses extend from 1957 to 2001 and, because they cover the whole stratosphere, were expected to provide a much better representation than previous analyses, which extended only up to 10 hPa. Such analyses (e.g., ECMWF ERA-15 reanalyses for the period 1978 to 1993) were used in studies discussed in WMO (2003). These ERA-40 reanalyses have now been quite extensively tested in long-term transport studies and the winds have been applied for ozone integrations. These studies have shown that the reanalyses are a very important resource for diagnosing past ozone changes but, due to some clear problems, some caution is needed in their use. The ERA-40 data has a much stronger circulation than the operational data, due to the less balanced assimilation procedure in 3D-VAR, which has been shown by ozone integrations (Laat et al., 2006). In addition, ERA-40 suffers from inhomogeneity, introduced by the use of spaceborne observations in the data assimilation as well as by changes in the satellite instrumentation. This was illustrated from different diagnoses, e.g., downward ozone fluxes (Van Noije et al., 2004) and water vapor distributions (Bengtsson et al., 2004). They showed significant discontinuities in the strength of the ozone flux at 100 hPa.

Different datasets of assimilated winds and temperature (operational and reanalyses) have been evaluated for the Arctic winter (Manney et al., 2003) and the 2002

Antarctic polar vortex (Manney et al., 2005) by comparisons with observations. The large-scale dynamical structures were well represented in all datasets, but noticeable differences appeared in several diagnoses. The REAN and NCEP show warm biases in the temperatures, while the ERA-40 dataset shows unrealistic spurious temperature oscillations, which were also reported by Simmons et al. (2005). Manney et al. (2005) also show that between the different meteorological datasets, there is little consensus in mixing of vortex air with midlatitudes. Overall, they concluded that caution must be taken when applying a certain assimilated wind dataset, and that the use of some reanalysis data for detailed studies of polar dynamics and chemistry is not recommended. Additional evidence of inhomogeneities in the reanalysis datasets was given by temperature and tropopause height trends analyses (Santer et al., 2004). However, they also concluded that the ERA-40 reanalysis has much improved compared with the earlier ERA-15 and NCEP-50 reanalyses. Birner et al. (2006) also noted the effect of data inhomogeneities on tropopause characteristics. Despite the caveats, the interannual variability of tracers using ERA-40 is simulated quite well (Hadjinicolaou et al., 2005; Feng et al., 2006).

Even when applying the operational 4D-VAR ECMWF data, the large-scale circulation in pressure-coordinate CTMs remains too strong (Meijer et al., 2004; Van Noije et al., 2006). However, there are different approaches to the use of analyzed winds to force an off-line CTM. For example, the use of an isentropic vertical coordinate results in less noisy vertical motion, shown by a reduction of air parcel dispersion in the tropical lower stratosphere and increased mean age of air (Mahowald et al., 2002; Schoeberl et al., 2003; Chipperfield, 2006). Another approach to reducing the noise in the wind data uses forecasts instead of analyses (Meijer et al., 2004; Scheele et al., 2005; Laat et al., 2006). In addition, the use of 3-hourly instead of the usual 6-hourly analyses has been shown to improve stratospheric tracer distribution at northern midlatitudes (Berthet et al., 2005).

Nevertheless, the apparent dispersive character of assimilated winds remains, and it seems inherently connected to the assimilation procedure. In addition, reducing present spurious variability and inhomogeneity as a result of temporal changes in spaceborne instrumentation and inter-instrumental biases is a major challenge for future improvements of reanalyses datasets. Data assimilation for the stratosphere is the subject of ongoing development. Improvements in the 3D-VAR and 4D-VAR assimilation procedures are currently being evaluated (Polavarapu et al., 2005; Monge Sanz et al., 2006), which may lead to improved reanalyses datasets. In the meantime, despite its shortcomings, the ERA-40 dataset is the best descrip-

tion we have of the meteorological state of the stratosphere over the past few decades (Randel et al., 2004). These reanalyses have been used in chemical and dynamical attribution studies discussed below (Sections 3.4.2 and 3.4.5).

3.4.2 Dynamical Processes

As reviewed in Section 4.6 of WMO (2003), changes in two specific dynamical transport processes can significantly influence midlatitude ozone trends. These are:

- (1) interannual and long-term changes in the strength of the stratospheric mean meridional (Brewer-Dobson) circulation, which is responsible for the winter-spring buildup of extratropical ozone (e.g., Fusco and Salby, 1999; Randel et al., 2002; Weber et al., 2003; Salby and Callaghan, 2004; Hood and Soukharev, 2005); and
- (2) changes in tropospheric circulation, particularly changes in the frequency of local nonlinear synoptic wave forcing events, which lead to the formation of extreme ozone minima (“mini-holes”) and associated large increases in tropopause height (Steinbrecht et al., 1998; Hood et al., 1997, 1999, 2001; Reid et al., 2000; Orsolini and Limpasuvan, 2001; Brönnimann and Hood, 2003; Hood and Soukharev, 2005; Koch et al., 2005).

It is therefore important to consider interannual changes in both the Brewer-Dobson circulation and the nonlinear synoptic wave forcing when estimating the component of interannual ozone variability and trends that can be attributed to dynamical transport processes. The bulk of the studies on this subject have looked at the northern midlatitudes, and this is reflected in the following discussion. The lack of published studies for the Southern Hemisphere is partly due to the apparently weaker signal of dynamical changes on ozone trends compared with the Northern Hemisphere.

When the stratospheric polar vortex is strong (positive North Atlantic Oscillation or Arctic Oscillation index), tropospheric wave forcing is weaker, the Brewer-Dobson circulation is weaker, and less ozone is transported to the extratropics in winter and spring. Also, when the polar vortex is strong, the zonal wind field in the midlatitude lower stratosphere is less cyclonic, implying a greater frequency of anticyclonic, poleward wave breaking events that lead to ozone mini-holes and localized tropopause height increases (Peters and Waugh, 1996; Hood et al., 1999; Orsolini and Limpasuvan, 2001). Therefore, at northern midlatitudes in winter-spring, these two dynamical transport mechanisms tend to reinforce one another.

During a period of increasing AO and NAO indices, such as the 1980s and early 1990s (Appenzeller et al., 2000; Hurrell, 1995; Graf et al., 1998; Zhou et al., 2001), a negative dynamically induced contribution to column ozone trends at northern midlatitudes is to be expected. As assessed below, several studies aimed at estimating empirically the contribution to ozone trends at northern midlatitudes due to one or both of the above transport mechanisms have been published during the past four years.

Reinsel et al. (2005) reported a multiple regression analysis of the version 7 TOMS and SBUV/SBUV(2) total ozone dataset over the 1979 to 2002 period. The statistical model included terms proportional to the Eliassen-Palm (EP) planetary wave flux averaged between 30° and 90° latitude in each hemisphere as well as the Arctic/Antarctic Oscillation (AO/AAO) indices. It was found that both dynamical variables had a substantial influence on total ozone at latitudes higher than ~40° in both hemispheres. Evidence was also obtained for a “large positive and significant” change in trend after 1996. The latter result was obtained both with and without the inclusion of dynamical index terms in the regression model. For the Southern Hemisphere, Malanca et al. (2005) found a sizeable, latitude-dependent slowdown in the ozone loss from the early 1990s, with significant longitudinal variations in the size of the change in trends. Although the zonal mean behavior is strongly linked to variations in chemical loss in the Antarctic vortex, the longitudinal asymmetry is due to dynamical influences.

Inclusion of AO/AAO or NAO indices alone in a regression model does not necessarily account completely for ozone variability associated with synoptic wave forcing. Also, the EP flux is more a measure of the ozone tendency associated with changes in the Brewer-Dobson circulation (e.g., Fusco and Salby, 1999; Randel et al., 2002) than of ozone itself. So this statistical analysis could not definitively determine whether or not the change in trend after 1996 was caused by dynamical transport contributions. Nevertheless, the statistical evidence for a change in trend after 1996 is not affected by these issues. A similar statistical analysis of total ozone from ground-based observations in Europe by Krzyścin et al. (2005) has also concluded that a positive change in ozone trend in this region has occurred since 1994.

Continuing the earlier work of Fusco and Salby (1999), Salby and Callaghan (2002, 2004) showed that total ozone interannual variability and trends in the Northern Hemisphere are both characterized by an out-of-phase relationship between low latitudes and high latitudes. This relationship is consistent with that expected from changes in the Brewer-Dobson circulation. It was therefore argued that a “systematic weakening” of the

latter transport influence was responsible for a major portion of the ozone decline between the 1980s and 1990s. Randel et al. (2002) also used correlative and regression relationships to estimate more specifically that net decreases in strength of the Brewer-Dobson circulation may have caused 20% to 30% of the column ozone trend at northern midlatitudes over the 1979 to 2000 period.

The importance of nonlinear synoptic wave forcing for ozone interannual variability and trends at northern midlatitudes has been indicated by several recent studies. Wohltmann et al. (2005) analyzed total ozone variability measured at European ground-based Dobson stations using a multiple regression statistical model that included an explanatory variable based on the equivalent latitude (i.e., potential vorticity or PV) profile at a given station. Their technique takes advantage of the near conservation of both ozone and PV on isentropic surfaces on a time scale less than a few weeks in order to transform the PV profile into a synthetic ozone profile using an ozone climatology. The resulting synthetic ozone column is then used as the explanatory variable. It accounts for both vertical lifting (sinking) of isentropes by tropospheric pressure systems and for horizontal isentropic advection of ozone. It was concluded that 30% to 50% of the observed long-term trend over Europe during the 1970 to 2002 period was attributable to long-term changes in tropospheric pressure systems. The latter consist primarily of increases in the number and amplitudes of anticyclonic systems associated with poleward planetary and synoptic wave events (e.g., Hood et al., 1999). Consistent with their results, Brönnimann and Hood (2003) analyzed historical data to show that low-ozone events over northwestern Europe in winter were much more frequent in 1990-2000 than in 1952-1963 and that changing atmospheric circulation strongly contributed to the observed increase in frequency. In an analysis of balloonborne ozonesonde data at several Canadian stations, Tarasick et al. (2005) report evidence for a positive change in ozone trends at all levels below 63 hPa after about 1993. Interannual variability was found to correlate well with the wintertime frequency of laminae in the ozone profile (defined here as a thin layer bounded by sudden changes in the ozone profile of at least 20 hPa), which represent southward excursions of ozone-rich Arctic, or polar vortex, air. It was suggested that much of the positive change in trends after the early 1990s could result from changes in circulation, since both the laminae time series and the ozone time series show a similar change in trend (see also Krizan and Lastovicka, 2005).

As also reviewed in the previous Assessment (Section 4.6.3.3 of WMO, 2003), it may be reasonably questioned whether the separate influences of the Brewer-Dobson circulation and tropospheric synoptic wave

GLOBAL OZONE

forcing on zonal mean ozone trends at a given latitude can simply be added together, because these two dynamical processes may not be entirely independent of one another. For example, tropospheric planetary-scale waves that are dominantly responsible for driving the Brewer-Dobson circulation are also associated with synoptic wave events and local tropopause height changes.

Hood and Soukharev (2005) used correlative and regression methods to estimate separately and in combination the portion of ozone interannual variability and trends over the 1979 to 2002 period that can be attributed to long-term changes in both the Brewer-Dobson circulation and nonlinear synoptic wave forcing. In approximate agreement with Randel et al. (2002), it was estimated that 18% to 25% of the observed maximum negative trend in February and March is due to long-term changes in the Brewer-Dobson circulation. In addition, 27% to 31% of the observed maximum midlatitude trend was estimated to be caused by synoptic wave forcing. No significant correlations were found between monthly mean EP flux variations (representing changes in Brewer-Dobson circulation strength) and monthly mean PV variations (representing changes in synoptic wave forcing) at northern midlatitudes. A significantly higher correlation, up to 0.7, was obtained using both the time-integrated EP flux and zonal mean PV as predictor variables than using either predictor variable alone. This indicates that contributions to total ozone variability from these processes are, at least to first order, independent and summable at northern midlatitudes. Together, these transport components could explain almost 50% of the observed interannual variance and maximum negative trend at northern midlatitudes in February and March (Figure 3-16). The empirical regression model was able to simulate approximately the leveling off and slight increase in column ozone anomalies that have been observed for some months and latitudes since the middle 1990s (Figure 3-16). Furthermore, Brönnimann et al. (2004a, b) provided evidence for dynamic coupling of strong and long-lasting El Niño-Southern Oscillation events with stratospheric ozone in the NH by analyzing the record high total ozone values observed in northern midlatitudes in the early 1940s.

Changes in dynamical processes also affect the polar vortex conditions and, as a result, polar ozone loss. The midlatitude ozone is influenced by polar loss via air-mass mixing after the polar vortex breakup in early spring, as discussed in Section 3.4.3.2. Using regression analysis, Dhomse et al. (2006) concluded that this mechanism is one of the main factors responsible for the recent increase in NH total ozone.

Finally, estimates of the dynamically induced contributions to ozone interannual variability and trends can

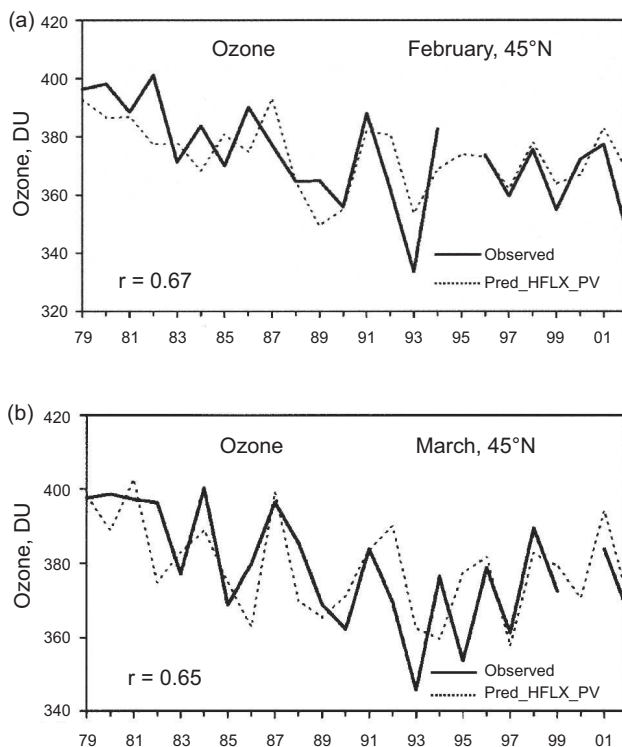


Figure 3-16. (a) Comparison of observed and empirically estimated column ozone at 45°N for February when both 350 K PV and EP flux, averaged over the 40°N to 70°N latitude band and integrated over January and February, are considered as predictor variables in the empirical model. (b) As in (a) but for March. In this case, EP flux is integrated over the January to March period. From Hood and Soukharev (2005).

be derived by using CTMs driven by observed temperature and wind fields (Hadjinicolaou et al., 1997, 2002, 2005). Most recently, Hadjinicolaou et al. (2005) have reported further integrations of the SLIMCAT 3-D chemical transport model with a parameterized ozone tracer and using the ECMWF ERA-40 meteorological analyses for 1979-2002. They find that the model simulates a large part of the observed ozone changes at northern midlatitudes (represented by the merged satellite dataset (see the Appendix 3A.1) averaged over the 35°N to 60°N latitude range), including the positive tendency after the mid-1990s. A linear regression analysis indicated that about one-third of the observed ozone trend from 1979 to 1993 at these latitudes and, within uncertainties, all of the positive trend thereafter could be explained by the model, which includes only transport-related changes. They argue that these changes are consistent with the changes in the Brewer-Dobson circulation in the observed positive tendency after the mid-1990s, but emphasized that this trans-

port process alone is unlikely to explain the relatively large change in slope of the ozone trend (modeled and observed) and that synoptic wave forcing may contribute significantly. Results from this study are included with full chemistry CTM studies, which also quantify the important role for halogen forcing, in the discussion of assessment models (Section 3.4.5 below).

The direct effects of dynamical factors on ozone described above are mainly limited to winter and spring. Through the summer season the total ozone changes from month to month are mainly controlled by nitrogen oxides (NO_x) abundance and photochemistry (Brühl et al., 1998). While the photochemical lifetime does not vary from year to year (e.g., Randel et al., 2002), the initial conditions for summertime ozone vary and depend on the winter-spring ozone abundance. As a result, ozone anomalies observed in late summer and early autumn are highly correlated with winter-spring anomalies (Fioletov and Shepherd, 2003; Dhomse et al., 2006). This suggests that summertime ozone is also indirectly influenced by dynamical processes in the preceding winter-spring.

In summary, both empirical and model studies using observed circulation changes continue to indicate that a major fraction (almost 50% in February-March) of the observed column ozone trends at northern midlatitudes from 1979 to the mid-1990s can be attributed to long-term changes in lower stratospheric circulation. Such circulation changes may also have been responsible, at least in part, for the increase that has been observed at these latitudes since the mid-1990s. The primary dynamical transport processes are (1) interannual and long-term changes in the strength of the mean meridional (Brewer-Dobson) circulation and (2) interannual and long-term changes in nonlinear synoptic wave forcing. Contributions from these two forcings appear to be comparable in amplitude and are, at least to first order, independent of one another. Zonal mean ozone decreases at northern midlatitudes in winter-spring caused by both forcings are larger when the tropospheric AO/NAO circulation indices are positive. The causes of the observed long-term trends in lower stratospheric circulation (including trends in the AO/NAO indices) are unclear. This question can be answered ultimately only with the aid of GCMs. Such models have so far indicated that it is unlikely that radiative changes from chemically induced ozone losses are responsible (e.g., Langematz et al., 2003). Remaining possibilities include long-term natural climate variability and greenhouse-gas-induced climate change.

3.4.3 Chemical Processes

3.4.3.1 UPDATE OF RELEVANT KINETICS

Based on the Jet Propulsion Laboratory (JPL) 2002 recommendation (Sander et al., 2003), updates to stratospheric reaction kinetics since the previous Assessment have generally been minor. No major new reaction pathways or rate changes have been uncovered since WMO (2003), which relied primarily on the *JPL 2000* evaluation (Sander et al., 2000). Several open issues from the previous Assessment have been resolved and some relatively minor updates are discussed here. Note that here we do not discuss any results from the very recent *JPL 2006* recommendation (Sander et al., 2006), which appeared after this Assessment was finalized.

Gas Phase

The *JPL 2002* recommendation (Sander et al., 2003) highlights several noteworthy changes from the previous stratospheric evaluation. Rates of some hydrocarbon reactions in the upper troposphere are considered, although their effect on the lower stratosphere is probably small. Reactions with hydroxyl radical (OH) and photolysis cross sections and quantum yields have been updated and added for numerous halocarbons. These will affect halocarbon lifetimes to some degree but do not have a major impact on stratospheric ozone.

Progress has been made in resolving several kinetics issues that were raised in WMO (2003). Regarding the product pernitrous acid (HOONO) in the reaction $\text{OH} + \text{NO}_2 + \text{M}$, *JPL 2002* recommends neglecting this channel in stratospheric models. The $\text{OH} + \text{ClO} \rightarrow \text{HCl}$ product channel has increased from 5 to 7% at 298 K in *JPL 2002*, and the $\text{HO}_2 + \text{ClO}$ updates discussed in WMO (2003) are included in *JPL 2002*, however, the impacts of these changes in models have not been published specifically. Peroxynitric acid (HO_2NO_2) overtone photolysis has been tested in comparison with aircraft and balloon data by Salawitch et al. (2002) and in a global model by Evans et al. (2003). This process significantly changes the model abundance of HO_2NO_2 globally and odd hydrogen (HO_x) particularly near sunrise/sunset, and improves comparison with observations. The maximum change of O_3 in the lower stratosphere is 1-2%. This process is not included in *JPL 2002*. Data on HO_x reactions with O_3 discussed in WMO (2003) are now included in *JPL 2002*, which is consistent with atmospheric measurements of OH/ HO_x .

GLOBAL OZONE

More recently, the reaction $\text{NO} + \text{HO}_2 \rightarrow \text{OH} + \text{NO}_2$ (a) has been found to have a second channel at low temperatures: $\text{NO} + \text{HO}_2 \rightarrow \text{HNO}_3$ (b), branching ratio (k_b/k_a) = 0.18 (298 K) and 0.87 (223 K) (Butkovskaya et al., 2005). Inclusion of this product channel will produce a HO_x sink in the upper troposphere and decrease NO_x/HNO_3 partitioning in the lower stratosphere, perhaps by as much as 10-15%. Global impacts have yet to be tested in models.

Low-temperature oxidation rates for several hydrocarbon species have been updated, including: $\text{CH}_3\text{CHO} + \text{OH} \rightarrow \text{CH}_3\text{CO} + \text{H}_2\text{O}$ (Sivakumaran and Crowley, 2003), $\text{H}_2\text{CO} + \text{OH}$ (Sivakumaran et al., 2003), and $\text{CH}_3\text{OH} + \text{OH} \rightarrow \text{products}$ (Dillon et al., 2005). These changes will affect upper troposphere calculations but are not expected to have a significant impact on stratospheric chemistry.

The assessment models discussed in Section 3.4.5 use an updated version of the *JPL 2002* kinetics. No significant differences from simulations using the standard *JPL 2002* are found.

Heterogeneous Chemistry

JPL 2002 provides updates to several heterogeneous processes, with particular focus on liquid binary $\text{H}_2\text{SO}_4 \cdot \text{H}_2\text{O}$ uptake, i.e., $\text{HOCl} + \text{HBr}$, $\text{HO}_2\text{NO}_2 + \text{HCl}$, and α (HOI), as well as $\text{HCl} + \text{HNO}_3$ on liquid ternary solution. None of these updates is expected to have a significant impact on global ozone, although a specific test has not been published.

Recent laboratory experiments yielded new information regarding uptake of gases on ice surfaces under atmospheric conditions corresponding to the upper troposphere/lower stratosphere (UT/LS). So far the knowledge of gas uptake on ice particles was primarily based on clouds in cold polar stratospheric conditions and no information was available for competitive and reactive uptake. Hynes et al. (2002) and Cox et al. (2005) found that the uptake of HCl was suppressed when HNO_3 was present on the ice surface at temperatures higher than 208 K (Hynes et al.) or 218 K (Cox et al.). Hence for temperatures greater than 208 K, there is a tendency to reduce uptake of hydrochloric acid (HCl) when competitive uptake is considered, which will reduce the potential for chlorine activation on cirrus clouds. Fernandez et al. (2005) found significant uptake of chlorine nitrate (ClONO_2) on pure and doped (HNO_3 , HCl) ice surfaces. No model study has included this information to estimate the effect of heterogeneous chemistry on aerosol and ice particles on ozone.

3.4.3.2 LOWER STRATOSPHERE

The major chemical processes expected to contribute to global ozone depletion were reviewed in previous Assessments (e.g., WMO 2003). There have been no significant changes to the understanding of these processes, although studies have provided new quantification. There have been relatively minor refinements in chemical rate constants and uncertainties (Section 3.4.3.1) but no major changes in our understanding of chemical processes. However, some new observations, related to likely minor processes of cirrus activation and pyroconvection, are discussed here. Then we discuss recent findings related to the more established and important process of aerosol chemistry, the role of bromine in the lower stratosphere, and export from the polar vortex.

Cirrus (Including Subvisible Cirrus)

In addition to the observed cirrus climatologies in the tropopause region reported earlier (see WMO, 2003), there is new observational evidence of thin cirrus clouds in the cold tropical (Peter et al., 2003) and midlatitude tropopause region (Ström et al., 2003; Keckhut et al., 2005a). Supporting these findings, there is further observational evidence of supersaturation with respect to ice in the same altitude range (Ovarlez et al., 2002; Spichtinger et al., 2004), though it is likely that the thin “ice” clouds consist of nitric acid trihydrate (NAT) (Popp et al., 2006). Gao et al. (2004) found observational evidence for a new HNO_3 -containing ice particle (delta-ice). However, the laboratory results from Delval and Rossi (2005) do not support the Gao et al. findings and suggest that small NAT particles, even H_2O -rich, can survive much longer in a subsaturated atmosphere than previously thought.

Following the first observations of possible chlorine activation in the lowermost stratosphere (Keim et al., 1996; Borrmann et al., 1997), Solomon et al. (1997) showed that these findings could lead to significant chemical ozone loss in the midlatitude lowermost stratosphere, but Bregman et al. (2002) calculated considerably less loss (see WMO, 2003). More recent observations by Thornton et al. (2003) showed much more in-situ observational evidence of chlorine monoxide (ClO) of several tens of parts per trillion by volume (pptv) in the lowermost stratosphere in the northern extratropics. The observed mixing ratios are significantly higher than can be explained by background gas-phase and heterogeneous chemistry on aerosols (Thornton et al., 2005). The observations were primarily performed during wintertime in the Northern Hemisphere and the enhancements were found between 55°N - 70°N . These observed levels of ClO were in very

close agreement with those calculated by Bregman et al. (2002), although no evaluation could be made regarding the temporal and spatial distribution of the ClO enhancements. However, the modeled bromine monoxide (BrO) levels in Bregman et al. were 2-4 pptv, which is a factor of two too small, according to recent estimates from Salawitch et al. (2005), implying that the calculated ozone loss is likely too small; consequently, this process may need further study.

The chemical composition of the ice cloud particles is important for their potential to activate halogens. In the tropical tropopause region there is ongoing discussion about the existence and occurrence frequency of the HNO₃-containing particles (Gao et al., 2004; Popp et al., 2006; Delval and Rossi., 2005).

Pyroconvection

It is well known that the presence of enhanced aerosols in the stratosphere can cause significant chemical ozone loss through heterogeneous chemical reactions, as demonstrated by many studies of the impact of the eruption of Mt. Pinatubo (see WMO, 2003). Apart from volcanic eruptions, a recently identified process, pyroconvection, may also cause enhanced stratospheric aerosol concentrations. Pyroconvection is induced by boreal fires or biomass burning, likely in combination with strong convective activity (Fromm and Servranckx, 2003; Jost et al., 2004; Fromm et al., 2005). The aerosol enhancements have been found in the lower stratosphere over all longitudes in the northern mid- and high latitudes. The particles likely consist of soot and smoke (Fromm and Servranckx, 2003).

Blumenstock et al. (2006) observed chlorine activation in the lower stratosphere in late Arctic winter under conditions well above the NAT temperatures. This was attributed to heterogeneous chemistry on an enhanced aerosol plume, originating from forest fires and injected by strong convection, as described in Gerding et al. (2003).

Ray et al. (2004) and Jost et al. (2004) attribute enhanced carbon monoxide (CO) and aerosol observed by aircraft measurements in the subtropical stratosphere to pyroconvection. Livesey et al. (2004) found enhanced acetonitrile (CH₃CN) in stratospheric data from the spaceborne Microwave Limb Sounder (MLS), associated with forest fires and thunderstorm lofting. Injection of aerosol and other fire-produced chemical species will affect ozone locally.

The occurrence frequency of pyroconvection remains an open issue, as does a quantification of its impact on ozone. However, given the impact of other established processes included in models that can gener-

ally reproduce past ozone changes, we can surmise that any effect will be relatively small.

Aerosol Effects

Sulfate aerosol in the lower stratosphere provides surfaces for the activation of chlorine. The distribution of sulfate surface area depends on background sulfur emissions and volcanic eruptions. The atmosphere is currently (since about 1999) near a background minimum (Section 3.3.1) and this sets the minimum for the nonvolcanic aerosol loading. Thus, the Mt. Pinatubo-to-present period gives a good span of potential heterogeneous effects, barring a huge future volcanic eruption. The reactions, as reviewed in previous Assessments, do not suggest significant missing processes or inaccurate rates. Sulfate surface area in models can be, and usually is, specified from observations for past-to-present runs.

A large chemical effect from volcanoes has been quantified in 2-D models (e.g., Tie et al., 1994; WMO 2003, Section 4.5.3.4) and 3-D models (e.g., Chipperfield, 1999; 2003; Stolarski et al., 2006). The volcanic effect on column ozone results from heterogeneous suppression of NO_x, via N₂O₅ + H₂O(l), which then interferes less with the halogen and HO_x ozone loss cycles in the lower stratosphere. Thus, chemical ozone losses from volcanic sulfate injection are largest at times of peak chlorine and bromine, and volcanic impact on ozone at preindustrial halogen levels is small or even positive (Tie and Brasseur, 1995).

Dynamical changes resulting from the Mt. Pinatubo eruption also contribute to ozone change and are present in meteorological analyses (Hadjinicolaou et al., 2005; see Sections 3.4.2, 3.4.5). An outstanding puzzle is the lack of a Pinatubo effect on observed ozone in the SH while the effect on NO₂ there is clear. Models all show a SH effect as large, or larger than, the NH effect. Stolarski et al. (2006) show that much of this apparent hemispheric discrepancy may be the result of interannual variability masking the volcanic effect in the ozone time series analysis.

Inorganic Bromine

A variety of observations have shown that that inorganic bromine in the stratosphere is underestimated when based on release from methyl bromide (CH₃Br), halons, and other long-lived source gases (see Chapter 2), as is usually assumed in global models. Although full resolution of this issue awaits further study (Sinnhuber et al., 2005), the potential impact of increased background stratospheric Br on O₃ loss is significant (Salawitch et al.,

GLOBAL OZONE

2005). Assuming the purported additional Br is of biogenic origin, and thus is constant with time, it contributes slightly to the O₃ column change from 1979 to present through reaction with Cl at low background aerosol amounts. The effect of the additional Br is large, however, during periods of volcanically enhanced stratospheric aerosol following El Chichón and Mt. Pinatubo (see Figures 3-14 and 3-25). Ozone loss via the BrO + ClO catalytic cycle is enhanced by a factor of two or more by the additional Br during periods of relatively high Cl resulting from heterogeneous reactions on volcanic sulfate. This enhancement generally improves the global model simulation of decadal O₃ change in comparison to observations (Chapter 2 Figure 2-12; see also 3-D results in Figure 3-25 below). This potential additional source of stratospheric Br is important to resolve and characterize because it will impact O₃ future projections as Cl decreases and if the Br source and/or transport processes change with climate.

Export from Vortex

The export of ozone-depleted or activated polar vortex air may have a significant contribution to observed ozone loss at midlatitudes in spring-summer. This effect exists in both hemispheres but is expected to be larger in the Southern Hemisphere due to the larger and more regular ozone depletion in the Antarctic vortex. Although transport is clearly involved in this process, the ultimate cause is chemical O₃ loss in the polar regions by Cl and Br species (see Chapter 4). Figure 3-17 shows that the mass of “missing” ozone in the ozone hole has the same order of magnitude as the mass deficit over southern middle and high latitudes in summer, and illustrates the strong correlation between loss in the ozone hole and in summer.

Konopka et al. (2003) investigated the fate of Arctic vortex remnants, and the chemistry occurring in those remnants, during the spring of 1997 and 2000 using a Lagrangian CTM. They found a different behavior in the lower and in the mid-stratosphere. Above 20 km, vortex remnants (Orsolini, 2001) remain long-lived in the summer westward circulation. Using balloonborne in-situ measurements of water vapor and methane, Durry and Hauchecorne (2005) indeed found evidence for such vortex remnants in the midlatitude summer stratosphere. Below 20 km, the subtropical jet bounds the meridional propagation of those remnants (Piani et al., 2002), and the remnants' lifetime is considerably reduced due to enhanced stirring by synoptic eddies. This picture is corroborated by satellite measurements of the breakup of the Antarctic polar vortex in 2004. Manney et al. (2005)

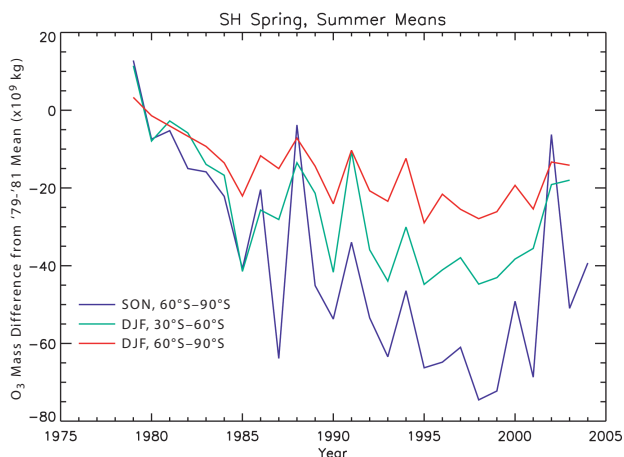


Figure 3-17. The change in mean ozone mass from the average of 1979-1981 over southern polar latitudes in spring (September-November; blue curve) and summer (December-February; red curve) compared with that over southern midlatitudes in summer (green curve). Derived from the NIWA Assimilated Dataset (see Appendix 3A).

reported that vortex remnants persisted in tracer measurements for over a month in the mid-stratosphere, but no more than a week in the lower stratosphere.

Seasonal model studies have been conducted to quantify the impact of the export of polar air on midlatitudes in particular years. Knudsen and Grooß (2000) found that about 40% of the observed midlatitude depletion in May 1995 and 1997 is due to dilution with polar-processed air. Including all years with large Arctic ozone depletion (1993, 1995, 1996, 1997, and 2000) Andersen and Knudsen (2002) found that the dilution explains 33% of the 1979-2002 midlatitude trend in the April-May period. The dilution has a tendency to occur mainly over the Eurasian continent, which helps to explain why ozone trends are larger over this region (Knudsen and Andersen, 2001). Using a high resolution CTM, Marchand et al. (2003) estimated that the dilution of polar vortex air during the cold winter 1999-2000 contributed up to 50% of ozone depletion at northern midlatitudes (45°-55°N) over the period from December 10 to April 30. Millard et al. (2003) studied the connection between polar and midlatitude ozone loss with a series of seasonal 3-D CTM simulations. During years 1994 to 2000, they found a large interannual variability (from -25 DU to almost 0) in the contribution of polar vortex air (90°-70°N) to midlatitude (60°-30°N) ozone loss from December 1 to May 31.

For the Southern Hemisphere, Ajtić et al. (2004) quantified the seasonal dilution effect of the Antarctic ozone hole by calculating ensemble diabatic trajectories

of ozone-depleted air parcels from October 15 to January 15 for a series of years. The mean calculated ozone reduction in 1998, 1999, and 2000 was 16-19 DU (5-6% of total column) between 30°S-60°S. This is 83-95% of the change observed by TOMS between 1979-1980 and 1998-2000. Part of this overestimate is due to the fact that photochemistry was not included. Based on Prather et al. (1990), who suggested there would be 20-30% production during this period, the dilution may therefore account for 58-76% of the summertime ozone depletion at southern midlatitudes

Multiannual model studies have been performed to investigate the accumulated effect of polar processing on midlatitudes. Hadjinicolaou and Pyle (2004) investigated the dilution of polar ozone loss in the 1990s using a decadal 3-D CTM run with parameterized ozone. They found a large interannual variability in the north related to winter-spring planetary wave activity and calculated a year-round midlatitude depletion of about 1% between 40°N-60°N,

compared with 2-4% in the south. Chipperfield (2003) used a full chemistry 3-D CTM for 1979-1995 and reported that for the overall modeled decrease of midlatitude ozone due to halogens, about 30% (NH) to 50% (SH) of the change is caused by ozone loss within the polar vortex.

Once the vortex breaks down, ozone is rapidly mixed throughout the extratropics, which makes summertime year-to-year ozone variations outside the tropics homogeneous in latitude. This holds for both short-term variations and long-term trends (Fioletov and Shepherd, 2005). Figure 3-18 (top) shows that the magnitudes of the summertime trends over middle and polar latitudes are nearly identical, while the corresponding springtime trends are quite different. Polar ozone depletion and export of depleted air from the vortex thus affects the seasonal structure of midlatitude ozone trends, and thereby accounts for the different seasonality of the midlatitude trends in the two hemispheres. Over 35°-60°N, the long-

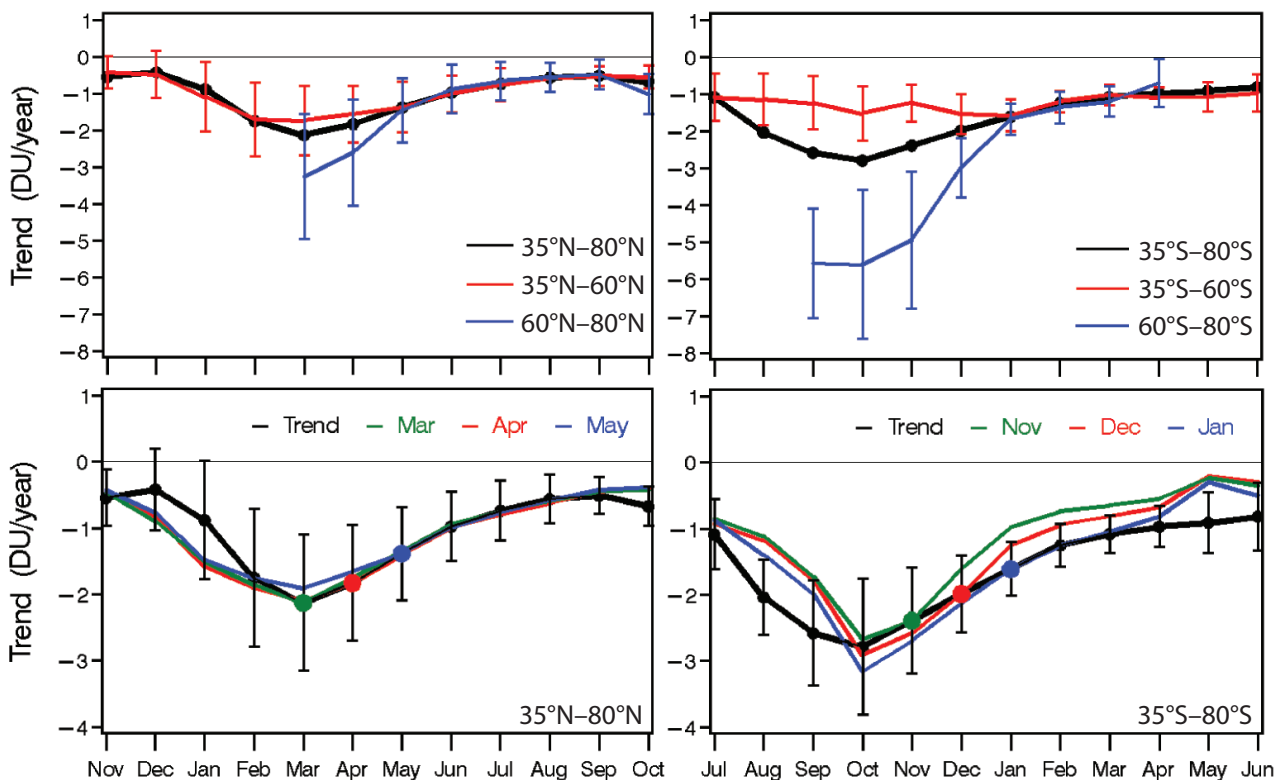


Figure 3-18. Top: The observed total ozone trends for 35°-60° (red), 60°-80° (blue), and 35°-80° (black) latitudinal belts for the Northern Hemisphere (left) and Southern Hemisphere (right). Bottom: The observed ozone trends for 35°-80°N and S (black line), and the trends estimated from the March, April, and May trends for the NH (November, December, and January trends for the SH) and regression coefficients estimated from detrended data. The trends were estimated for the period 1979-2003 using regression to an EESC curve and converted to DU/year using the variation of EESC with time in the 1980s. The error bars represent the 95% confidence intervals. From Fioletov and Shepherd (2005).

GLOBAL OZONE

term trends are in line with interannual variability, with a maximum in spring and a minimum in autumn. In particular, the trend magnitudes from late spring through to early autumn are related to the trend in April in the same way that the corresponding monthly ozone anomalies are related to the April anomaly in the detrended data (Fioletov and Shepherd, 2003). In contrast, the summer ozone long-term decline over 35°-60°S is stronger than one would expect purely from photochemical decay of the spring trend there, and is in fact of comparable magnitude to the spring trend. However for the entire 35°-80° belt, the long-term trends in SH ozone have a clear seasonal structure and are in line with interannual variability, as shown in Figure 3-18 (bottom). The implication is that the near constancy of the SH midlatitude trends throughout the year, in striking contrast to the behavior in the NH, reflects the much greater influence of polar processes in the SH compared with the NH. Indeed, Fioletov and Shepherd (2005) estimated from total ozone observations that about 39% of the observed southern midlatitude long-term ozone decline in December can be attributed to the polar ozone depletion achieved up to November. In the Northern Hemisphere, the corresponding contribution is about 15%, but the statistical uncertainty is too large to make an accurate estimate.

3.4.3.3 UPPER STRATOSPHERE

There have been no changes in our understanding that ozone trends in the upper stratosphere (around 40 km) are caused by changes in chlorine acting through the ClO + O cycle. The chemistry of the upper stratosphere will be affected by the trend in temperature (Chapter 5) and the partitioning of ClO and HCl, which will affect loss via the ClO + O cycle, will also be affected by changes in methane (CH₄) (Chapter 1). Trends in these quantities also need to be observed and compared with models for a rigorous test of our understanding. Overall, our understanding, as expressed in current models, is qualitatively consistent with observations, though as discussed in Section 3.4.5, there appears to be quantitative discrepancies in the simultaneous modeling of all relevant trends. This, however, should be considered as a problem for these models to simulate realistically the distribution of the precursors and species that control ozone, rather than a measure of uncertainty in the upper stratosphere chemical processes for which we have a good understanding (e.g., WMO, 1999). Chapter 6 (Section 6.5.1) summarizes observations of recent changes in ozone in the upper stratosphere, in the context of EESC levels, and discusses the implications for recovery from halogen-induced loss.

3.4.4 Solar Cycle Variations

A decadal variation of total column ozone is observed to be in phase with the solar cycle, with an amplitude of 2-3% from solar minimum to maximum in the tropics (Figure 3-4) and over the 60°S-60°N band (Figure 3-1). The detailed vertical structure of the ozone variation is still a topic of current research (for a review, see Hood, 2004) but, despite some uncertainty due to the limited record length (see discussion below), this decadal variation appears to be a dominant form of long-term ozone variability and should be carefully considered when evaluating anthropogenic trends at all latitudes and altitudes (Steinbrecht et al., 2004a, b; Cunnold et al., 2004).

The stratospheric ozone response to 11-year solar forcing has been estimated as a function of altitude, latitude, and season by a number of analysts based mainly on long-term, near-global satellite remote sensing datasets (Chandra and McPeters, 1994; McCormack and Hood, 1996; McCormack et al., 1997; Hood, 1997; Wang et al., 1996; Lee and Smith, 2003; Soukharev and Hood, 2006). Figure 3-19 compares the annually averaged solar cycle response derived from two long-term satellite ozone profile datasets (SBUV and SAGE) with the predictions of four models that account for observed 11-year changes in solar ultraviolet spectral irradiance. The observed ozone change from solar minimum to maximum is estimated using a multiple regression statistical model containing QBO, volcanic aerosol, solar cycle, and linear trend explanatory variables as well as a first-order autoregressive term. Figure 3-19a presents the signal in ozone averaged over the 55°S-55°N band (essentially the whole region covered by the satellites), while Figure 3-19b shows only the tropical response (25°S-25°N). The satellite datasets used are SBUV(/2) version 8 from 1979-2003 (Frith et al., 2004; updated from Hood, 2004) and SAGE I+II version 6.20 from 1979 to 2005, excluding several years after the Mt. Pinatubo eruption (updated from Stolarski and Randel, 1998). Analyses of SAGE II and UARS HALOE data (Soukharev and Hood, 2006), as well as comparisons between SBUV and TOMS data (e.g., Hood, 1997), suggest that most or all of the apparent total ozone solar cycle variation originates primarily in the lower stratosphere. Thus the observed variation in the ozone column of 2-3% (as discussed above) can be taken to represent the integrated values below about 25 km and 30 km for the 55°S-55°N and 25°S-25°N bands.

The theoretical curves in Figure 3-19 include results from two 2-D radiative-chemical transport models (Brasseur, 1993; Haigh, 1994) and two fully interactive, 3-D Chemistry-Climate Models (Tourpali et al., 2003; Egorova et al., 2004). Although the models have very dif-

ferent dynamical formulations, their predictions for the ozone solar response in the low-to-middle stratosphere (15-35 km) are very similar, and also representative of the results from other published modeling studies. In the upper stratosphere the model predictions diverge, probably due to their different representations of photochemical processes in the mesosphere.

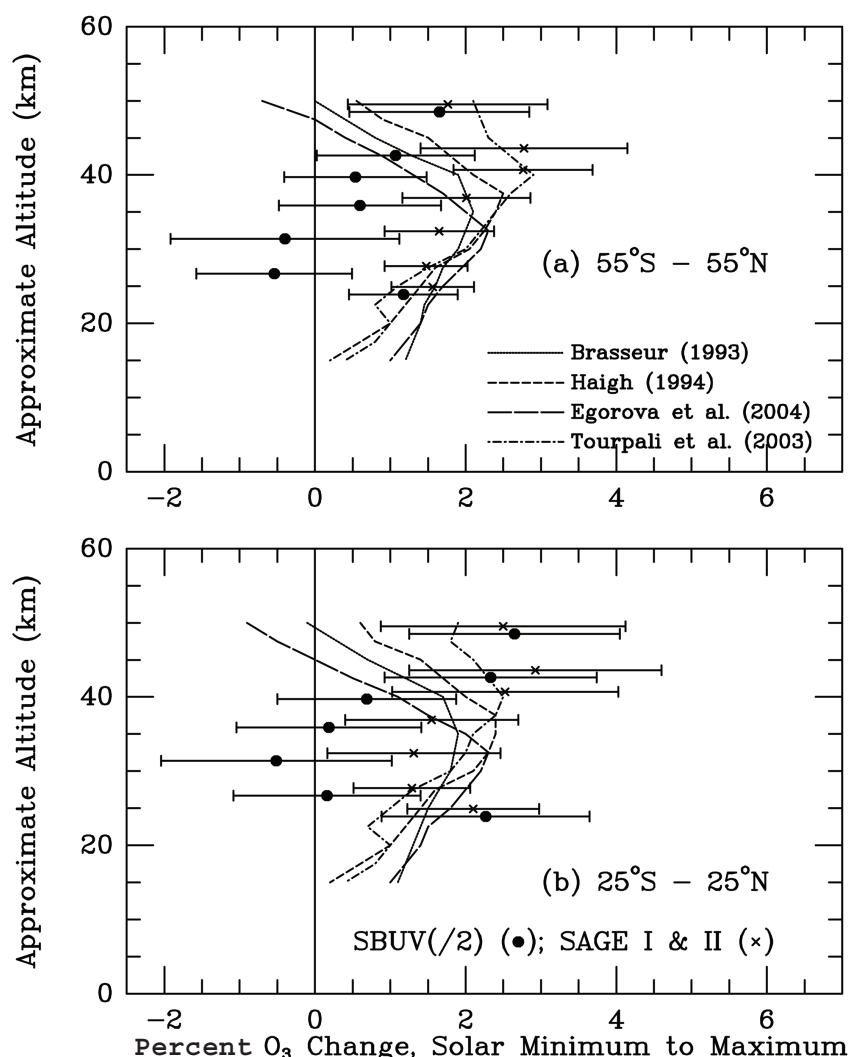
Over the 55°S-55°N band (Figure 3-19a), the model predictions lie within the error bars of the SAGE data analysis, and of the SBUV analysis in the upper and lower stratosphere, but tend to overestimate the signal found in the middle stratosphere in the SBUV data. The models are also generally consistent with the 1.5% lower stratospheric (ozone column) signal. However, in comparing the predicted model ozone responses to the observationally derived responses in the tropics (Figure 3-19b), some possible differences on the 11-year time scale are evident. Near the stratopause (~50 km altitude), the observed response appears to be larger than expected from the

models while in the middle stratosphere (~30 – 35 km), the reverse is true, especially relative to SBUV data. In the lower stratosphere, the mean observed response appears to increase again while the model responses decrease.

A number of possible explanations for the apparent differences between the observationally derived and model-predicted tropical ozone responses may be considered. First, it is possible that there are significant uncertainties in the observations because of problems in the cross-calibration of instruments (see Section 3.2.3), overall short record lengths, and the relative size of the solar effect (a few percent). Only after another several decades of data are acquired will these uncertainties be reduced.

One physical explanation suggested for the unexpected altitude dependence of the tropical ozone response is increased odd nitrogen in the upper stratosphere caused by enhanced precipitation of energetic electrons when the

Figure 3-19. Annual mean solar cycle response calculated from two long-term satellite ozone profile datasets with the predictions of four stratospheric models that account for observed 11-year changes in solar ultraviolet spectral irradiance, for (a) 55°S-55°N and (b) 25°S-25°N. Datasets are the monthly zonal mean version 8 SBUV/SBUV(/2) ozone profile dataset of Frith et al. (2004) over the 1979 through 2003 period (updated from Hood, 2004) and version 6.20 SAGE I and II ozone profile data over the 1979 to 2005 period, except for several years following the Mt. Pinatubo eruption (updated from Stolarski and Randel, 1998). Model results are from the 3-D models of Tourpali et al. (2003) and Egorova et al. (2004) and the 2-D models of Brasseur (1993) and Haigh (1994).



GLOBAL OZONE

Sun is less active (Callis et al., 2000, 2001). Some model simulations (Langematz et al., 2005; Rozanov et al., 2005) have produced a response of opposite sign (a “self-healing effect”) in the mid-stratosphere but only in response to massive electron precipitation events producing very large NO_x signals, which have not been detected in satellite data (Hood and Soukharev, 2006). At this time, therefore, there is no evidence for particle-induced NO_x being responsible for the apparent difference between models and observations in the tropics.

Several possible explanations for the reduced solar cycle ozone response in the tropical middle stratosphere may be considered. First, it is possible that the multiple regression statistical analysis is being biased by interference from the QBO and major volcanic eruptions. Lee and Smith (2003) have applied a two-dimensional chemical-dynamical-radiative model with a prescribed QBO to show that such interference can occur, especially from the QBO, and can potentially lead to small or even negative solar cycle regression coefficients in the equatorial lower and middle stratosphere. It remains to be seen whether some of this response is an artifact due to the highly idealized form used by Lee and Smith for the QBO, but interference from the QBO should be carefully considered in future evaluations of the observed tropical response minimum. It is also possible that the QBO itself may be modulated slightly by the solar cycle (Salby and Callaghan, 2000; McCormack, 2003; but see also Hamilton, 2002). If so, then additional dynamical effects on the net ozone change over a solar cycle could be implied. Finally, one relatively simple possible explanation for the tropical ozone response minimum is that the unexpectedly large ozone response in the upper stratosphere effectively reduces the ozone production rate in the middle stratosphere through increased absorption of UV radiation (a form of “self-healing”), but this remains to be tested. On short time scales (i.e., that of the ~27-day solar rotation period), the observed ozone response to solar UV variations in the tropical middle and upper stratosphere agrees very well with photochemical model predictions (see, e.g., Chen et al., 1997).

The origin of the apparent solar cycle ozone variation in the lower stratosphere also remains uncertain. It has been questioned whether the lower stratospheric decadal ozone variation is of solar origin at all because of the occurrence of two major volcanic perturbations about 9 years apart in 1982 and 1991 (e.g., Solomon et al., 1996). However, the increase in tropical total ozone approaching the most recent solar maximum, when no major eruptions have occurred, supports the view that volcanic eruptions alone cannot explain this decadal variation. A remaining hypothesis is that the direct upper stratospheric effects of

solar ultraviolet radiation (and possibly particle precipitation) are able to modify the development of stratospheric circulation in such a way as to modify the effective upwelling rate in the tropical and subtropical lower stratosphere. Possible mechanisms for this, and for the subsequent transmission of a solar signal into the troposphere, are discussed in Section 5.2.1.1 of Chapter 5.

3.4.5 Assessment Model Simulations

A range of model runs have been performed for this Assessment to simulate both the past and future atmosphere. Different types of two-dimensional (2-D) latitude-height models and three-dimensional (3-D) models are described in Box 5-1 (Chapter 5). Simulations using 2-D models and 3-D coupled Chemistry-Climate Models (CCMs) are described in Chapter 6 (Appendix 6A), where they are used to investigate future changes in stratospheric ozone. These models were also used, in certain experiments, to simulate the past atmosphere. In this section we make use of these simulations of the recent past to understand the causes of past changes in ozone. Descriptions of the 2-D models and 3-D CCMs used in this chapter may be found in Tables 6-3 and 6-4 of Chapter 6. In addition to the 2-D models and CCMs, we also use results from off-line 3-D chemical transport models (CTMs). Because the CTM results are only used in this chapter, we summarize details of the runs available in Table 3-1. Generally, for the CTMs we have used existing, published simulations and reanalyzed the output to compare with recent observations. The NASA Goddard Space Flight Center (GSFC) CTM provided one simulation (Stolarski et al., 2006), which was forced by GCM winds. The Global Modeling Initiative (GMI) CTM, which is technically very similar to the GSFC CTM and is based on much of the same code, provided two simulations. These used repeating climatological GCM winds corresponding to a “cold” and a “warm” Arctic winter. The SLIMCAT CTM was forced by analyzed ECMWF winds. In one experiment the model used a parameterized ozone tracer (see Hadjinicolaou et al., 2005). The model was also used to perform three experiments with full chemistry: A run with time-dependent halogen loading, a similar run but without an assumed 5 pptv of inorganic bromine (Br_y) from short-lived species, and a run with fixed halogen loadings.

Two-dimensional models have been used extensively in previous Assessments and we use them again here for comparison with the 3-D CTM runs. We have used output from the P5 runs (see Chapter 6), as these have the most realistic bromine loadings. In addition to the basic model setups described in Appendix 6A, the non-interactive GSFC 2-D model also performed a run in

Table 3-1. Participating 3-D chemical transport models.

Model Name	Institution(s)	Investigators	Forcing Winds and Temperatures	Resolution and Domain	Chemistry / PSC Scheme	Reference
GSFC CTM	NASA Goddard, U.S.	A. Douglass S.R. Kawa R. Stolarski	GEOS-4 GCM	2° × 2.5° Surface to 0.4 hPa	Full chemistry / Considine et al. (2000)	Stolarski et al. (2006)
GMI CTM	Several institutions, U.S.	A. Douglass S. Strahan R. Stolarski	GEOS-4 GCM	2° × 2.5° Surface to 0.015 hPa (33 levels)	Full chemistry / Considine et al. (2000)	Douglass et al. (2004)
SLIMCAT	University of Leeds, U.K.	M.P. Chipperfield W. Feng	ECMWF (ERA-40, operational)	7.5° × 7.5° Surface to 55 km	Full chemistry / Equilibrium	Chipperfield (1999) Feng et al. (2006)
	University of Cambridge, U.K.	P. Hadjinicolaou J. A. Pyle	ECMWF (ERA-40, operational)	5.6° × 5.6° 8 to 55 km	Parameterized O ₃ tracer / (No time dependence)	Hadjinicolaou et al. (2005)

which the model was forced with an interannually varying circulation (run GSFC-IDV in discussion below). These 2-D models and the 3-D CTMs have been compared with observations for ozone column and profiles in both the Northern and Southern Hemispheres, which extends on published work. The status of CCMs is much less mature and for these simulations we show just a basic comparison of the range of models with column ozone.

Figure 3-20 shows the deseasonalized zonal mean column ozone for global (60°N-60°S), NH (60°N-35°N) and SH (35°S-60°S) regions for a selection of the 2-D models and 3-D CTMs. There is a wide range in the predicted absolute column O₃ from the different models, which is due mainly to differences in the model transport. Clearly, the 2-D models, with their climatological circulation, do not capture the interannual variability in the observations. The GSFC CTM, forced by GCM winds, does well in tracking the variations in global ozone (as shown in Stolarski et al., 2006) but overestimates the SH values by around 20 DU. The interannual variability in this model, driven by the GCM winds, would not be expected to correlate with observed variations. For the 2-D models (except GSFC-IDV, not shown in Figure 3-20), the weak interannual variations will be driven by only aerosol changes and source gas trends. The SLIMCAT CTM, which is forced by analyzed winds, does capture more variability. This was demonstrated for the NH by Hadjinicolaou et al. (2005), who ran the model for the stratosphere with parameterized O₃ and showed the very

good agreement for 35°N-60°N. The full chemistry SLIMCAT run extends to the surface and tends to have larger columns due to overestimating O₃ in the lowermost stratosphere. However, these model runs are characterized by a large, spurious positive deviation in O₃ in the late 1980s that is caused by inaccurate interannual variability in the forcing (ERA-40) analyzed winds.

Figure 3-21 shows the global, equatorial, NH mid-latitude, and SH midlatitude anomalies of the annual average O₃ from the 2-D models and 3-D CTMs. As seen in WMO (2003), the 2-D models perform better in reproducing the observed variations in the NH, although there is still a spread in model results. In particular, the decrease in these models around 1992 is due to enhanced aerosol from the Mt. Pinatubo eruption. In the SH and globally, the 2-D models produce a wider spread of results, likely reflecting different treatments of the Antarctic ozone hole. The 3-D CTMs also appear more successful in simulating the NH midlatitudes than the SH midlatitudes. Aside from the large positive (late 1980s) and negative (early 1990s) deviations in the SLIMCAT runs, which use ERA-40 winds, the CTMs perform well in capturing the overall variations, which will be dominated by changes in aerosol loading and halogens. The SLIMCAT parameterized O₃ run is that discussed in Hadjinicolaou et al. (2005), where they show results for 35°N-60°N (see Section 3.4.2). This run has no time-dependence in the chemistry parameterization and clearly does not capture the overall trend from 1980-2004. However, the run does produce an increase in

GLOBAL OZONE

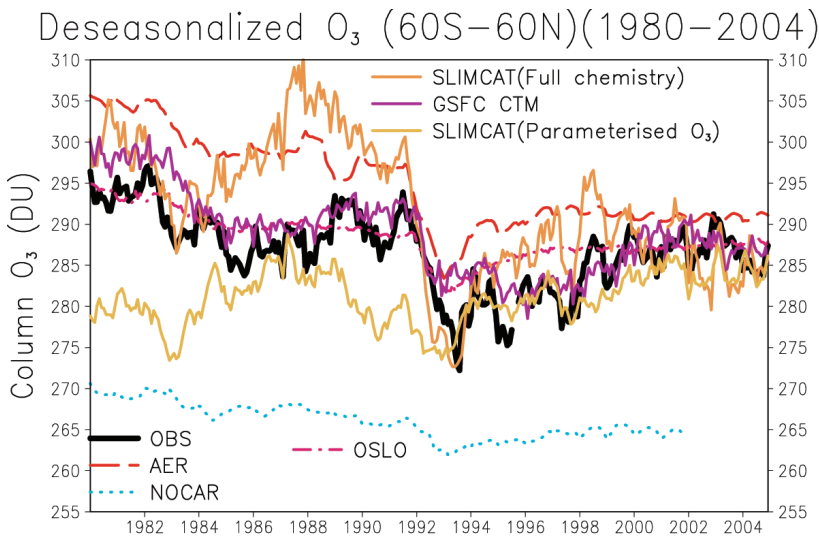


Figure 3-20. Time series of deseasonalized mean column O_3 for (top panel) $60^{\circ}S-60^{\circ}N$, (middle panel) $35^{\circ}N-60^{\circ}N$, and (bottom panel) $60^{\circ}S-35^{\circ}S$ from 1980-2004 for three selected 2-D models and three 3-D CTMs. Also shown are the observations from the merged satellite data-set (black line). See Tables 6-3 and 6-4 of Chapter 6 for information about the models.

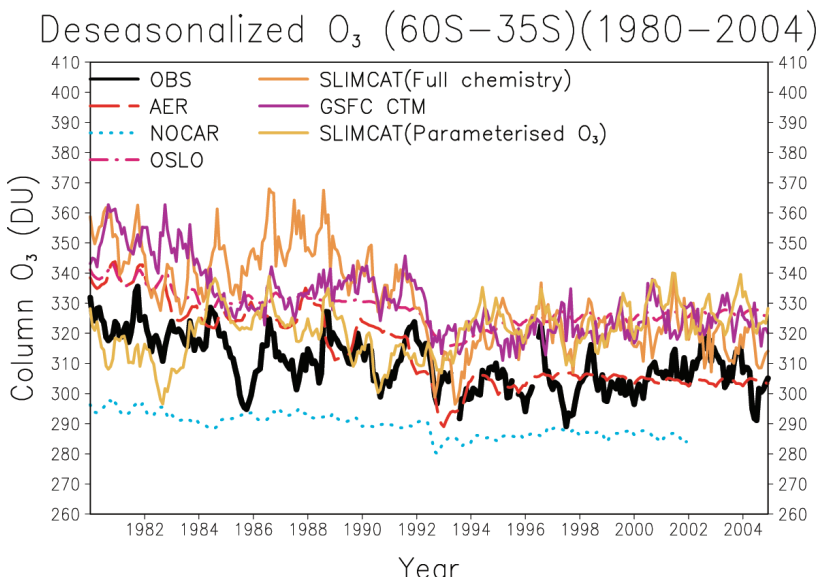
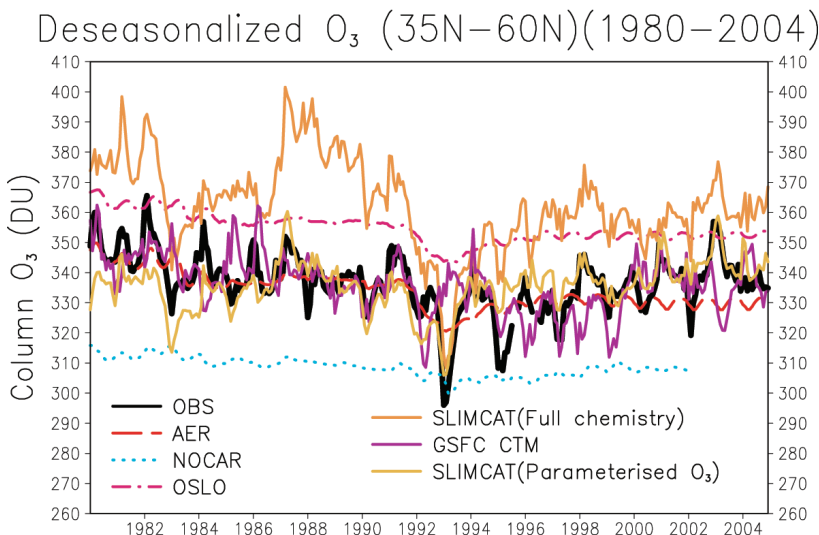
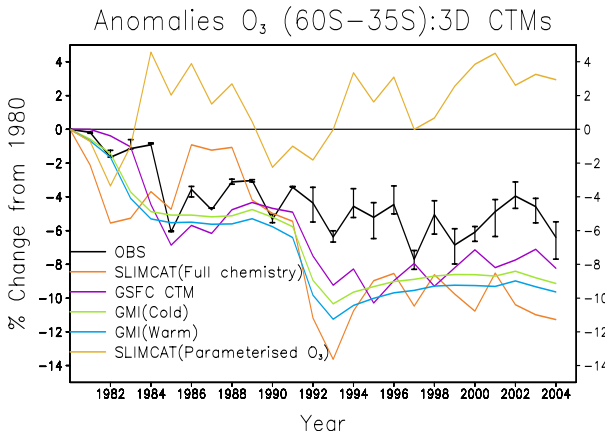
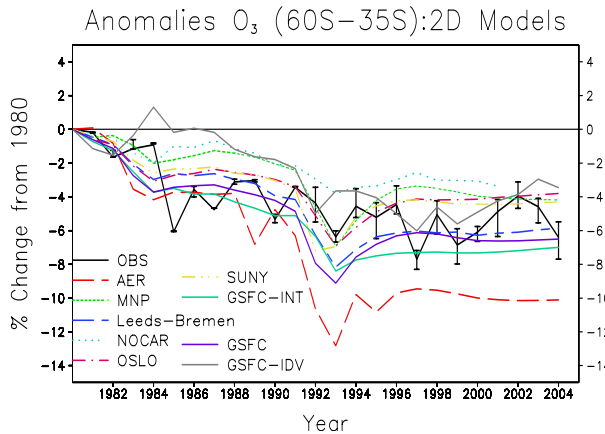
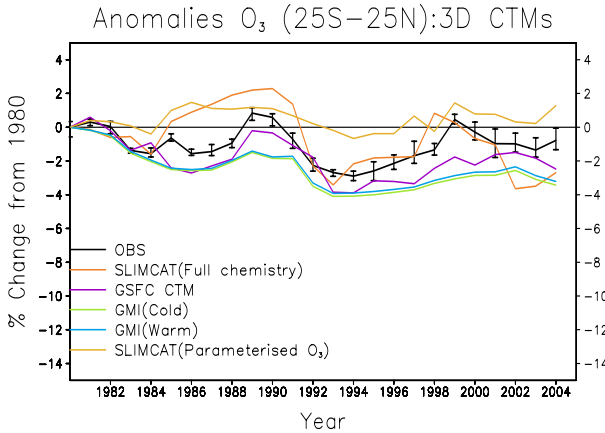
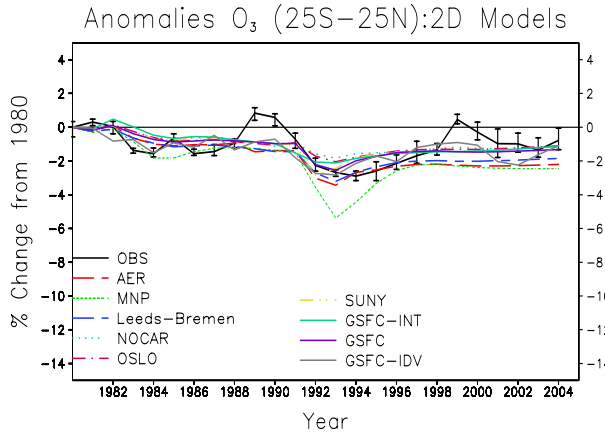
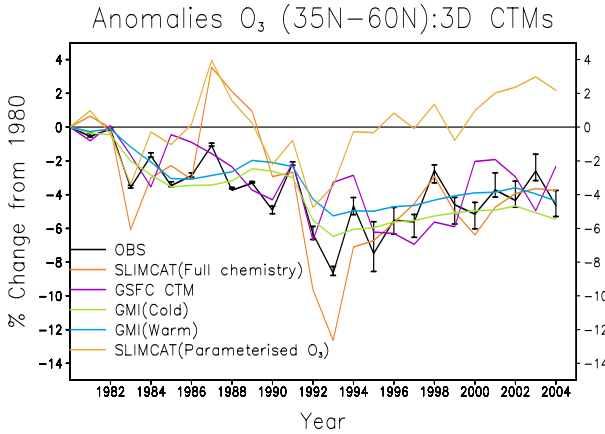
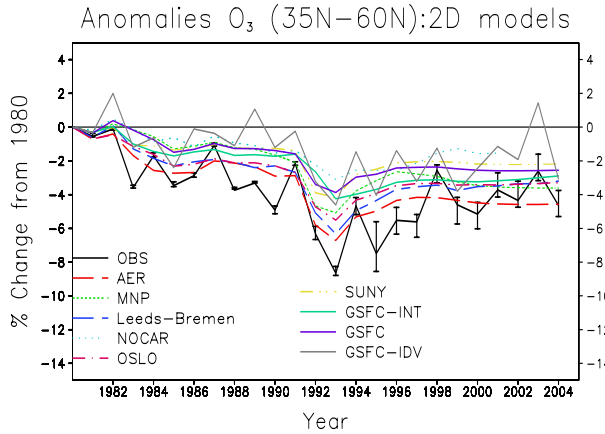
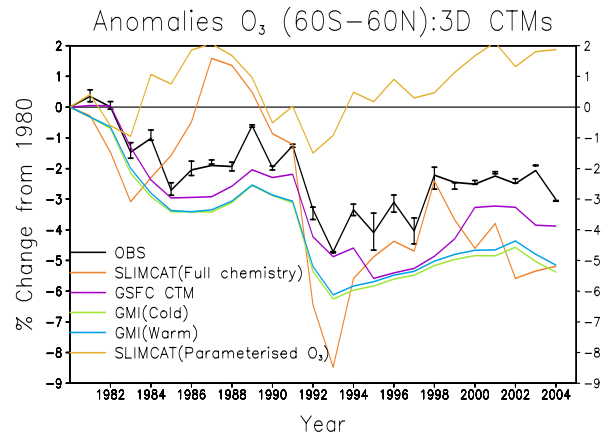
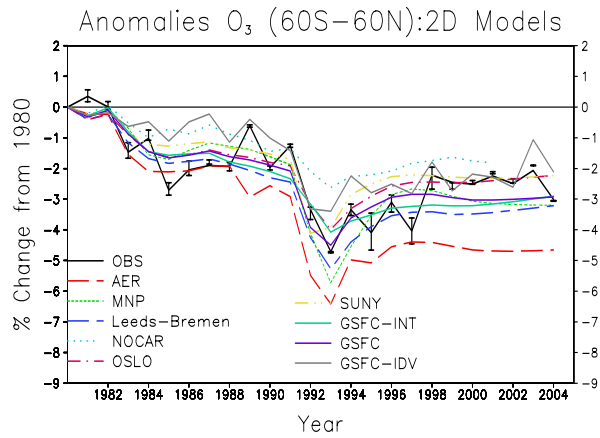


Figure 3-21. (On the right.) Time series of annual mean column ozone variations from observations (black line) and from eight 2-D model runs (left) and five 3-D CTM runs (right) for latitude bands of (top) $60^{\circ}S-60^{\circ}N$, $35^{\circ}N-60^{\circ}N$, $25^{\circ}N-25^{\circ}S$, and (bottom) $60^{\circ}S-35^{\circ}S$. Changes are calculated in percent with respect to 1980 values for each time series. Observations are from the merged satellite dataset; see Appendix 3A. The error bars on the observations represent the spread of different datasets, which provides a minimum estimate of their uncertainty. The SLIMCAT run with parameterized O_3 does not include any chemical changes and is therefore not expected to follow the other model curves. See Tables 6-3 and 6-4 of Chapter 6 for information about the models.



GLOBAL OZONE

NH column O_3 after the mid-1990s and this was presented as evidence that circulation changes are leading to O_3 increases. Interestingly, the GMI CTM runs with repeating meteorology also model an increase in O_3 during this period, which, like any changes in the 2-D models except GSFC-IDV, is related to aerosol trends. The GMI run with “cold” Arctic meteorology gives around 1% lower O_3 than the run with “warm” meteorology, which is a measure of the impact of different polar loss in this run. The different CTM runs give similar simulations for the SH, again with more variability in the SLIMCAT run, but the full chemistry CTMs clearly underestimate the observed O_3 from the early 1990s on. These models produce a realistically large O_3 hole and this appears to be having a large impact on the model SH midlatitudes. The models shown here are a mixture of those that include feedback between chemistry and dynamics (e.g., some of the 2-D models) and models without any coupling (e.g., the off-line 3-D CTMs). However, the impact of the modeled midlatitude O_3 loss on dynamics is not likely to be important. Using a GCM with parameterized O_3 chemistry, Braesicke and Pyle (2003) showed the impact of an imposed midlatitude O_3 loss did not produce an additional feedback on the O_3 distribution. The effect of dynamical changes on ozone is discussed in Section 3.4.2.

Results from the 2-D models and 3-D CTMs have been analyzed for ozone trends. This was done with a similar statistical model to that used in Section 3.2.1 and the trend term was regressed onto an EESC curve. Figure 3-22 shows the modeled O_3 trends from 1980-2004 (fitted using EESC and converted to %/decade using the EESC-time variation in the 1980s) as a function of latitude. As shown in WMO (2003) the 2-D models tend to reproduce the observed trends in the NH midlatitudes but show a wide variation in the SH. The 2-D models also produce a negative trend of 1-2%/decade in the tropics where the observations indicate a zero trend. The 3-D CTMs also fall in the range of observations in the NH and produce a negative trend in the tropics with the exception of the SLIMCAT run forced by analyzed winds. This run produces a zero trend in the tropics (see also Figure 3-21), which may indicate that the ECMWF analyzed winds succeed in isolating this region more efficiently (see Monge Sanz et al., 2006). In the SH, the CTMs are quite consistent with each other but again tend to overestimate the observed midlatitude trend.

Figure 3-23 shows the modeled and observed column ozone trends versus month for the NH and SH. The NH observations show a seasonality with the largest trend of around -4%/decade in March and a minimum

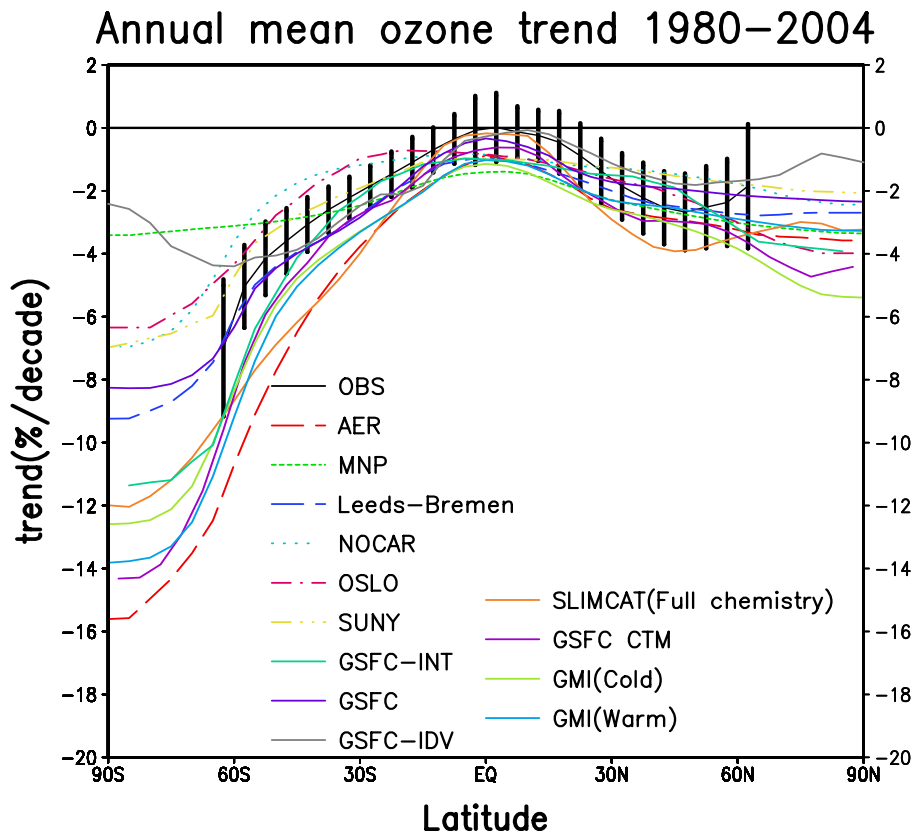


Figure 3-22. Latitudinal profile of annual mean column ozone trends from observations (black line) compared with results from 2-D models and 3-D CTMs for 1980-2004. The trends were estimated using regression to an EESC curve and converted to %/decade using the variation of EESC with time in the 1980s. Observations are from the merged satellite dataset; see Appendix 3A. The error bars for the observations indicate the 2σ uncertainties.

trend in late summer. The models generally capture the magnitude of this trend and its seasonal variation. There is a wide variation in the 2-D model results, which is similar to WMO (2003); this is expected, as these models will not have evolved substantially over this period. The CTMs capture the seasonal variations but tend to overestimate the trend in late spring. In contrast, the comparison in the SH is very poor. The observations show a trend of -4% decade with only a small seasonal variation. This lack of seasonal variation is produced by some 2-D models but there is a wide range in magnitude of trend, reflecting the extent of the models' SH polar loss. The 3-D CTMs, with their expected more realistic treatment of the SH polar loss and vortex dynamics, produce a trend which is larger than observed and shows a clear seasonal cycle. In these runs the formation of the Antarctic ozone hole in August-September seems to impact midlatitudes and increase the trend there. Given the better physical basis for the 3-D models, the apparently better agreement for the seasonality of the trend from some 2-D models should not be taken to mean that this modeling approach is better.

The trends in the vertical profile of O_3 from the models and observations are shown in Figure 3-24. The observations show a characteristic double peak with loss around 40 km due to the $ClO + O$ cycle and loss in the lower stratosphere due to halogen/aerosol chemistry and the impact of loss at higher latitudes. In the upper stratosphere the 3-D CTMs and model 2-D models produce trends similar to the observations, with a peak around 40-45 km. The Leeds-Bremen, NOCAR, and GSFC-INT 2-D models produce a trend that is about a factor of two less than observed. These three models, in contrast to the other 2-D models and CTMs, calculate interactive temperatures in the upper stratosphere. On this basis they might be expected to be more realistic than models that use fixed temperatures, although yearly varying analyses should also be realistic. However, this depends on the accuracy of the modeled temperature trends and any trends that causes in circulation. The interactive 2-D models produce a peak upper stratospheric cooling over the same time period of around 1-1.4 K/decade (not shown), which is in reasonable agreement with observations (Chapter 5) and clearly better than models that assume no trend. These interactive 2-D models also produce the largest CH_4 trend in the upper stratosphere, indicating a feedback in these models that increases the meridional circulation (not shown). Both of these factors act to reduce the magnitude of the ozone trend. Overall these comparisons shown that while we have a reasonable understanding of upper stratospheric ozone depletion, we still do not have full quantitative agreement between models and observations. Around 20 km in the NH lower stratosphere, the models again

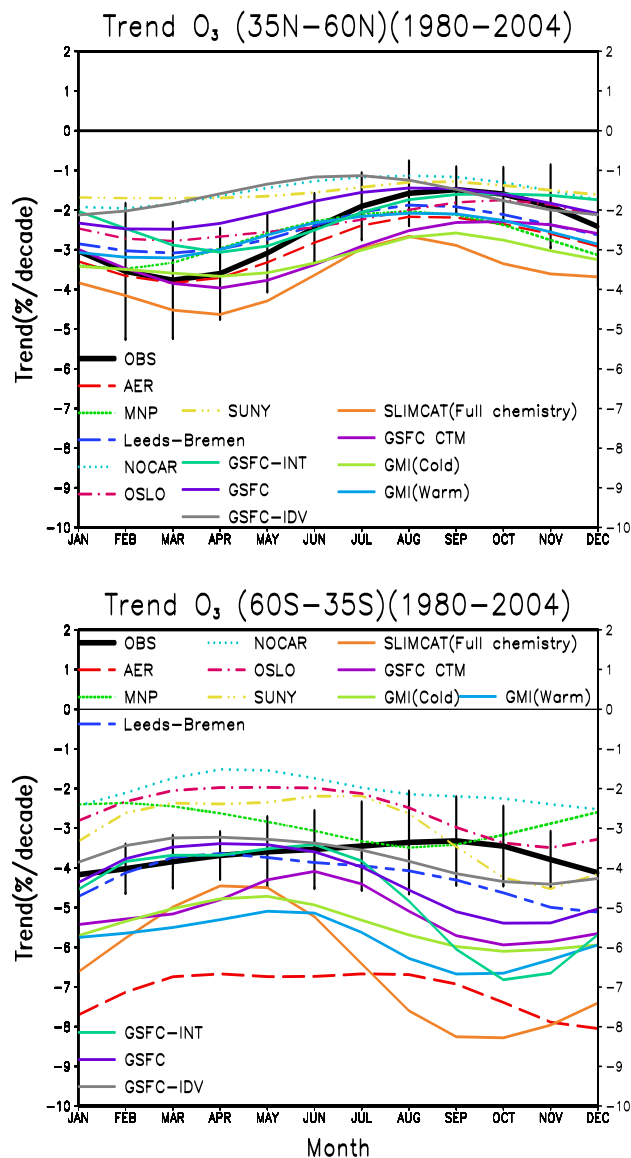


Figure 3-23. Seasonal variation of observed (black line) and modeled column ozone trends at (top) 35°N-60°N and (bottom) 35°S-60°S. The model results are from 2-D models and 3-D CTMs. The trends were estimated using regression to an EESC curve and converted to %/decade using the variation of EESC with time in the 1980s. Observed trends were estimated from the merged satellite dataset, with error bars denoting 2σ uncertainties.

overall produce a similar trend to that observed. There are no trend estimates from observations below 20 km in the SH but, consistent with the SH comparisons shown above, there is a large variation between the models. The CTMs give similar results while the 2-D models can give very small trends, or in the case of the AER model, a large trend between 10-15 km.

GLOBAL OZONE

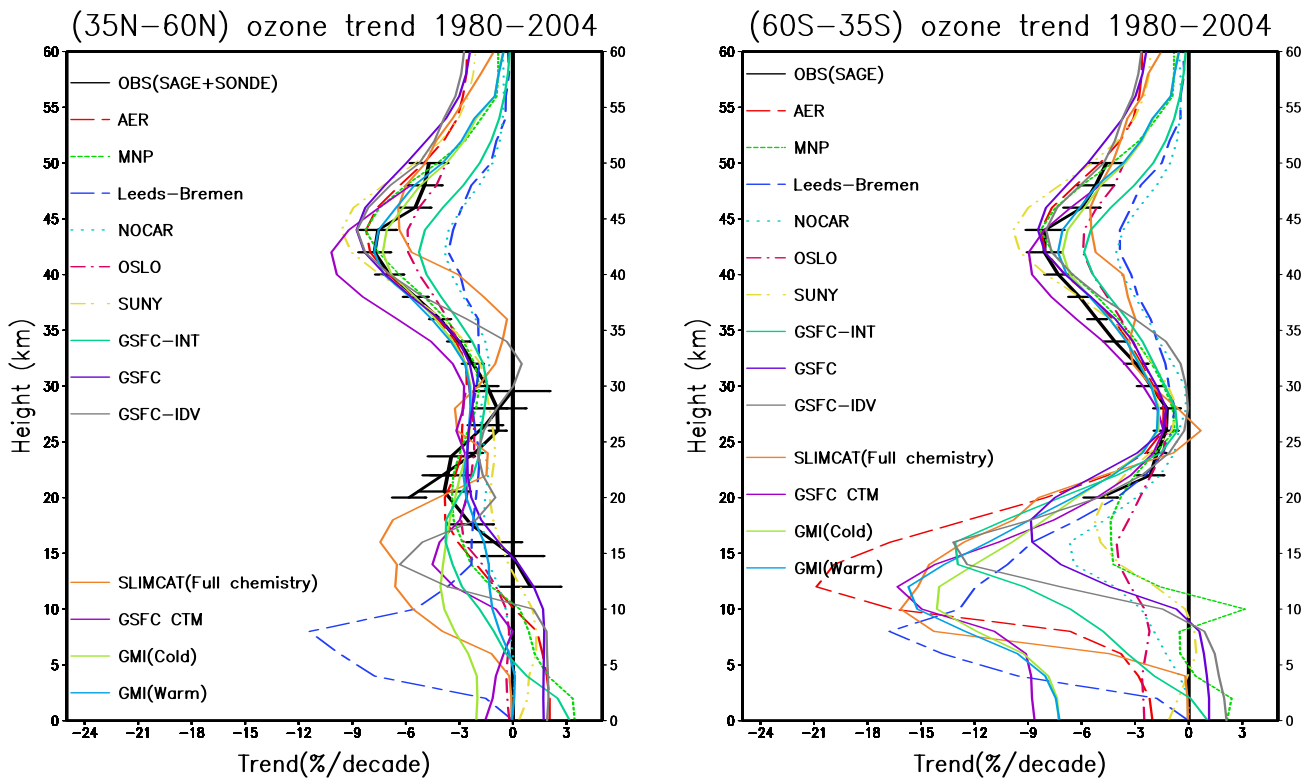


Figure 3-24. Vertical profiles of ozone trends over the period 1980-2004 from observations compared with 2-D models and 3-D CTMs for (left) 60°N-35°N and (right) 35°S-60°S. The trends were estimated using regression to an EESC curve and converted to %/decade using the variation of EESC with time in the 1980s. The observations are from SAGE I+II in the upper stratosphere and from ozonesondes in the lower stratosphere (NH only).

On the basis of these comparisons, it is evident that many broad features of the observed ozone trends are consistent with models that are forced with observed variations in halogens and aerosols. The models generally perform better in the Northern Hemisphere than in the south. Overall, the 3-D CTMs perform as least as well as the 2-D models, although there are fewer of them to compare. In particular, the behavior of the models in the SH is more similar, though they do show a significant discrepancy with the observed magnitude and seasonality of the trend.

We now use results from the SLIMCAT CTM runs to diagnose the roles of chemistry and dynamics in past ozone changes in more detail. As discussed in Section 3.4.2, CTMs forced by meteorological analyses have been used to estimate the role of dynamics on (NH) midlatitude ozone. Full chemistry CTMs can also be used to quantify the effect of different chemical forcings. For example, Chipperfield (2003) reported a similar SLIMCAT CTM integration to Hadjinicolaou et al. (2002) but including detailed chemistry for cases with and without the inclusion of halogen loading and time-dependent aerosol. For most months and latitudes, the run with halogen loading and aerosol data yielded a better agreement with observed

ozone time series. Moreover, the magnitude of the modeled halogen effect was similar to the observed long-term decrease. It was therefore concluded that the modeled ozone decrease at all latitudes up to the early 1990s, including northern midlatitudes, was dominantly caused by halogen-related trends in combination with heterogeneous chemistry on lower stratospheric polar stratospheric clouds (PSCs)/aerosols. The runs discussed above (Table 3-1) update these studies using ERA-40 winds (Hadjinicolaou et al., 2005; Feng et al., 2006). Feng et al. (2006) ran the CTM from 1977 until 2005, using ERA-40 winds until the end of 2001 followed by operational analyses. In addition to the basic model run with time-dependent source gases, they performed a run with fixed (1980 troposphere) halogen loadings and a run without a 6 pptv contribution of Br_y from very short-lived substances (VSLS). As shown in Figure 3-25, the comparison of the basic model runs with the TOMS/SBUV anomaly is similar to that shown in Hadjinicolaou et al. (2005) (Figure 3-21), where the model captures some observed variability but, through the use of ERA-40 winds, produces some features (variability) which are not observed. As discussed in Section 3.4.1, the use of meteorological analyses for

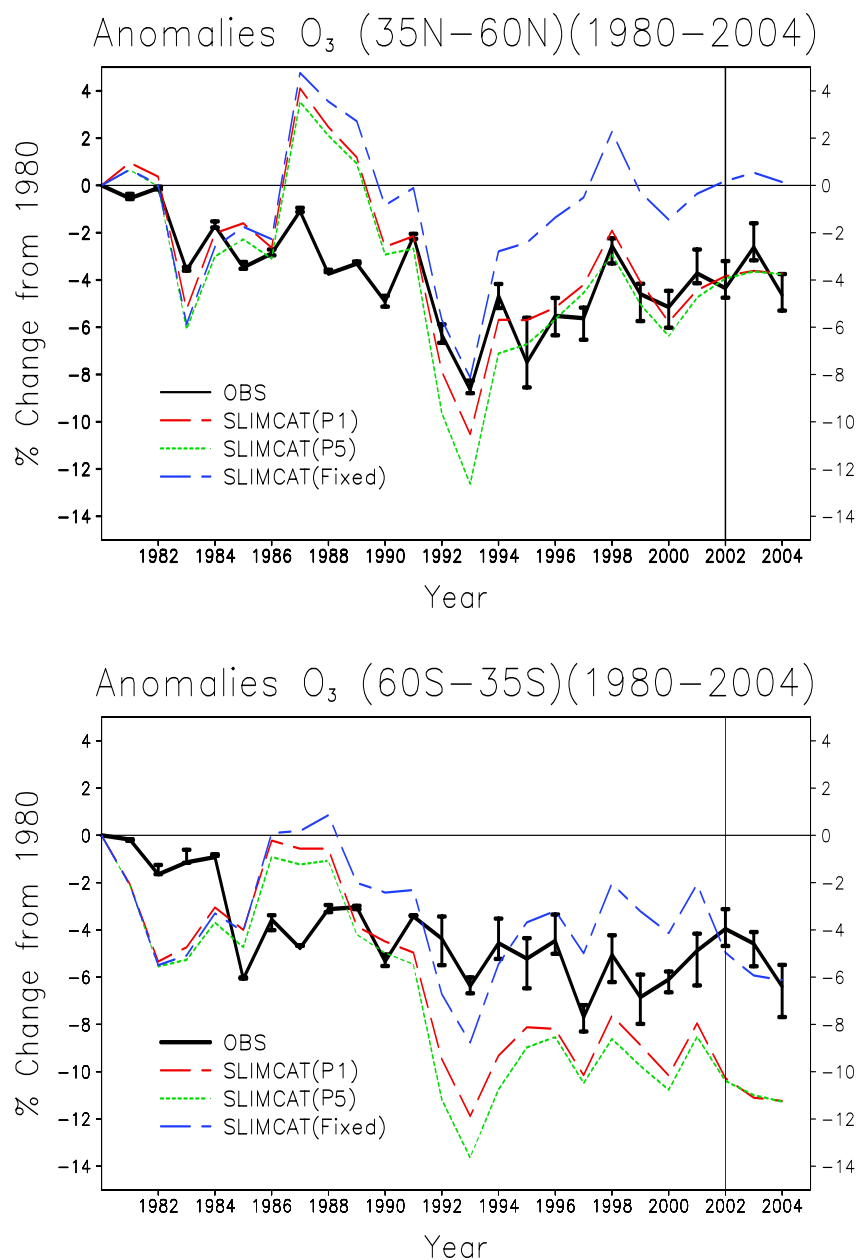
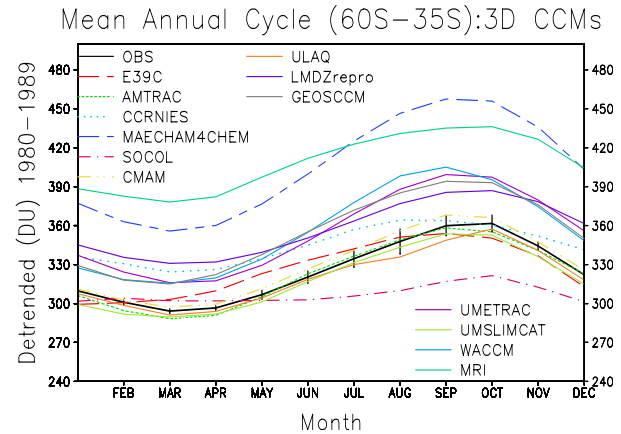
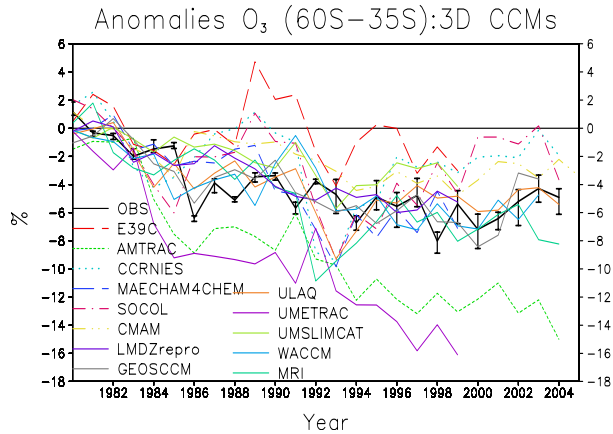
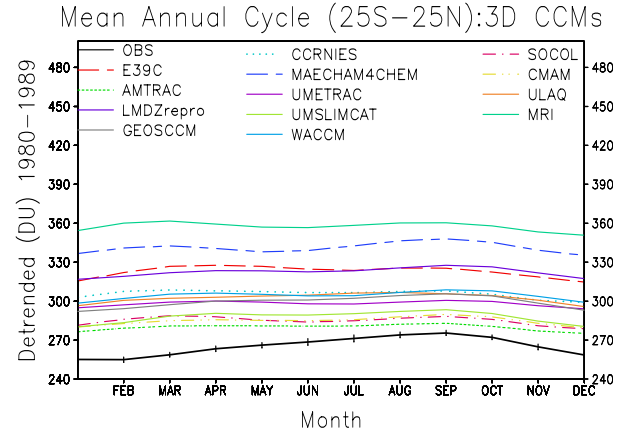
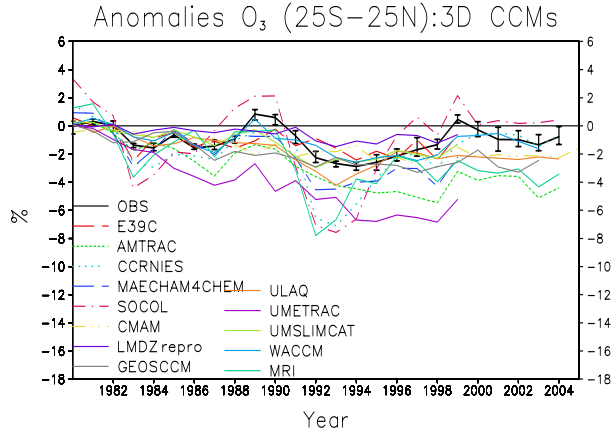
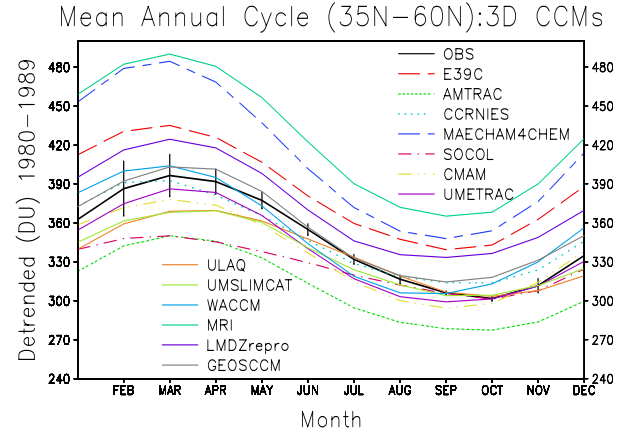
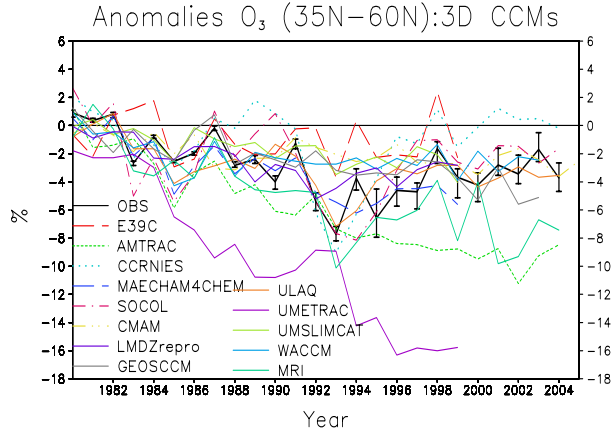
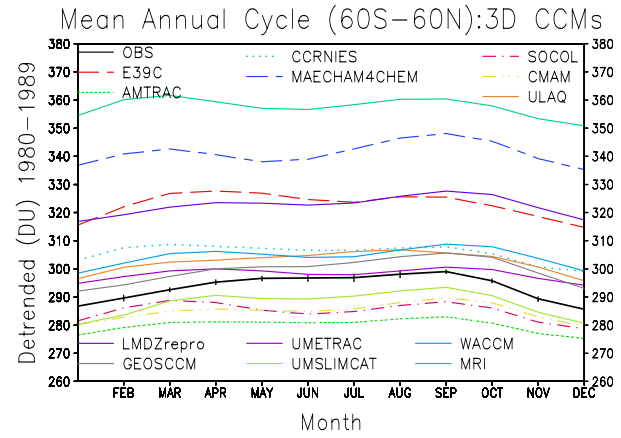
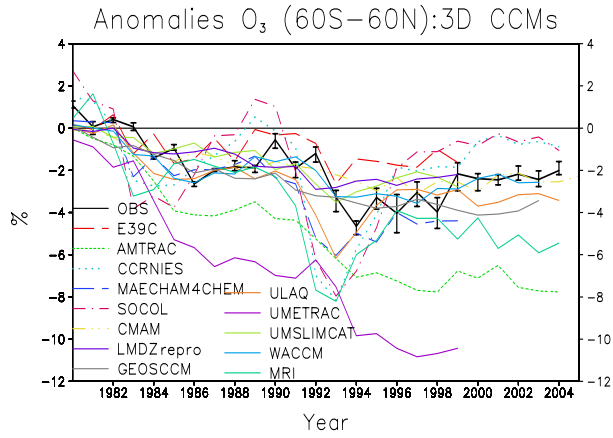


Figure 3-25. Time series of annual mean anomalies (with respect to 1980) for three simulations of the SLIMCAT 3-D CTM compared with observations (black line). The SLIMCAT simulations considered full time-dependent halogen chemistry (run P5, green dotted line), a simulation without 6 pptv Br_y from short-lived species (run P1, red dashed line), and a simulation with fixed (1980 tropospheric) halogen loadings (blue dashed line). The vertical line at the start of 2002 indicates where the CTM forcing changed from ECMWF ERA-40 analyses to ECMWF operational.

trend studies needs to be treated with caution. Assuming that the analyses are able to give a realistic circulation in the model, then the CTM can be used for chemical experiments, although these are not coupled (i.e., any indirect circulation effect of a chemical forcing will not be captured). Figure 3-25 shows that when the model is run with fixed halogen loadings, there is a difference of about 4–7% in the NH and SH anomalies, or 20–22 DU of the column, in the model ozone by 2000 relative to the run with time-varying halogens, confirming the important overall role of the halogen trends. The 3-D CTM results in Figure 3-25 also confirm the 2-D results of Salawitch et al. (2005) (see Section 3.4.3). An additional 6 pptv of Br_y

in the lower stratosphere decreases the model O_3 column by about 10 DU (Feng et al., 2006) but, when expressed as an anomaly relative to 1980 (a low aerosol period), an additional relative depletion is only noticeable around the time of the Mt. Pinatubo eruption. Finally, we can note that by about 2000, and before the model results are affected by the switch of analyses, the modeled contribution from halogens to midlatitude ozone loss is starting to decrease slightly, i.e., there is only a small contribution of halogen changes to recent changes in ozone. Using a photochemical box model, Yang et al. (2006) argued that the increase in ozone for altitudes below 18 km is most likely driven by changes in transport (see Section 3.4.2), rather

GLOBAL OZONE



than by declining chlorine and bromine, but the cessation of ozone depletion between 18-25 km altitude is consistent with a leveling off of stratospheric abundances of chlorine and bromine.

As discussed in Chapter 6, there are now many coupled Chemistry-Climate Models (CCMs) that have been developed to study past and future changes in the stratosphere. These models have chemistry schemes similar to those in 2-D models and CTMs, but they calculate their own interactive circulation, which will be much more variable than interactive 2-D models. The models are also computationally expensive and often can only run one scenario either as a single simulation or as a few-member ensemble. Hence, these models have not yet been applied to diagnosing past changes in midlatitude ozone; rather the models themselves are still at the validation stage. Andersen et al. (2006) presented results of three CCMs compared with the 2-D models used in WMO (2003); the CCM results varied significantly. More recently, Eyring et al. (2006) compared results from 13 CCMs that ran with the same external forcings. These were the REF1 simulations described in Chapter 6 of this Assessment. The CCMs produce a good simulation of the global temperature fields. Results of the stratospheric age of air and tropical tape recorder signal showed a large spread of results, although about half of the models were realistic; this shows an improvement compared with CCMs used in previous Assessments. Eyring et al. (2006) also discussed the performance of these models in reproducing polar ozone depletion. Overall the differences in modeled transport, and likely the treatment of lower stratospheric chemical processes at all latitudes, leads to a range in modeled global ozone trends over the past 20 years.

Figure 3-26 shows the results from 13 CCMs for the seasonal cycle in column ozone and its anomaly for various latitude bands (see Chapter 6 for model details), extending on the analysis of Eyring et al. (2006). At NH and SH midlatitudes the models all capture the expected seasonal cycle but the modeled column varies by up to 160 DU. The models also all tend to overestimate the tropical column ozone. In the tropics some CCMs capture the

Figure 3-26. Time series of mean annual anomalies, expressed as a % deviation from the detrended 1980-1989 mean annual cycle (left), and mean 1980-1989 detrended seasonal cycle (right) for latitude bands 60°N-60°S, 60°N-35°N, 25°N-25°S, and 35°S-60°S for the REF1 simulations of 13 coupled Chemistry-Climate Models (CCMs) described in Chapter 6 (Table 6-4 and Appendix 6A). Also shown are the merged satellite observations. (Note: observations in right panels are mean over years 1980-2004.)

observed small long-term change but many, as in the case of 2-D models and 3-D CTMs, produce a large long-term decrease. Note that only some of the CCM simulations include a treatment of the solar cycle (see Chapter 6). For the midlatitude anomalies, the models generally show a decreasing trend through to the 1990s, in response to the imposed halogen and aerosol variations, but again there is a wide range in the model predictions. However, as noted in Chapter 6, some of the outlying simulations should be ignored due to unrealistic levels of inorganic chlorine in the lower stratosphere. Still, given the expected dynamical variability in the models, it is not possible to draw robust conclusions from this range of model runs.

REFERENCES

- Ajtić, J., B.J. Connor, B.N. Lawrence, G.E. Bodeker, K.W. Hoppel, J.E. Rosenfield, and D.N. Heuff, Dilution of the Antarctic ozone hole into southern midlatitudes, 1998-2000, *J. Geophys. Res.*, *109*, D17107, doi: 10.1029/2003JD004500, 2004.
- Andersen, S.B., and B.M. Knudsen, The influence of vortex ozone depletion on Arctic ozone trends, *Geophys. Res. Lett.*, *29* (21), 2013, doi: 10.1029/2001GL014595, 2002.
- Andersen, S.B., E.C. Weatherhead, A. Stevermer, J. Austin, C. Brühl, E.L. Fleming, J. de Grandpré, V. Grewe, I. Isaksen, G. Pitari, R.W. Portmann, B. Rognerud, J.E. Rosenfield, S. Smyshlyaev, T. Nagashima, G.J.M. Velders, D.K. Weisenstein, and J. Xia, Comparison of recent modeled and observed trends in total column ozone, *J. Geophys. Res.*, *111*, D02303, doi: 10.1029/2005JD006091, 2006.
- Appenzeller, C., A.K. Weiss, and J. Staehelin, North Atlantic Oscillation modulates total ozone winter trends, *Geophys. Res. Lett.*, *27* (8), 1131-1134, 2000.
- Attmanspacher, W., and H.U. Dütsch, International ozone sonde; intercomparison at the observatory Hohenpeissenberg, 19 January - 5 February 1970, *Berichte des Deutschen Wetterdienstes, Nr. 120 (Bd. 16)*, 74p., 1970.
- Bengtsson, L., S. Hagemann, and K.I. Hodges, Can climate trends be calculated from reanalysis data?, *J. Geophys. Res.*, *109*, D11111, doi: 10.1029/2004JD004536, 2004.
- Berthet, G., N. Huret, F. Lefèvre, G. Moreau, C. Robert, M. Chartier, V. Catoire, B. Barret, I. Pissot, and L. Pomathiod, On the ability of chemical transport models to simulate the vertical structure of the N₂O, NO₂ and HNO₃ species in the mid-latitude stratosphere, *Atmos. Chem. Phys.*, *6*, 1599-1609, 2005.
- Bhartia, P.K., C.G. Wellemeyer, S.L. Taylor, N. Nath, and

GLOBAL OZONE

- A. Gopalan, Solar Backscatter Ultraviolet (SBUV) version 8 profile algorithm, in *Ozone Vol. I, Proceedings of the XX Quadrennial Ozone Symposium*, 1-8 June 2004, Kos, Greece, edited by C.S. Zerefos, 295-296, Int. Ozone Comm., Athens, Greece, 2004.
- Birner, T., D. Sankey, and T.G. Shepherd, The tropopause inversion layer in models and analyses, *Geophys. Res. Lett.*, *33*, L14804, doi: 10.1029/2006GL026549, 2006.
- Bloom, S., A. de Silva, D. Dee (Senior Authors), M. Bosilovich, J-D. Chern, S. Pawson, S. Schubert, M. Sienkiewicz, I. Stajner, W-W. Tan, and M-L. Wu, Documentation and Validation of the Goddard Earth Observing System (GEOS) Data Assimilation System – Version 4, NASA/TM-2005-104606, 26, 2005.
- Blumenstock, T., G. Kopp, F. Hase, G. Hochschild, S. Mikuteit, U. Raffalski, and R. Ruhnke, Observation of unusual chlorine activation by ground-based infrared and microwave spectroscopy in the late Arctic winter 2000/01, *Atmos. Chem. Phys.*, *6*, 897-905, 2006.
- Bodeker, G.E., J.C. Scott, K. Kreher, and R.L. McKenzie, Global ozone trends in potential vorticity coordinates using TOMS and GOME intercompared against the Dobson network: 1978-1998, *J. Geophys. Res.*, *106* (D19), 23029-23042, 2001.
- Bodeker, G.E., H. Shiona, and H. Struthers, The NIWA assimilated total column ozone data base and assimilated trace gas profile data base for validation of CCMs, paper presented at *CCMVal 2005 Workshop*, October 2005, Boulder, Colo. Available: http://www.pa.op.dlr.de/workshops/CCMVal2005/CCMVal2005_abstract.html, 2005.
- Bojkov, R.D., and V.E. Fioletov, Total ozone variations in the tropical belt: An application for quality of ground based measurements, *Meteorol. Atmos. Phys.*, *58* (1-4), 223-240, 1996.
- Bojkov, R.D., C.S. Zerefos, D.S. Balis, I.C. Ziomas, and A.F. Bais, Record low total ozone during northern winters of 1992 and 1993, *Geophys. Res. Lett.*, *20* (13), 1351-1354, 1993.
- Bojkov, R.D., E. Kosmidis, J.J. DeLuisi, I. Petropavlovskikh, V.E. Fioletov, S. Godin, and C. Zerefos, Vertical ozone distribution characteristics deduced from ~44,000 re-evaluated Umkehr profiles (1957-2000), *Meteorol. Atmos. Phys.*, *79* (3-4), 127-158, 2002.
- Borrmann, S., S. Solomon, L. Avallone, D. Toohey, and D. Baumgardner, On the occurrence of ClO in cirrus clouds and volcanic aerosol in the tropopause region, *Geophys. Res. Lett.*, *24* (16), 2011-2014, 1997.
- Bortz, S.E., M.J. Prather, J.-P. Cammas, V. Thouret, and H. Smit, Ozone, water vapor, and temperature in the upper tropical troposphere: Variations over a decade of MOZAIC measurements, *J. Geophys. Res.*, *111*, D05305, doi: 10.1029/2005JD006512, 2006.
- Braesicke, P., and J.A. Pyle, Changing ozone and changing circulation in northern mid-latitudes: Possible feedbacks?, *Geophys. Res. Lett.*, *30* (2), 1059, doi: 10.1029/2002GL015973, 2003.
- Brasseur, G., The response of the middle atmosphere to long-term and short-term solar variability: A two-dimensional model, *J. Geophys. Res.*, *98* (D12), 23079-23090, 1993.
- Bregman, B., P.-H. Wang, and J. Lelieveld, Chemical ozone loss in the tropopause region on subvisible ice clouds, calculated with a chemistry-transport model, *J. Geophys. Res.*, *107* (D3), 4032, doi: 10.1029/2001JD000761, 2002.
- Brinksma, E.J., Y.J. Meijer, B.J. Connor, G.L. Manney, J.B. Bergwerff, G.E. Bodeker, I.S. Boyd, J.B. Liley, W. Hogervorst, J.W. Hovenier, N.J. Livesey, and D.P.J. Swart, Analysis of record-low ozone values during the 1997 winter over Lauder, New Zealand, *Geophys. Res. Lett.*, *25* (15), 2785-2788, 1998.
- Brönnimann, S., and L.L. Hood, Frequency of low-ozone events over northwestern Europe in 1952-1963 and 1990-2000, *Geophys. Res. Lett.*, *30* (21), 2118, doi: 10.1029/2003GL018431, 2003.
- Brönnimann, S., J. Staehelin, S.F.G. Farmer, J.C. Cain, T. Svendby, and T. Svenøe, Total ozone observations prior to the IGY. I: A history, *Quart. J. Roy. Meteorol. Soc.*, *129* (593), 2797-2817, 2003a.
- Brönnimann, S., J.C. Cain, J. Staehelin, and S.F.G. Farmer, Total ozone observations prior to the IGY. II: Data and quality, *Quart. J. Roy. Meteorol. Soc.*, *129* (593), 2819-2843, 2003b.
- Brönnimann, S., J. Luterbacher, J. Staehelin, and T. Svendby, An extreme anomaly in stratospheric ozone over Europe in 1940-1942, *Geophys. Res. Lett.*, *31*, L08101, doi: 10.1029/2004GL019611, 2004a.
- Brönnimann, S., J. Luterbacher, J. Staehelin, T.M. Svendby, G. Hansen, and T. Svenøe, Extreme climate of the global troposphere and stratosphere in 1940-42 related to El Niño, *Nature*, *431* (7011), 971-974, 2004b.
- Brühl, C., P.J. Crutzen, and J.U. Groöb, High-latitude, summertime NO_x activation and seasonal ozone decline in the lower stratosphere: Model calculations based on observations by HALOE on UARS,

- J. Geophys. Res.*, 103 (D3), 3587-3597, 1998.
- Brunner, D., J. Staehelin, H.-R. Künsch, and G.E. Bodeker, A Kalman filter reconstruction of the vertical ozone distribution in an equivalent latitude – potential temperature framework from TOMS/GOME/SBUV total ozone observations, *J. Geophys. Res.*, 111, D12308, doi: 10.1029/2005JD006279, 2006.
- Burrows, J.P., M. Weber, M. Buchwitz, V. Rozanov, A. Ladstaeetter-Weissenmayer, A. Richter, R. de Beek, R. Hoogen, K. Bramstedt, K.U. Eichmann, and M. Eisinger, The Global Ozone Monitoring Experiment (GOME): mission concept and first scientific results, *J. Atmos. Sci.*, 56 (2), 151-175, 1999.
- Butkovskaya, N.I., A. Kukui, N. Pouvesle, and G. Le Bras, Formation of nitric acid in the gas-phase HO₂ + NO reaction: effects of temperature and water vapor, *J. Phys. Chem. A*, 109 (29), 6509-6520, 2005.
- Calisesi, Y., R. Stübi, N. Kämpfer, and P. Viatte, Investigation of systematic uncertainties in Brewer-Mast ozone soundings using observations from a ground-based microwave radiometer, *J. Atmos. Oceanic Technol.*, 20 (11), 1543-1551, 2003.
- Callis, L.B., M. Natarajan, and J.D. Lambeth, Calculated upper stratospheric effects of solar UV flux and NO_y variations during the 11-year solar cycle, *Geophys. Res. Lett.*, 27 (23), 3869-3872, 2000.
- Callis, L.B., M. Natarajan, and J.D. Lambeth, Solar-atmospheric coupling by electrons (SOLACE): 3. Comparisons of simulations and observations, 1979-1997, issues and implications, *J. Geophys. Res.*, 106 (D7), 7523-7539, 2001.
- Chandra, S., and R.D. McPeters, The solar cycle variation of ozone in the stratosphere inferred from Nimbus-7 and NOAA-11 satellites, *J. Geophys. Res.*, 99 (D10), 20665-20671, 1994.
- Chen, L., J. London, and G. Brasseur, Middle atmospheric ozone and temperature responses to solar irradiance variations over 27-day periods, *J. Geophys. Res.*, 102 (D25), 29957-29980, 1997.
- Chipperfield, M.P., Multiannual simulations with a three-dimensional chemical transport model, *J. Geophys. Res.*, 104 (D1), 1781-1805, 1999.
- Chipperfield, M.P., A three-dimensional model study of long-term mid-high latitude lower stratosphere ozone changes, *Atmos. Chem. Phys.*, 3, 1253-1265, 2003.
- Chipperfield, M.P., New version of the TOMCAT/SLIMCAT off-line chemical transport model: Intercomparison of stratospheric tracer experiments, *Quart. J. Roy. Meteorol. Soc.*, 132 (617), 1179-1203, 2006.
- Clancy, R.T., and D.O. Muhleman, Ground-based microwave spectroscopy of the Earth's stratosphere and mesosphere, Chapter 7 in *Atmospheric Remote Sensing by Microwave Radiometry*, edited by M.A. Janssen, 335-381, John Wiley & Sons, Inc., New York, 1993.
- Coldewey-Egbers, M., M. Weber, L.N. Lamsal, R. de Beek, M. Buchwitz, and J.P. Burrows, Total ozone retrieval from GOME UV spectral data using the weighting function DOAS approach, *Atmos. Chem. Phys.*, 5, 1015-1025, 2005.
- Connor, B.J., G.E. Bodeker, R.L. McKenzie, and I.S. Boyd, The total ozone anomaly at Lauder, NZ in 1997, *Geophys. Res. Lett.*, 26 (2), 189-192, 1999.
- Considine, D.B., A.R. Douglass, P.S. Connell, D.E. Kinnison, and D.A. Rotman, A polar stratospheric cloud parameterization for the global modeling initiative three-dimensional model and its response to stratospheric aircraft, *J. Geophys. Res.*, 105 (D3), 3955-3974, 2000.
- Cordero, E.C., and T.R. Nathan, An examination of anomalously low column ozone in the Southern Hemisphere midlatitudes during 1997, *Geophys. Res. Lett.*, 29 (7), 1123, doi: 10.1029/2001GL013948, 2002.
- Cox, R.A., M.A. Fernandez, A. Symington, M. Ullerstam, and J.P.D. Abbatt, A kinetic model for uptake of HNO₃ and HCl on ice in a coated wall flow system, *Phys. Chem. Chem. Phys.*, 7 (19), 3434-3442, 2005.
- Cunnold, D.M., J.M. Zawodny, W.P. Chu, J.P. Pommereau, F. Goutail, J. Lenoble, M.P. McCormick, R.E. Veiga, D. Murcray, N. Iwagami, K. Shibasaki, P.C. Simon, and W. Peetermans, Validation of SAGE II NO₂ measurements, *J. Geophys. Res.*, 96 (D7), 12913-12925, 1991.
- Cunnold, D.M., E.-S. Yang, M.J. Newchurch, G.C. Reinsel, J.M. Zawodny, and J.M. Russell III, Comment on "Enhanced upper stratospheric ozone: Sign of recovery or solar cycle effect?" by W. Steinbrecht et al., *J. Geophys. Res.*, 109, D14305, doi: 10.1029/2004JD004826, 2004.
- Daniel, J.S., S. Solomon, and D.L. Albritton, On the evaluation of halocarbon radiative forcing and global warming potentials, *J. Geophys. Res.*, 100 (D1), 1271-1285, 1995.
- Delval, C., and M.J. Rossi, Influence of monolayer amounts of HNO₃ on the evaporation rate of H₂O over ice in the range 179 to 208 K: A quartz crystal microbalance study, *J. Phys. Chem. A*, 109 (32), 7151-7165, 2005.
- Deshler, T., R. Anderson-Sprecher, H. Jäger, J. Barnes, D.J. Hofmann, B. Clemesha, D. Simonich, M. Osborn, R.G. Grainger, and S. Godin-Beekmann,

GLOBAL OZONE

- Trends in the nonvolcanic component of stratospheric aerosol over the period 1971-2004, *J. Geophys. Res.*, *111*, D01201, doi: 10.1029/2005JD006089, 2006.
- Dhomse, S., M. Weber, I. Wohltmann, M. Rex, and J.P. Burrows, On the possible causes of recent increases in NH total ozone from a statistical analysis of satellite data from 1979 to 2003, *Atmos. Chem. Phys.*, *6*, 1165-1180, 2006.
- Dillon, T.J., D. Hölscher, V. Sivakumaran, A. Horowitz, and J.N. Crowley, Kinetics of the reactions of HO with methanol (210-351 K) and with ethanol (216-368 K), *Phys. Chem. Chem. Phys.*, *7* (2), 349-355, 2005.
- Donovan, D.P., H. Fast, Y. Makino, J.C. Bird, A.I. Carswell, J. Davies, T.J. Duck, J.W. Kaminski, C.T. McElroy, R.L. Mittermeier, S.R. Pal, V. Savastiouk, D. Velkov, and J.A. Whiteway, Ozone, column ClO, and PSC measurements made at the NDSC Eureka observatory (80°N, 86°W) during the spring of 1997, *Geophys. Res. Lett.*, *24* (22), 2709-2712, 1997.
- Douglass, A.R., R.S. Stolarski, S.E. Strahan, and P.S. Connell, Radicals and reservoirs in the GMI chemistry and transport model: Comparison to measurements, *J. Geophys. Res.*, *109*, D16302, doi: 10.1029/2004JD004632, 2004.
- Durry, G., and A. Hauchecorne, Evidence for long-lived polar vortex air in the mid-latitude summer stratosphere from in situ laser diode CH₄ and H₂O measurements, *Atmos. Chem. Phys.*, *5*, 1467-1472, 2005.
- Dütsch, H.U., and J. Staehelin, Results of the new and old Umkehr algorithm compared with ozone soundings, *J. Atmos. Terr. Phys.*, *54* (5), 557-569, 1992.
- Egorova, T., E. Rozanov, E. Manzini, M. Haberer, W. Schmutz, V. Zubov, and T. Peter, Chemical and dynamical response to the 11-year variability of the solar irradiance simulated with a chemistry-climate model, *Geophys. Res. Lett.*, *31*, L06119, doi: 10.1029/2003GL019294, 2004.
- Eskes, H.J., R.J. van der A, E.J. Brinksma, J.P. Veefkind, J.F. de Haan, and P.J.M. Valks, Retrieval and validation of ozone columns derived from measurements of SCIAMACHY on Envisat, *Atmos. Chem. Phys. Discuss.*, *5* (4), 4429-4475, 2005.
- Evans, J.T., M.P. Chipperfield, H. Oelhaf, M. Stowasser, and G. Wetzell, Effect of near-IR photolysis of HO₂NO₂ on stratospheric chemistry, *Geophys. Res. Lett.*, *30* (5), 1223, doi: 10.1029/2002GL016470, 2003.
- Eyring, V., N. Butchart, D.W. Waugh, H. Akiyoshi, J. Austin, S. Bekki, G.E. Bodeker, B.A. Boville, C. Brühl, M.P. Chipperfield, E. Cordero, M. Dameris, M. Deushi, V.E. Fioletov, S.M. Frith, R.R. Garcia, A. Gettelman, M.A. Giorgetta, V. Grewe, L. Jourdain, D.E. Kinnison, E. Mancini, E. Manzini, M. Marchand, D.R. Marsh, T. Nagashima, P.A. Newman, J.E. Nielsen, S. Pawson, G. Pitari, D.A. Plummer, E. Rozanov, M. Schraner, T.G. Shepherd, K. Shibata, R.S. Stolarski, H. Struthers, W. Tian, and M. Yoshiki, Assessment of temperature, trace species, and ozone in chemistry-climate model simulations of the recent past, *J. Geophys. Res.*, *111*, D22308, doi: 10.1029/2006JD007327, 2006.
- Feng, W., M.P. Chipperfield, M. Dorf, and K. Pfeilsticker, Mid-latitude ozone changes: Studies with a 3-D CTM forced by ERA-40 analyses, *Atmos. Chem. Phys. Discuss.*, *6*, 6695-6722, 2006.
- Fernandez, M.A., R.G. Hynes, and R.A. Cox, Kinetics of ClONO₂ reactive uptake on ice surfaces at temperatures of the upper troposphere, *J. Phys. Chem. A*, *109* (44), 9986-9996, 2005.
- Fioletov, V.E., and T.G. Shepherd, Seasonal persistence of midlatitude total ozone anomalies, *Geophys. Res. Lett.*, *30* (7), 1417-1420, 2003.
- Fioletov, V.E., and T.G. Shepherd, Summertime total ozone variations over middle and polar latitudes, *Geophys. Res. Lett.*, *32*, L04807, doi: 10.1029/2004GL022080, 2005.
- Fioletov, V.E., G.E. Bodeker, A.J. Miller, R.D. McPeters, and R. Stolarski, Global and zonal total ozone variations estimated from ground-based and satellite measurements: 1964-2000, *J. Geophys. Res.*, *107* (D22), 4647, doi: 10.1029/2001JD001350, 2002.
- Fioletov, V.E., J.B. Kerr, C.T. McElroy, D.I. Wardle, V. Savastiouk, and T.S. Grajnar, The Brewer reference triad, *Geophys. Res. Lett.*, *32*, L20805, doi: 10.1029/2005GL024244, 2005.
- Fioletov, V.E., D.W. Tarasick, and I. Petropavlovskikh, Estimating ozone variability and instrument uncertainties from SBUV(2), ozonesonde, Umkehr, and SAGE II measurements: Short-term variations, *J. Geophys. Res.*, *111*, D02305, doi: 10.1029/2005JD006340, 2006.
- Frith, S., R. Stolarski, and P.K. Bhartia, Implications of Version 8 TOMS and SBUV data for long-term trend analysis, in *Ozone Vol. I, Proceedings of the XX Quadrennial Ozone Symposium*, 1-8 June 2004, Kos, Greece, edited by C.S. Zerefos, 65-66, Int. Ozone Comm., Athens, Greece, 2004.
- Fromm, M.D., and R. Servranckx, Transport of forest fire smoke above the tropopause by supercell convection, *Geophys. Res. Lett.*, *30* (10), 1542, doi: 10.1029/2002GL016820, 2003.
- Fromm, M., R. Bevilacqua, R. Servranckx, J. Rosen, J.P.

- Thayer, J. Herman, and D. Larko, Pyrocumulonimbus injection of smoke to the stratosphere: Observations and impact of a super blowup in northwestern Canada on 3-4 August 1998, *J. Geophys. Res.*, *110*, D08205, doi: 10.1029/2004JD005350, 2005.
- Fusco, A.C., and M.L. Salby, Interannual variations of total ozone and their relationship to variations of planetary wave activity, *J. Clim.*, *12* (6), 1619-1629, 1999.
- Gao, R.S., P.J. Popp, D.W. Fahey, T.P. Marcy, R.L. Herman, E.M. Weinstock, D.G. Baumgardner, T.J. Garrett, K.H. Rosenlof, T.L. Thompson, P.T. Bui, B.A. Ridley, S.C. Wofsy, O.B. Toon, M.A. Tolbert, B. Karcher, T. Peter, P.K. Hudson, A.J. Weinheimer, and A.J. Heymsfield, Evidence that nitric acid increases relative humidity in low-temperature cirrus clouds, *Science*, *303* (5657), 516-520, 2004.
- Gerding, M., G. Baumgarten, U. Blum, J.P. Thayer, K.-H. Fricke, R. Neuber, and J. Fiedler, Observations of an unusual mid-stratospheric aerosol layer in the Arctic: possible sources and implications for polar vortex dynamics, *Ann. Geophys.*, *21* (4), 1057-1069, 2003.
- Gleason, J.F., P.K. Bhartia, J.R. Herman, R. McPeters, P. Newman, R.S. Stolarski, L. Flynn, G. Labow, D. Larko, C. Seftor, C. Wellemeyer, W.D. Komhyr, A.J. Miller, and W. Planet, Record low global ozone in 1992, *Science*, *260* (5107), 523-526, 1993.
- Godin, S., V. Bergeret, S. Bekki, C. David, and G. Mégie, Study of the interannual ozone loss and the permeability of the Antarctic polar vortex from aerosol and ozone lidar measurements in Dumont d'Urville (66.4°S, 140°E), *J. Geophys. Res.*, *106* (D1), 1311-1330, 2001.
- Godin, S., M. Marchand, A. Hauchecorne, and F. Lefèvre, Influence of Arctic polar ozone depletion on lower stratospheric ozone amounts at Haute-Provence Observatory (43.92°N, 5.71°E), *J. Geophys. Res.*, *107* (D20), 8272, doi: 10.1029/2001JD000516, 2002.
- Graf, H.-F., I. Kirchner, and J. Perlwitz, Changing lower stratospheric circulation: The role of ozone and greenhouse gases, *J. Geophys. Res.*, *103* (D10), 11251-11261, 1998.
- Griffin, R.E.M., V. Fioletov, and J.C. McConnell, Measurements of historical total ozone from the Chalonge-Divan stellar spectrum program: A reanalysis of the 1953-1972 data and a comparison with simultaneous Dobson Arosa measurements, *J. Geophys. Res.*, *111*, D12309, doi: 10.1029/2005JD006476, 2006.
- Guillas, S., M.L. Stein, D.J. Wuebbles, and J. Xia, Using chemistry transport modeling in statistical analysis of stratospheric ozone trends from observations, *J. Geophys. Res.*, *109*, D22303, doi: 10.1029/2004JD005049, 2004.
- Guirlet, M., P. Keckhut, S. Godin, and G. Mégie, Description of the long-term ozone data series obtained from different instrumental techniques at a single location: the Observatoire de Haute-Provence (43.9°N, 5.7°E), *Ann. Geophys.*, *18* (10), 1325-1339, 2000.
- Hadjinicolaou, P., and J.A. Pyle, The impact of Arctic ozone depletion on northern middle latitudes: interannual variability and dynamical control, *J. Atmos. Chem.*, *47* (1), 25-43, 2004.
- Hadjinicolaou, P., J.A. Pyle, M.P. Chipperfield, and J.A. Kettleborough, Effect of interannual meteorological variability on mid-latitude O₃, *Geophys. Res. Lett.*, *24* (23), 2993-2996, 1997.
- Hadjinicolaou, P., A. Jrrar, J.A. Pyle, and L. Bishop, The dynamically driven long-term trend in stratospheric ozone over northern middle latitudes, *Quart. J. Roy. Meteorol. Soc.*, *128* (583), 1393-1412, 2002.
- Hadjinicolaou, P., J.A. Pyle, and N.R.P. Harris, The recent turnaround in stratospheric ozone over northern middle latitudes: A dynamical modeling perspective, *Geophys. Res. Lett.*, *32*, L12821, doi: 10.1029/2005GL022476, 2005.
- Haigh, J.D., The role of stratospheric ozone in modulating the solar radiative forcing of climate, *Nature*, *370* (6490), 544-546, 1994.
- Hamilton, K., On the quasi-decadal modulation of the stratospheric QBO period, *J. Clim.*, *15* (17), 2562-2565, 2002.
- Hansen, G., and T. Svenøe, Multilinear regression analysis of the 65-year Tromsø total ozone series, *J. Geophys. Res.*, *110*, D10103, doi: 10.1029/2004JD005387, 2005.
- Harris, J.M., S.T. Oltmans, G.E. Bodeker, R. Stolarski, R.D. Evans, and D.M. Quincy, Long-term variations in total ozone derived from Dobson and satellite data, *Atmos. Environ.*, *37* (23), 3167-3175, 2003.
- Hartogh, P., C. Jarchow, G.R. Sonnemann, and M. Grygalashvyly, On the spatiotemporal behavior of ozone within the upper mesosphere/mesopause region under nearly polar night conditions, *J. Geophys. Res.*, *109*, D18303, doi: 10.1029/2004JD004576, 2004.
- Hofmann, D.J., S.J. Oltmans, W.D. Komhyr, J.M. Harris, J.A. Lathrop, A.O. Langford, T. Deshler, B.J. Johnson, A. Torres, and W.A. Matthews, Ozone loss in the lower stratosphere over the United States in

GLOBAL OZONE

- 1992-1993: Evidence for heterogeneous chemistry on the Pinatubo aerosol, *Geophys. Res. Lett.*, 21 (1), 65-68, 1994.
- Hollandsworth, S.M., R.D. McPeters, L.E. Flynn, W. Planet, A.J. Miller, and S. Chandra, Ozone trends deduced from combined Nimbus-7 SBUV and NOAA-11 SBUV/2 data, *Geophys. Res. Lett.*, 22 (8), 905-908, 1995.
- Hood, L.L., The solar cycle variation of total ozone: Dynamical forcing in the lower stratosphere, *J. Geophys. Res.*, 102 (D1), 1355-1370, 1997.
- Hood, L.L., Effects of solar UV variability on the stratosphere, in *Solar Variability and its Effect on the Earth's Atmospheric and Climate System*, edited by J. Pap, P. Fox, C. Frohlich, H. Hudson, J. Kuhn, J. McCormack, G. North, W. Sprigg, and S.T. Wu, 283-304, American Geophysical Union, Washington, D.C., 2004.
- Hood, L.L., and B.E. Soukharev, Interannual variations of total ozone at northern midlatitudes correlated with stratospheric EP flux and potential vorticity, *J. Atmos. Sci.*, 62 (10), 3724-3740, 2005.
- Hood, L.L., and B.E. Soukharev, Solar induced variations of odd nitrogen: Multiple regression analysis of UARS HALOE data, *Geophys. Res. Lett.*, 33, L22805, doi: 10.1029/2006GL028122, 2006.
- Hood, L.L., R.D. McPeters, J.P. McCormack, L.E. Flynn, S.M. Hollandsworth, and J.F. Gleason, Altitude dependence of stratospheric ozone trends based on Nimbus-7 SBUV data, *Geophys. Res. Lett.*, 20 (23), 2667-2670, 1993.
- Hood, L.L., J.P. McCormack, and K. Labitzke, An investigation of dynamical contributions to midlatitude ozone trends in winter, *J. Geophys. Res.*, 102 (D11), 13079-13093, 1997.
- Hood, L.L., S. Rossi, and M. Beulen, Trends in lower stratospheric zonal winds, Rossby wave breaking behavior, and column ozone at northern midlatitudes, *J. Geophys. Res.*, 104 (D20), 24321-24339, 1999.
- Hood, L.L., B.E. Soukharev, M. Fromm, and J. McCormack, Origin of extreme ozone minima at middle to high northern latitudes, *J. Geophys. Res.*, 106 (D18), 20925-20940, 2001.
- Hurrell, J.W., Decadal trends in the North Atlantic Oscillation regional temperatures and precipitation, *Science*, 269 (5224), 676-679, 1995.
- Hynes, R.G., M.A. Fernandez, and R.A. Cox, Uptake of HNO₃ on water-ice and coadsorption of HNO₃ and HCl in the temperature range 210-235 K, *J. Geophys. Res.*, 107 (D24), 4797, doi: 10.1029/2001JD001557, 2002.
- Jonson, J.E., D. Simpson, H. Fagerli, and S. Solberg, Can we explain the trends in European ozone levels?, *Atmos. Chem. Phys.*, 6, 51-66, 2006.
- Jost, H.-J., K. Drdla, A. Stohl, L. Pfister, M. Loewenstein, J.P. Lopez, P.K. Hudson, D.M. Murphy, D.J. Cziczo, M. Fromm, T.P. Bui, J. Dean-Day, C. Gerbig, M.J. Mahoney, E.C. Richard, N. Spichtinger, J.V. Pittman, E.M. Weinstock, J.C. Wilson, and I. Xueref, In-situ observations of mid-latitude forest fire plumes deep in the stratosphere, *Geophys. Res. Lett.*, 31, L11101, doi: 10.1029/2003GL019253, 2004.
- Kanamitsu, M., W. Ebisuzaki, J. Woollen, S.K. Yang, J.J. Hnilo, M. Fiorino, and G.L. Potter, NCEP-DOE AMIP-II reanalysis (R-2), *Bull. Amer. Meteorol. Soc.*, 83 (11), 1631-1643, 2002.
- Keckhut, P., A. Hauchecorne, S. Bekki, A. Colette, C. David, and J. Jumelet, Indications of thin cirrus clouds in the stratosphere at mid-latitudes, *Atmos. Chem. Phys.*, 5, 3407-3414, 2005a.
- Keckhut, P., I. McDermid, D. Swart, T. McGee, S. Godin-Beekmann, A. Adriani, J. Barnes, J.L. Baray, H. Bencherif, H. Claude, A.G. di Sarra, G. Fiocco, G. Hansen, A. Hauchecorne, T. Leblanc, C.H. Lee, S. Pal, G. Mégie, H. Nakane, R. Neuber, W. Steinbrecht, and J. Thayer, Review of ozone and temperature lidar validations performed within the framework of the Network for the Detection of Stratospheric Change, *J. Environ. Monit.*, 6 (9), 721-733, 2005b.
- Keim, E.R., D.W. Fahey, L.A. DelNegro, E.L. Woodbridge, R.S. Gao, P.O. Wennberg, R.C. Cohen, R.M. Stimpfle, K.K. Kelly, E.J. Hints, J.C. Wilson, H.H. Jonsson, J.E. Dye, D. Baumgardner, S.R. Kawa, R.J. Salawitch, M.H. Proffitt, M. Loewenstein, J.R. Podolske, and K.R. Chan, Observations of large reductions in the NO/NO_y ratio near the mid-latitude tropopause and the role of heterogeneous chemistry, *Geophys. Res. Lett.*, 23 (22), 3223-3226, 1996.
- Kerr, J.B., C.T. McElroy, and R.A. Olafson, Measurements of ozone with the Brewer spectrophotometer, in *Proceedings of the Quadrennial International Ozone Symposium*, 4-9 August 1980, Boulder, Colo., edited by J. London, 74-79, National Center for Atmospheric Research, 1981.
- Kerr, J.B., D.I. Wardle, and D.W. Tarasick, Record low ozone values over Canada in early 1993, *Geophys. Res. Lett.*, 20 (18), 1979-1982, 1993.
- Klein, U., K. Lindner, S. Bagdohn, I. Wohltmann, and K.F. Kuenzi, Microwave measurements of arctic chlorine monoxide and computed chemical ozone loss in

- spring 2000, *Adv. Space Res.*, 29, 1719-1723, 2002.
- Knudsen, B.M., and S.B. Andersen, Geophysics: Longitudinal variation in springtime ozone trends, *Nature*, 413 (6857), 699-700, 2001.
- Knudsen, B.M., and J.-U. Grooß, Northern midlatitude stratospheric ozone dilution in spring modeled with simulated mixing, *J. Geophys. Res.*, 105 (D5), 6885-6890, doi: 10.1029/1999JD901076, 2000.
- Koch, G., H. Wernli, C. Schwierz, J. Staehelin, and T. Peter, A composite study on the structure and formation of ozone miniholes and minihighs over central Europe, *Geophys. Res. Lett.*, 32, L12810, doi: 10.1029/2004GL022062, 2005.
- Konopka, P., J.U. Grooß, S. Bausch, R. Müller, D.S. McKenna, O. Morgenstern, and Y. Orsolini, Dynamics and chemistry of vortex remnants in late Arctic spring 1997 and 2000: Simulations with the Chemical Lagrangian Model of Stratosphere (CLaMS), *Atmos. Chem. Phys.*, 3 (3), 839-849, 2003.
- Krizan, P., and J. Lastovicka, Trends in positive and negative ozone laminae in the Northern Hemisphere, *J. Geophys. Res.*, 110, D10107, doi: 10.1029/2004JD005477, 2005.
- Krzyżcin, J.W., Change in ozone depletion rates beginning in the mid 1990s: Trend analyses of the TOMS/SBUV merged total ozone data, 1978-2003, *Ann. Geophys.*, 24 (2), 493-502, 2006.
- Krzyżcin, J.W., J. Jaroslawski, and B. Rajewska-Wiech, Beginning of the ozone recovery over Europe? Analysis of the total ozone data from the ground-based observations, 1964-2004, *Ann. Geophys.*, 23 (5), 1685-1695, 2005.
- Laat, J. de, J. Landgraf, O. Hasekamp, I. Aben, and B. Bregman, Assimilated winds for global modelling: Evaluation with space- and balloon-borne ozone observations, *J. Geophys. Res.*, in press, 2006.
- Langematz, U., M. Kunze, K. Krüger, K. Labitzke, and G.L. Roff, Thermal and dynamical changes of the stratosphere since 1979 and their link to ozone and CO₂ changes, *J. Geophys. Res.*, 108 (D1), 4027, doi: 10.1029/2002JD002069, 2003.
- Langematz, U., J.L. Grenfell, K. Matthes, P. Mieth, M. Kunze, B. Steil, and C. Brühl, Chemical effects in 11-year solar cycle simulations with the Freie Universität Berlin Climate Middle Atmosphere Model with online chemistry (FUB-CMAM-CHEM), *Geophys. Res. Lett.*, 32, L13803, doi: 10.1029/2005GL022686, 2005.
- Leblanc, T., and I.S. McDermid, Stratospheric ozone climatology from lidar measurements at Table Mountain (34.4°N, 117.7°W) and Mauna Loa (19.5°N, 155.6°W), *J. Geophys. Res.*, 105 (D11), 14613-14623, 2000.
- Leblanc, T., and I.S. McDermid, Quasi-biennial oscillation signatures in ozone and temperature observed by lidar at Mauna Loa, Hawaii (19.5°N, 155.6°W), *J. Geophys. Res.*, 106 (D14), 14869-14874, 2001.
- Lee, H., and A.K. Smith, Simulation of the combined effects of solar cycle, quasi-biennial oscillation, and volcanic forcing on stratospheric ozone changes in recent decades, *J. Geophys. Res.*, 108 (D2), 4049, doi: 10.1029/2001JD001503, 2003.
- Lelieveld, J., J. van Aardenne, H. Fischer, M. de Reus, J. Williams, and P. Winkler, Increasing ozone over the Atlantic Ocean, *Science*, 304 (5676), 1483-1487, 2004.
- Li, J.L., D.M. Cunnold, H.J. Wang, E.S. Yang, and M.J. Newchurch, A discussion of upper stratospheric ozone asymmetries and SAGE trends, *J. Geophys. Res.*, 107 (D23), 4705, doi: 10.1029/2001JD001398, 2002.
- Liley, J.B., P.V. Johnston, R.L. McKenzie, A.J. Thomas, and I.S. Boyd, Stratospheric NO₂ variations from a long time series at Lauder, New Zealand, *J. Geophys. Res.*, 105 (D9), 11633-11640, 2000.
- Livesey, N., M.D. Fromm, J.W. Waters, G.L. Manney, M.L. Santee, and W.G. Read, Enhancements in lower stratospheric CH₃CN observed by the Upper Atmosphere Research Satellite Microwave Limb Sounder following boreal forest fires, *J. Geophys. Res.*, 109, D06308, doi: 10.1029/2003JD004055, 2004.
- Logan, J.A., Trends in the vertical distribution of ozone: An analysis of ozonesonde data, *J. Geophys. Res.* 99 (D12), 25553-25585, 1994.
- Logan, J.A., I.A. Megretskaya, A.J. Miller, G.C. Tiao, D. Choi, L. Zhang, R.S. Stolarski, G.J. Labow, S.M. Hollandsworth, G.E. Bodeker, H. Claude, D. De Muer, J.B. Kerr, D.W. Tarasick, S.J. Oltmans, B. Johnson, F. Schmidlin, J. Staehelin, P. Viatte, and O. Uchino, Trends in the vertical distribution of ozone: A comparison of two analyses of ozonesonde data, *J. Geophys. Res.*, 104 (D21), 26373-26399, 1999.
- Mahieu, E., R. Zander, P. Demoulin, M. De Mazière, F. Mélen, C. Servais, G. Roland, L. Delbouille, J. Poels, and R. Blomme, Fifteen years-trend characteristics of key stratospheric constituents monitored by FTIR above the Jungfraujoch, in *Stratospheric Ozone 1999, Proc. 5th European Symp.*, 27 September-1 October 1999, St. Jean de Luz, France, edited by N.R.P. Harris, M. Guirlet, and G.T. Amanatidis, *Air Pollution Research Rep. 73, EUR 19340*, 99-102, European Commission, Luxembourg, 2000.
- Mahowald, N.M., R.A. Plumb, P.J. Rasch, J. del Corral, F.

GLOBAL OZONE

- Sassi, and W. Heres, Stratospheric transport in a three-dimensional isentropic coordinate model, *J. Geophys. Res.*, 107 (D15), 4254, doi: 10.1029/2001JD001313, 2002.
- Malanca, F.E., P.O. Canziani, and G.A. Arguello, Trends evolution of ozone between 1980 and 2000 at mid-latitudes over the Southern Hemisphere: Decadal differences in trends, *J. Geophys. Res.*, 110, D05102, doi:10.1029/2004JD004977, 2005.
- Manney, G.L., L. Froidevaux, M.L. Santee, N.J. Livesey, J.L. Sabutis, and J.W. Waters, Variability of ozone loss during Arctic winter (1991-2000) estimated from UARS Microwave Limb Sounder measurements, *J. Geophys. Res.*, 108 (D4), 4149, doi: 10.1029/2002JD002634, 2003.
- Manney, G.L., D.R. Allen, K. Krueger, B. Naujokat, M.L. Santee, J.L. Sabutis, S. Pawson, R. Swinbank, C.E. Randall, A.J. Simmons, and C. Long, Diagnostic comparison of meteorological analyses during the 2002 Antarctic winter, *Mon. Wea. Rev.*, 133 (5), 1261-1278, 2005.
- Marchand, M., S. Godin, A. Hauchecorne, F. Lefèvre, S. Bekki, and M. Chipperfield, Influence of polar ozone loss on northern midlatitude regions estimated by a high-resolution chemistry transport model during winter 1999/2000, *J. Geophys. Res.*, 108 (D5), 8326, doi: 10.1029/2001JD000906, 2003.
- Mateer, C.L., H.U. Dutsch, and J. Staehelin, Influence of a priori profiles on trend calculations from Umkehr data, *J. Geophys. Res.*, 101 (D11), 16779-16787, 1996.
- McCormack, J.P., The influence of the 11-year solar cycle on the quasi-biennial oscillation, *Geophys. Res. Lett.*, 30 (22), 2162, doi: 10.1029/2003GL018314, 2003.
- McCormack, J.P., and L.L. Hood, Apparent solar cycle variations of upper stratospheric ozone and temperature: Latitude and seasonal dependences, *J. Geophys. Res.*, 101 (D15), 20933-20944, 1996.
- McCormack, J.P., L.L. Hood, R. Nagatani, A.J. Miller, W.G. Planet, and R.D. McPeters, Approximate separation of volcanic and 11-year signals in the SBUV-SBUV/2 total ozone record over the 1979-1995 period, *Geophys. Res. Lett.*, 24 (22), 2729-2732, 1997.
- McCormick, M.P., J.M. Zawodny, R.E. Viegas, J.C. Larsen, and P.-H. Wang, An overview of SAGE I and II ozone measurements, *Planet. Space Sci.*, 37 (12), 1567-1586, 1989.
- McPeters, R.D., T. Miles, L.E. Flynn, C.G. Wellemeyer, and J.M. Zawodny, Comparison of SBUV and SAGE II ozone profiles: Implications for ozone trends, *J. Geophys. Res.*, 99 (D10), 20513-20524, 1994.
- McPeters, R.D., J.A. Logan, and G.J. Labow, Ozone climatological profiles for version 8 TOMS and SBUV retrievals, *Eos Trans. Amer. Geophys. Union*, 84, Abstract A21D-0998, 2003.
- McPeters, R., C. Wellemeyer, and A. Ahn, The validation of version 8 ozone profiles: Is SBUV ready for prime time?, in *Ozone Vol. I, Proceedings of the XX Quadrennial Ozone Symposium*, 1-8 June 2004, Kos, Greece, edited by C.S. Zerefos, 113-114, Int. Ozone Comm., Athens, Greece, 2004.
- Meijer, E.W., B. Bregman, A. Segers, and P.F.J. van Velthoven, The influence of data assimilation on the age of air calculated with a global chemistry-transport model using ECMWF wind fields, *Geophys. Res. Lett.*, 31, L23114, doi: 10.1029/2004GL021158, 2004.
- Millard, G.A., A.M. Lee, and J.A. Pyle, A model study of the connection between polar and midlatitude ozone loss in the Northern Hemisphere lower stratosphere, *J. Geophys. Res.*, 108 (D5), 8323, doi: 10.1029/2001JD000899, 2003.
- Miller, A.J., R.M. Nagatani, L.E. Flynn, S. Kondragunta, E. Beach, R. Stolarski, R.D. McPeters, P.K. Bhartia, M.T. DeLand, C.H. Jackman, D.J. Wuebbles, K.O. Patten, and R.P. Cebula, A cohesive total ozone data set from the SBUV(/2) satellite system, *J. Geophys. Res.*, 107 (D23), 4701, doi: 10.1029/2001JD000853, 2002.
- Miller, A.J., A. Cai, G. Taio, D.J. Wuebbles, L.E. Flynn, S.-K. Yang, E.C. Weatherhead, V. Fioletov, I. Petropavlovskikh, X.-L. Meng, S. Guillas, R.M. Nagatani, and G.C. Reinsel, Examination of ozone-sonde data for trends and trend changes incorporating solar and Arctic oscillation signals, *J. Geophys. Res.*, 111, D13305, doi: 10.1029/2005JD006684, 2006.
- Monge Sanz, B., M.P. Chipperfield, A. Simmons, and S. Uppala, Mean age of air and transport in a CTM: Comparison of different ECMWF analyses, *Geophys. Res. Lett.*, in press, 2006.
- Nagahama, T., H. Nakane, Y. Fujinuma, H. Ogawa, A. Mizuno, and Y. Fukui, A semiannual variation of ozone in the middle mesosphere observed with the millimeter-wave radiometer at Tsukuba, Japan, *J. Geophys. Res.*, 108 (D21), 4684, doi: 10.1029/2003JD003724, 2003.
- Naja, M., and H. Akimoto, Contribution of regional pollution and long-range transport to the Asia-Pacific region: Analysis of long-term ozonesonde data over Japan, *J. Geophys. Res.*, 109, D21306, doi:

- 10.1029/2004JD004687, 2004.
- Nazaryan, H., and M.P. McCormick, Comparisons of Stratospheric Aerosol and Gas Experiment (SAGE II) and Solar Backscatter Ultraviolet Instrument (SBUV/2) ozone profiles and trend estimates, *J. Geophys. Res.*, *110*, D17302, doi: 10.1029/2004JD005483, 2005.
- Nazaryan, H., M.P. McCormick, and J.M. Russell III, New studies of SAGE II and HALOE ozone profile and long-term change comparisons, *J. Geophys. Res.*, *110*, D09305, doi: 10.1029/2004JD005425, 2005.
- Newchurch, M.J., E.-S. Yang, D.M. Cunnold, G.C. Reinsel, J.M. Zawodny, and J.M. Russell III, Evidence for slowdown in stratospheric ozone loss: First stage of ozone recovery, *J. Geophys. Res.*, *108* (D16), 4507, doi: 10.1029/2003JD003471, 2003.
- Newman, P.A., S.R. Kawa, and E.R. Nash, On the size of the Antarctic ozone hole, *Geophys. Res. Lett.*, *31*, L21104, doi: 10.1029/2004GL020596, 2004.
- Newman, P.A., E.R. Nash, S.R. Kawa, S.A. Montzka, and S.M. Schauffler, When will the Antarctic ozone hole recover?, *Geophys. Res. Lett.*, *33*, L12814, doi: 10.1029/2005GL025232, 2006.
- Notholt, J., B.P. Luo, S. Füglistaler, D. Weisenstein, M. Rex, M.G. Lawrence, H. Bingemer, I. Wohltmann, T. Corti, T. Warneke, R. von Kuhlmann, and T. Peter, Influence of tropospheric SO₂ emissions on particle formation and the stratospheric humidity, *Geophys. Res. Lett.*, *32*, L07810, doi: 10.1029/2004GL022159, 2005.
- Oltmans, S.J., A.S. Lefohn, J.M. Harris, I. Galbally, H.E. Scheel, G. Bodeker, E. Brunke, H. Claude, D. Tarasick, B.J. Johnson, P. Simmonds, D. Shadwick, K. Anlauf, K. Hayden, F. Schmidlin, T. Fujimoto, K. Akagi, C. Meyer, S. Nichol, J. Davies, A. Redondas, and E. Cuevas, Long-term changes in tropospheric ozone, *Atmos. Environ.*, *40* (17), 3156-3173, 2006.
- Orsolini, Y.J., Long-lived tracer patterns in the summer polar stratosphere, *Geophys. Res. Lett.*, *28* (20), 3855-3858, 2001.
- Orsolini, Y.J., and V. Limpasuvan, The North Atlantic Oscillation and the occurrences of ozone miniholes, *Geophys. Res. Lett.*, *28* (21), 4099-4102, 2001.
- Ovarlez, J., J.F. Gayet, K. Gierens, J. Strom, H. Ovarlez, F. Auriol, R. Busen, and U. Schumann, Water vapour measurements inside cirrus clouds in Northern and Southern hemispheres during INCA, *Geophys. Res. Lett.*, *29* (16), 1813-1817, 2002.
- Parrish, A., Millimeter-wave remote sensing of ozone and trace constituents in the stratosphere, *Proc. IEEE.*, *82* (12), 1915-1929, 1994.
- Peter, T., B.P. Luo, M. Wirth, C. Kiemle, H. Flentje, V.A. Yushkov, V. Khattatov, V. Rudakov, A. Thomas, S. Borrmann, G. Toci, P. Mazzinghi, J. Beuermann, C. Schiller, F. Cairo, G. Di Donfrancesco, A. Adriani, C.M. Volk, J. Strom, K. Noone, V. Mitev, R.A. MacKenzie, K.S. Carslaw, T. Trautmann, V. Santacesaria, and L. Stefanutti, Ultrathin Tropical Tropopause Clouds (UTTCS): I. Cloud morphology and occurrence, *Atmos. Chem. Phys.*, *3*, 1083-1091, 2003.
- Peters, D., and D. Waugh, Influence of barotropic shear on the poleward advection of upper-tropospheric air, *J. Atmos. Sci.*, *53* (21), 3013-3031, 1996.
- Petropavlovskikh, I., C. Ahn, P.K. Bhartia, and L.E. Flynn, Comparison and covalidation of ozone anomalies and variability observed in SBUV(2) and Umkehr northern midlatitude ozone profile estimates, *Geophys. Res. Lett.*, *32*, L06805, doi: 10.1029/2004GL022002, 2005a.
- Petropavlovskikh, I., P.K. Bhartia, and J.J. DeLuisi, New Umkehr ozone profile retrieval algorithm optimized for climatological studies, *Geophys. Res. Lett.*, *32*, L16808, doi: 10.1029/2005GL023323, 2005b.
- Piani, C., W.A. Norton, A.M. Iwi, E.A. Ray, and J.W. Elkins, Transport of ozone-depleted air on the breakup of the stratospheric polar vortex in spring/summer 2000, *J. Geophys. Res.*, *107* (D20), 8270, doi: 10.1029/2001JD000488, 2002.
- Polavarapu, S., S.Z. Ren, Y. Rochon, D. Sankey, N. Ek, J. Koshyk, and D. Tarasick, Data assimilation with the Canadian Middle Atmosphere Model, *Atmos. Ocean*, *43* (1), 77-100, 2005.
- Popp, P.J., T.P. Marcy, E.J. Jensen, B. Karcher, D.W. Fahey, R.S. Gao, T.L. Thompson, K.H. Rosenlof, E.C. Richard, R.L. Herman, E.M. Weinstock, J.B. Smith, R.D. May, H. Vomel, J.C. Wilson, A.J. Heymsfield, M.J. Mahoney, and A.M. Thompson, The observation of nitric acid-containing particles in the tropical lower stratosphere, *Atmos. Chem. Phys.*, *6*, 610-611, 2006.
- Prather, M.J., M.M. Garcia, A.R. Douglass, C.H. Jackman, M.K.W. Ko, and N.D. Sze, The space shuttle's impact on the stratosphere, *J. Geophys. Res.*, *95* (D11), 18583-18590, 1990.
- Randel, W.J., and F. Wu, A stratospheric ozone profile data set for 1979-2005: variability, trends, and comparisons with column ozone data, *J. Geophys. Res.*, *111*, doi:10.1029/2006JD007339, in press, 2006.
- Randel, W.J., F. Wu, and R. Stolarski, Changes in column ozone correlated with the stratospheric EP flux, *J. Meteorol. Soc. Japan*, *80* (4B), 849-862, 2002.
- Randel, W., P. Udelhofen, E. Fleming, M. Geller, M.

GLOBAL OZONE

- Gelman, K. Hamilton, D. Karoly, D. Ortland, S. Pawson, R. Swinbank, F. Wu, M. Baldwin, M.L. Chanin, P. Keckhut, K. Labitzke, E. Remsberg, A. Simmons, and D. Wu, The SPARC intercomparison of middle atmosphere climatologies, *J. Clim.*, *17* (5), 986-1003, 2004.
- Randel, W.J., F. Wu, H. Vömel, G.E. Nedoluha, and P. Forster, Decreases in stratospheric water vapor after 2001: Links to changes in the tropical tropopause and the Brewer-Dobson circulation, *J. Geophys. Res.*, *111*, D12312, doi:10.1029/2005JD006744, 2006.
- Ray, E.A., K.H. Rosenlof, E.C. Richard, P.K. Hudson, D.J. Cziczo, M. Loewenstein, H.J. Jost, J. Lopez, B. Ridley, A. Weinheimer, D. Montzka, D. Knapp, S.C. Wofsy, B.C. Daube, C. Gerbig, I. Xueref, and R.L. Herman, Evidence of the effect of summertime midlatitude convection on the subtropical lower stratosphere from CRYSTAL-FACE tracer measurements, *J. Geophys. Res.*, *109*, D18304, doi: 10.1029/2004JD004655, 2004.
- Reid, S.J., A.F. Tuck, and G. Kiladis, On the changing abundance of ozone minima at northern midlatitudes, *J. Geophys. Res.*, *105* (D10), 12169-12180, 2000.
- Reinsel, G.C., E.C. Weatherhead, G.C. Tiao, A.J. Miller, R.M. Nagatani, D.J. Wuebbles, and L.E. Flynn, On detection of turnaround and recovery in trend for ozone, *J. Geophys. Res.*, *107* (D10), 4078, doi: 10.1029/2001JD000500, 2002.
- Reinsel, G.C., A.J. Miller, E.C. Weatherhead, L.E. Flynn, R. Nagatani, G.C. Tiao, and D.J. Wuebbles, Trend analysis of total ozone data for turnaround and dynamical contributions, *J. Geophys. Res.*, *110*, D16306, doi: 10.1029/2004JD004662, 2005.
- Ricaud, P., P. Baron, and J. De La Noë, Quality assessment of ground-based microwave measurements of chlorine monoxide, ozone, and nitrogen dioxide from the NDSC radiometer at the Plateau de Bure, *Ann. Geophys.*, *22* (6), 1903-1915, 2004.
- Rind, D., J. Lerner, and J. Zawodny, A complementary analysis for SAGE II data profiles, *Geophys. Res. Lett.*, *32*, L07812, doi: 10.1029/2005GL022550, 2005.
- Rosenfield, J.E., S.M. Frith, and R.S. Stolarski, Version 8 SBUV ozone profile trends compared with trends from a zonally averaged chemical model, *J. Geophys. Res.*, *110*, D12302, doi: 10.1029/2004JD005466, 2005.
- Rozanov, E., L. Callis, M. Schlesinger, F. Yang, N. Andronova, and V. Zubov, Atmospheric response to NO_y source due to energetic electron precipitation, *Geophys. Res. Lett.*, *32*, L14811, doi: 10.1029/2005GL023041, 2005.
- Salawitch, R.J., P.O. Wennberg, G.C. Toon, B. Sen, and J.F. Blavier, Near IR photolysis of HO₂NO₂: Implications for HO_x, *Geophys. Res. Lett.*, *29* (16), 1762, doi: 10.1029/2002GL015006, 2002.
- Salawitch, R.J., D.K. Weisenstein, L.J. Kovalenko, C.E. Sioris, P.O. Wennberg, K. Chance, M.K.W. Ko, and C.A. McLinden, Sensitivity of ozone to bromine in the lower stratosphere, *Geophys. Res. Lett.*, *32*, L05811, doi: 10.1029/2004GL021504, 2005.
- Salby, M., and P. Callaghan, Connection between the solar cycle and the QBO: The missing link, *J. Clim.*, *13* (14), 2652-2662, 2000.
- Salby, M.L., and P.F. Callaghan, Interannual changes of the stratospheric circulation: Relationship to ozone and tropospheric structure, *J. Clim.*, *15* (24), 3673-3685, 2002.
- Salby, M.L., and P.F. Callaghan, Systematic changes of Northern Hemisphere ozone and their relationship to random interannual changes, *J. Clim.*, *17* (23), 4512-4521, 2004.
- Sander, S.P., R.R. Friedl, W.B. DeMore, D.M. Golden, M.J. Kurylo, R.F. Hampson, R.E. Huie, G.K. Moortgat, A.R. Ravishankara, C.E. Kolb, and M.J. Molina, *Chemical Kinetics and Photochemical Data for Use in Stratospheric Modeling, Evaluation No. 13, JPL Publication 00-03*, Jet Propulsion Laboratory, Pasadena, Calif., 2000.
- Sander, S.P., R.R. Friedl, D.M. Golden, M.J. Kurylo, R.E. Huie, V.L. Orkin, G.K. Moortgat, A.R. Ravishankara, C.E. Kolb, M.J. Molina, and B.J. Finlayson-Pitts, *Chemical Kinetics and Photochemical Data for Use in Atmospheric Studies: Evaluation Number 14, JPL Publication 02-25*, Jet Propulsion Laboratory, Pasadena, Calif., 2003.
- Sander, S.P., R.R. Friedl, D.M. Golden, M.J. Kurylo, G.K. Moortgat, H. Keller-Rudek, P.H. Wine, A.R. Ravishankara, C.E. Kolb, M.J. Molina, B.J. Finlayson-Pitts, R.E. Huie, and V.L. Orkin, *Chemical Kinetics and Photochemical Data for Use in Atmospheric Studies: Evaluation Number 15, JPL Publication 06-2*, Jet Propulsion Laboratory, Pasadena, Calif., 2006.
- Santer, B.D. T.M.L. Wigley, A.J. Simmons, P.W. Kallberg, G.A. Kelly, S.M. Uppala, C. Ammann, J.S. Boyle, W. Bruggemann, C. Doutriaux, M. Fiorino, C. Mears, G.A. Meehl, R. Sausen, K.E. Taylor, W.M. Washington, M.F. Wehner, and F.J. Wentz, Identification of anthropogenic climate change using a second-generation reanalysis, *J. Geophys. Res.*,

- 109, D21104, doi: 10.1029/2004JD005075, 2004.
- Saraf, N., and G. Beig, Long-term trends in tropospheric ozone over the Indian tropical region, *Geophys. Res. Lett.*, *31*, L05101, doi: 10.1029/2003GL018516, 2004.
- Scheele, M.P., P.C. Siegmund, and P.F.J. van Velthoven, Stratospheric age of air computed with trajectories based on various 3D-var and 4D-var datasets, *Atmos. Chem. Phys.*, *5*, 1-7, 2005.
- Schneider, N., O. Lezeaux, J. La Noe, J. Urban, and P. Ricaud, Validation of ground-based observations of stratomesospheric ozone, *J. Geophys. Res.*, *108* (D17), 4540, doi: 10.1029/2002JD002925, 2003.
- Schoeberl, M.R., A.R. Douglass, Z.X. Zhu, and S. Pawson, A comparison of the lower stratospheric age spectra derived from a general circulation model and two data assimilation systems, *J. Geophys. Res.*, *108* (D3), 4113, doi: 10.1029/2002JD002652, 2003.
- Shalomyanskij, A.M., I.L. Karol, L.P. Klyagina, and K.I. Romashkina, Total ozone over regions of the Russian Federation and adjacent countries from measurements at surface stations for 30 years, *Russ. Meteorol. Hydrol.*, *8*, 24-36, 2004.
- Simmonds P.G., R.G. Derwent, A.L. Manning, and G. Spain, Significant growth in surface ozone at Mace Head, Ireland, 1987-2003, *Atmos. Env.*, *38* (28), 4769-4778, 2004.
- Simmons, A.J., M. Hortal, G. Kelly, A. McNally, A. Untch, and S. Uppala, ECMWF analyses and forecasts of stratospheric winter polar vortex breakup: September 2002 in the Southern Hemisphere and related events, *J. Atmos. Sci.*, *62* (3), 668-689, 2005.
- Sinnhuber, B.-M., A. Rozanov, N. Sheode, O.T. Afe, A. Richter, M. Sinnhuber, F. Wittrock, J.P. Burrows, G.P. Stiller, T. von Clarmann, and A. Linden, Global observations of stratospheric bromine monoxide from SCIAMACHY, *Geophys. Res. Lett.*, *32*, L20810, doi: 10.1029/2005GL023839, 2005.
- Sivakumaran, V., and J.N. Crowley, Reaction between OH and CH₃CHO, Part 2. Temperature dependent rate coefficients (201-348 K), *Phys. Chem. Chem. Phys.*, *5* (1), 106-111, 2003.
- Sivakumaran, V., D. Holscher, T.J. Dillon, and J.N. Crowley, Reaction between OH and HCHO: temperature dependent rate coefficients (202-399K) and product pathways (298 K), *Phys. Chem. Chem. Phys.*, *5* (21), 4821-4827, 2003.
- Solomon, S., R.W. Portmann, R.R. Garcia, L.W. Thomason, L.R. Poole, and M.P. McCormick, The role of aerosol variations in anthropogenic ozone depletion at northern midlatitudes, *J. Geophys. Res.*, *101* (D3), 6713-6727, 1996.
- Solomon, S., S. Bormann, R.R. Garcia, R. Portmann, L. Thomason, L.R. Poole, D. Winker, and M.P. McCormick, Heterogeneous chlorine chemistry in the tropopause region, *J. Geophys. Res.*, *102* (D17), 21411-21430, 1997.
- Soukharev, B.E., and L.L. Hood, Solar cycle variation of stratospheric ozone: Multiple regression analysis of long-term satellite data sets and comparisons with models, *J. Geophys. Res.*, *111* (D20314), doi: 10.1029/2006JD007107, 2006.
- SPARC (Stratospheric Processes And their Role in Climate), *SPARC/IOC/GAW Assessment of Trends in the Vertical Distribution of Ozone*, edited by N. Harris, R. Hudson, and C. Phillips, *SPARC Report No. 1, WMO Global Ozone Research and Monitoring Project Report No. 43*, 289 pp., Verrières le Buisson, France, 1998.
- SPARC (Stratospheric Processes And their Role in Climate), *SPARC Assessment of Stratospheric Aerosol Properties*, edited by L. Thomason, and Th. Peter, *World Climate Research Program Report 124, SPARC Report 4*, 346 pp., Verrières le Buisson, France, 2006.
- Spichtinger, P., K. Gierens, H.G.J. Smit, J. Ovarlez, and J.F. Gayet, On the distribution of relative humidity in cirrus clouds, *Atmos. Chem. Phys.*, *4*, 639-647, 2004.
- Stahelin, J., J. Kerr, R. Evans, and K. Vanicek, *Comparison of Total Ozone Measurements of Dobson and Brewer Spectrophotometers and Recommended Transfer Functions*, WMO/TD No. 1147, World Meteorological Organization, Geneva, Switzerland, 2003.
- Steinbrecht, W., H. Claude, and U. Köhler, Correlations between tropopause height and total ozone: Implications for long-term changes, *J. Geophys. Res.*, *103* (D15), 19183-19192, 1998.
- Steinbrecht, W., H. Claude, and P. Winkler, Enhanced upper stratospheric ozone: Sign of recovery or solar cycle effect?, *J. Geophys. Res.*, *109*, D14305, doi: 10.1029/2004JD004826, 2004a.
- Steinbrecht, W., H. Claude, and P. Winkler, Reply to comment by D.M. Cunnold et al. on "Enhanced upper stratospheric ozone: Sign of recovery or solar cycle effect?" *J. Geophys. Res.*, *109*, D14306, doi: 10.1029/2004JD004948, 2004b.
- Steinbrecht, W., H. Claude, F. Schöenborn, I.S. McDermid, T. Leblanc, S. Godin, T. Song, D.P.J. Swart, Y.J. Meijer, G.E. Bodeker, B.J. Connor, N. Kämpfer, K. Hocke, Y. Calisesi, N. Schneider, J. de la Noë, A.D. Parrish, I.S. Boyd, C. Brühl, B. Steil, M.A. Giorgetta, E. Manzini, L.W. Thomason, J.M.

GLOBAL OZONE

- Zawodny, M.P. McCormick, J.M. Russell III, P.K. Bhartia, R.S. Stolarski, and S.M. Hollandsworth-Frith, Long-term evolution of upper stratospheric ozone at selected stations of the Network for the Detection of Stratospheric Change (NDSC), *J. Geophys. Res.*, *111*, D10308, doi: 10.1029/2005JD006454, 2006.
- Stolarski, R.S., and S. Frith, Search for evidence of trend slow-down in the long-term TOMS/SBUV total ozone data record: the importance of instrument drift uncertainty and fingerprint detection, *Atmos. Chem. Phys. Discuss.*, *6*, 3883-3912, 2006.
- Stolarski, R., and W. Randel, Ozone change as a function of altitude, Chapter 3 in *SPARC/IOC/GAW Assessment of Trends in the Vertical Distribution of Ozone*, edited by N. Harris, R. Hudson, and C. Phillips, *SPARC Report No. 1, WMO Global Ozone Research and Monitoring Project Report No. 43*, 289 pp., Verrières le Buisson, France, 1998.
- Stolarski, R.S., G.J. Labow, and R.D. McPeters, Springtime Antarctic total ozone measurements in the early 1970s from the BUUV instrument on Nimbus 4, *Geophys. Res. Lett.*, *24* (5), 591-594, 1997.
- Stolarski, R.S., A.R. Douglass, S. Steenrod, and S. Pawson, Trends in stratospheric ozone: Lessons learned from a 3D Chemical Transport Model, *J. Atmos. Sci.*, *63* (3), 1028-1041, 2006.
- Strahan, S.E., and A.R. Douglass, Evaluating the credibility of transport processes in simulations of ozone recovery using the Global Modeling Initiative three-dimensional model, *J. Geophys. Res.*, *109*, D05110, doi: 10.1029/2003JD004238, 2004.
- Ström, J., M. Seifert, B. Kärcher, J. Ovarlez, A. Minikin, J.-F. Gayet, R. Krejci, A. Petzold, F. Auriol, W. Haag, R. Busen, U. Schumann, and H.C. Hansson, Cirrus cloud occurrence as a function of ambient relative humidity: A comparison of observations obtained during the INCA experiment, *Atmos. Chem. Phys.*, *3*, 1807-1816, 2003.
- Svenby, T.M., and A. Dahlback, Statistical analysis of total ozone measurements in Oslo, Norway, 1978-1998, *J. Geophys. Res.*, *109*, D16107, doi: 10.1029/2004JD004679, 2004.
- Swinbank, R., N.B. Ingleby, P.M. Boorman, and R.J. Renshaw, *A 3D Variational Data Assimilation System for the Stratosphere and Troposphere*, Forecasting Research Division Scientific Paper No. 71, U.K. Met. Office, NWP Division, Berkshire, U.K., 2002.
- Tan, W.W., M.A. Geller, S. Pawson, and A. da Silva, A case study of excessive subtropical transport in the stratosphere of a data assimilation system, *J. Geophys. Res.*, *109*, D11102, doi: 10.1029/2003JD004057, 2004.
- Tarasick, D.W., V.E. Fioletov, D.I. Wardle, J.B. Kerr, and J. Davies, Changes in the vertical distribution of ozone over Canada from ozonesondes: 1980-2001, *J. Geophys. Res.*, *110*, D02304, doi: 10.1029/2004JD004643, 2005.
- Terao, Y., and J.A. Logan, Consistency of time series and trends of stratospheric ozone as seen by ozone-sonde, SAGE II, HALOE, and SBUV (/2), *J. Geophys. Res.*, in press, 2006.
- Thompson, A.M., J.C. Witte, R.D. McPeters, S.J. Oltmans, F.J. Schmidlin, J.A. Logan, M. Fujiwara, V.W.J.H. Kirchhoff, F. Posny, G.J.R. Coetzee, B. Hoegger, S. Kawakami, T. Ogawa, B.J. Johnson, H. Vömel, and G. Labow, Southern Hemisphere Additional Ozonesondes (SHADOZ) 1998-2000 tropical ozone climatology 1. Comparison with Total Ozone Mapping Spectrometer (TOMS) and ground-based measurements, *J. Geophys. Res.*, *108* (D2), 8238, doi: 10.1029/2001JD000967, 2003.
- Thornton, B.F., D.W. Toohey, L.M. Avallone, H. Harder, M. Martinez, J.B. Simpas, W.H. Brune, and M.A. Avery, In situ observations of ClO near the winter polar tropopause, *J. Geophys. Res.*, *108* (D8), 8333, doi: 10.1029/2002JD002839, 2003.
- Thornton, B.F., D.W. Toohey, L.M. Avallone, A.G. Hallar, H. Harder, M. Martinez, J.B. Simpas, W.H. Brune, M. Koike, Y. Kondo, N. Takegawa, B.E. Anderson, and M.A. Avery, Variability of active chlorine in the lowermost Arctic stratosphere, *J. Geophys. Res.*, *110*, D22304, doi: 10.1029/2004JD005580, 2005.
- Tie, X.X., and G.P. Brasseur, The response of stratospheric ozone to volcanic eruptions: Sensitivity to atmospheric chlorine loading, *Geophys. Res. Lett.*, *22* (22), 3035-3038, 1995.
- Tie, X.X., G.P. Brasseur, B. Briegleb, and C. Granier, Two-dimensional simulation of Pinatubo aerosol and its effect on stratospheric ozone, *J. Geophys. Res.*, *99* (D10), 20545-20562, 1994.
- Tourpali, K., C.J.E. Schuurmans, R. van Dorland, B. Steil, and C. Brühl, Stratospheric and tropospheric response to enhanced solar UV radiation: A model study, *Geophys. Res. Lett.*, *30* (5), 1231, doi: 10.1029/2002GL016650, 2003.
- Tsou, J.J., B.J. Connor, A. Parrish, R.B. Pierce, I.S. Boyd, G.E. Bodeker, W.P. Chu, J.M. Russell III, D.P.J. Swart, and T.J. McGee, NDSC millimeter wave ozone observations at Lauder, New Zealand, 1992-1998: Improved methodology, validation, and variation study, *J. Geophys. Res.*, *105* (D19), 24263-24281, 2000.

- Uppala, S.M., P.W. Kallberg, A.J. Simmons, U. Andrae, V.D. Bechtold, M. Fiorino, J.K. Gibson, J. Haseler, A. Hernandez, G.A. Kelly, X. Li, K. Onogi, S. Saarinen, N. Sokka, R.P. Allan, E. Andersson, K. Arpe, M.A. Balmaseda, A.C.M. Beljaars, L. Van De Berg, J. Bidlot, N. Bormann, S. Caires, F. Chevallier, A. Dethof, M. Dragosavac, M. Fisher, M. Fuentes, S. Hagemann, E. Holm, B.J. Hoskins, L. Isaksen, P. Janssen, R. Jenne, A.P. McNally, J.F. Mahfouf, J.J. Morcrette, N.A. Rayner, R.W. Saunders, P. Simon, A. Sterl, K.E. Trenberth, A. Untch, D. Vasiljevic, P. Viterbo, and J. Woollen, The ERA-40 re-analysis, *Quart. J. Roy. Meteorol. Soc.*, *131* (612), 2961-3012, 2005.
- Van Noije, T.P.C., H.J. Eskes, M. van Weele, and P.F.J. van Velthoven, Implications of the enhanced Brewer-Dobson circulation in European Centre for Medium-Range Weather Forecasts reanalysis ERA-40 for the stratosphere-troposphere exchange of ozone in global chemistry transport models, *J. Geophys. Res.*, *109*, D19308, doi: 10.1029/2004JD004586, 2004.
- Van Noije, T.P.C., A.J. Segers, and P.F.J. van Velthoven, Time series of the stratosphere-troposphere exchange of ozone simulated with reanalyzed and operational forecast data, *J. Geophys. Res.*, *111*, D03301, doi: 10.1029/2005JD006081, 2006.
- Van Roozendaal, M., D. Loyola, R. Spurr, D. Balis, J.-C. Lambert, Y. Livschitz, P. Valks, T. Ruppert, P. Kenter, C. Fayt, and C. Zehner, Ten years of GOME/ERS2 total ozone data—The new GOME Data Processor (GDP) Version 4 1. Algorithm description, *J. Geophys. Res.*, *111*, D14311, doi: 10.1029/2005JD006375, 2006.
- Vogler, C., S. Brönnimann, and G. Hansen, Re-evaluation of the 1950-1962 total ozone record from Longyearbyen, Svalbard, *Atmos. Chem. Phys. Discuss.*, *6*, 3913-3943, 2006.
- Wang, H.J., D.M. Cunnold, and X. Bao, A critical analysis of Stratospheric Aerosol and Gas Experiment ozone trends, *J. Geophys. Res.*, *101* (D7), 12495-12514, 1996.
- Wang, H.J., D.M. Cunnold, L.W. Thomason, J.M. Zawodny, and G.E. Bodeker, Assessment of SAGE version 6.1 ozone data quality, *J. Geophys. Res.*, *107* (D23), 4691, doi: 10.1029/2002JD002418, 2002.
- Weatherhead, E.C., G.C. Reinsel, G.C. Tiao, X.L. Meng, D.S. Choi, W.K. Cheang, T. Keller, J. DeLuisi, D.J. Wuebbles, J.B. Kerr, A.J. Miller, S.J. Oltmans, and J.E. Frederick, Factors affecting the detection of trends: Statistical considerations and applications to environmental data, *J. Geophys. Res.*, *103* (D14), 17149-17161, 1998.
- Weatherhead, E.C., G.C. Reinsel, G.C. Tiao, C.H. Jackman, L. Bishop, S.M. Hollandsworth, J. Frith, T. DeLuisi, S.J. Keller, S.J. Oltmans, E.L. Fleming, D.J. Wuebbles, J.B. Kerr, A.J. Miller, J. Herman, R. McPeters, R.M. Nagatani, and J.E. Frederick, Detecting the recovery of total column ozone, *J. Geophys. Res.*, *105* (D17), 22201-22210, 2000.
- Weber, M., S. Dhomse, F. Wittrock, A. Richter, B.-M. Sinnhuber, and J.P. Burrows, Dynamical control of NH and SH winter/spring total ozone from GOME observations in 1995-2002, *Geophys. Res. Lett.*, *30* (11), 1583, doi: 10.1029/2002GL016799, 2003.
- Weber, M., L.N. Lamsal, M. Coldewey-Egbers, K. Bramstedt, and J. Burrows, Pole-to-pole validation of GOME WFOAS total ozone with groundbased data, *Atmos. Chem. Phys.*, *5*, 1341-1355, 2005.
- Wohltmann, I., M. Rex, D. Brunner, and J. Mader, Integrated equivalent latitude as a proxy for dynamical changes in ozone column, *Geophys. Res. Lett.*, *32*, L09811, doi: 10.1029/2005GL022497, 2005.
- WMO (World Meteorological Organization), *Scientific Assessment of Ozone Depletion: 1991, Global Ozone Research and Monitoring Project—Report No. 25*, Geneva, Switzerland, 1992.
- WMO (World Meteorological Organization), *Scientific Assessment of Ozone Depletion: 1994, Global Ozone Research and Monitoring Project—Report No. 37*, Geneva, Switzerland, 1995.
- WMO (World Meteorological Organization), *Scientific Assessment of Ozone Depletion: 1998, Global Ozone Research and Monitoring Project—Report No. 44*, Geneva, Switzerland, 1999.
- WMO (World Meteorological Organization), *Scientific Assessment of Ozone Depletion: 2002, Global Ozone Research and Monitoring Project—Report No. 47*, Geneva, Switzerland, 2003.
- Yang, E.S., D.M. Cunnold, M.J. Newchurch, and R.J. Salawitch, Change in ozone trends at southern high latitudes, *Geophys. Res. Lett.*, *32*, L12812, doi: 10.1029/2004GL022296, 2005.
- Yang, E.S., D.M. Cunnold, R.J. Salawitch, M.P. McCormick, J.M. Russell III, J.M. Zawodny, S. Oltmans, and M.J. Newchurch, Attribution of recovery in lower-stratospheric ozone, *J. Geophys. Res.*, *111*, D17309, doi: 10.1029/2005JD006371, 2006.
- Zanis, P., E. Maillard, J. Staehelin, C. Zerefos, E. Kosmidis, K. Tourpali, and I. Wohltmann, On the turnaround of stratospheric ozone trends deduced from the reevaluated Umkehr record of Arosa, Switzerland, *J. Geophys. Res.*, *111*, D22307, doi:

GLOBAL OZONE

10.1029/2005JD006886, 2006.

- Zbinden, R.M., J.-P. Cammas, V. Thouret, P. Nedelec, F. Karcher, and P. Simon, Mid-latitude tropospheric ozone columns from the MOZAIC program: climatology and interannual variability, *Atmos. Chem. Phys.*, *6*, 1053-1073, 2006.
- Zhou, S., A.J. Miller, J. Wang, and J. Angell, Trends of NAO and AO and their associations with strato-

spheric processes, *Geophys. Res. Lett.*, *28* (21), 4107-4110, 2001.

- Ziemke, J.R., S. Chandra, and P.K. Bhartia, A 25-year data record of atmospheric ozone in the Pacific from Total Ozone Mapping Spectrometer (TOMS) cloud slicing: Implications for ozone trends in the stratosphere and troposphere, *J. Geophys. Res.*, *110*, D15105, doi: 10.1029/2004JD005687, 2005.

Appendix 3A

DESCRIPTION OF THE OZONE DATASETS

3A.1 Column Ozone Data

Ground-Based Data

Three types of ground-based instruments are used for long-term monitoring of total ozone content. Their characteristics and performance have been discussed in numerous WMO Assessments (e.g., WMO, 1995, 1999, 2003), and therefore only a brief description of new developments is provided here. The longest records of continuous reliable measurements are available from stations equipped with Dobson spectrophotometers. The first regular Dobson measurements started in the 1920s. The quality of total ozone data available from 17 Dobson sites prior to 1957 was assessed by Brönnimann et al. (2003a, b). About half of these pre-1957 datasets are reliable for analysis of total ozone variability; however, uncertainties in the absolute calibrations make all sets unsuitable for trend analysis. Several old Dobson records have been recently re-evaluated: from Tromsø, Norway, 1935-1972 (Hansen and Svenøe, 2005); Svalbard, Spitzbergen, Norway, 1950-1962 (Vogler et al., 2006); and Hradec Kralove, Czech Republic, 1962-2003. Griffin et al. (2006) reanalyzed datasets of 1953-1972 astronomical observations from Haute Provence, France, and Jungfrauoch, Switzerland, to calculate nightly column ozone. The retrieved values agree well with Arosa Dobson observations, but with a bias of 6-7%. The Brewer spectrophotometer was developed in the early 1980s (Kerr et al., 1981). There are now about 200 instruments installed around the world. They are regularly calibrated against a traveling standard. The traveling standard itself is calibrated against the set of three Brewer instruments located in Toronto and known as the Brewer Reference Triad (Fioletov et al., 2005). Small systematic differences between Dobson and Brewer total ozone measurements have been reported (Staehelin et al., 2003). Filter ozonometers are widely used in the former Soviet Union countries, and long-term reliable records are available from 1972 (Shalomyanskij et al., 2004). This instrument is less accurate than the Dobson and Brewer instruments, and the calibration is traceable to the Dobson reference. Dobson, Brewer, and filter ozonometer data are available from the World Ozone and UV Data Centre (WOUDC) at <http://www.woudc.org>. The ground-based dataset used in the Assessment is an updated version of the ground-based zonal mean dataset (Fioletov et al., 2002).

Total Ozone Mapping Spectrometer (TOMS)

Data from a series of TOMS instruments (on Nimbus 7, Meteor 3, and Earth Probe) have been reprocessed using a new version 8 algorithm (Bhartia, et al., 2004). The calibration was reviewed and updated during this process to be consistent from instrument to instrument. The TOMS version 8 algorithm uses a more detailed, improved a priori in the retrieval. The Nimbus 7 TOMS calibration has a slightly different time dependence than in version 7 because of a reassessment of how to handle the uncertainties in noise when TOMS started exhibiting occasional chopper non-synchronization effects in the mid-1980s. The Earth Probe TOMS data began to have a scan-mirror problem starting in about year 2000 that could not be corrected. The data should probably not be used for trend determination beyond year 2000. By 2002, there were latitude-dependent errors of 4% to 10%. TOMS data prior to July 1999 were included in the Merged satellite dataset described below. Data are available from the TOMS web site at <http://toms.gsfc.nasa.gov/>.

Backscatter Ultraviolet (BUV)

The BUV instrument launched on Nimbus 4 in April of 1970 provided the first global measurements of ozone from space (Stolarski et al., 1997). Data from this instrument are valuable for extending the satellite data record into the pre-ozone depletion period. Data from 1970 through 1972 provide good global coverage, but thereafter coverage is more sparse after the partial failure of the solar power array. Data from BUV were recently processed through the latest (version 8) SBUV algorithm (Bhartia et al., 2004). The calibration of BUV has always been questionable because of very rapid degradation of its solar diffuser plate. For the recent reprocessing, Umkehr data were used to establish the basic long-term calibration. The soft calibration techniques that were developed to calibrate SBUV instruments were used to establish the absolute accuracy of BUV. Comparison with Dobson data from that period shows that the resulting data were reasonably well calibrated.

GLOBAL OZONE

Solar Backscatter Ultraviolet (SBUV, SBUV/2)

The SBUV data have also been reprocessed using a new profile retrieval algorithm (Bhartia et al., 2004). This one is also designated version 8, and while there are some similarities, it is not the same algorithm as used for TOMS. The SBUV algorithm, in contrast to TOMS, now has a time-independent a priori to remove the possibility that a trend in the a priori could contribute to the deduced trend in ozone. The calibrations for the SBUV instrument on Nimbus 7 and for the SBUV/2 instruments on the sequence of NOAA satellites (9, 11, 14, 16, 17, and 18) have now been put on a consistent scale. The data for upper stratosphere profile can now be used for trend analyses directly without adjustment (though with some associated uncertainties). Data are available from <http://www.cpc.ncep.noaa.gov/products/stratosphere/sbuv2to>. The observational data used for this Assessment are zonally averaged, integrated vertical profile SBUV/2 data (version 8) from the period from 1979 to 2005 (updated from Miller et al., 2002).

Global Ozone Monitoring Experiment (GOME)

The GOME on board the European Space Agency's ERS-2 satellite is the first European experiment dedicated to global ozone measurements (Burrows et al., 1999). ERS-2 was launched in April 1995. GOME has been operational since June 1995, but spatial coverage has been limited since July 2003 due to problems with tape storage on ERS-2. GOME measures the backscattered radiances from 240-790 nm in the nadir-viewing geometry. In the relevant region for total ozone retrieval (320-340 nm), the spectral resolution is about 0.17 nm. The maximum scan width in the nadir is 960 km across track on the ground and global coverage is achieved within three days.

Three algorithms were developed for GOME applications in 2003 and used to reprocess the GOME total ozone data. These algorithms are all based on the DOAS (Differential Optical Absorption Spectroscopy) technique. They are (1) the WFDOS algorithm (Coldewey-Egbers et al., 2005; Weber et al., 2005; <http://www.iup.uni-bremen.de/gome/wfdoas/>); (2) the TOGOMI/TOSOMI algorithm (Eskes et al., 2005; <http://www.temis.nl/protocols/O3total.html>); and (3) the GDOAS algorithm (Van Roozendaal et al., 2006; <http://wdc.dlr.de/sensors/gome/gdp4.html>). For all three algorithms, retrieved GOME total ozone show excellent agreement with each other and with ground-based Brewer and Dobson measurements at midlatitudes, so only one GOME dataset is shown in Figures 3-2, 3-3, 3-4, and 3-5 (WFDOS version 1 algorithm).

Merged TOMS+SBUV/2

The merged dataset consists of monthly-mean zonal and gridded average datasets constructed by merging individual TOMS and SBUV/2 satellite datasets (Frith et al., 2004). An external calibration adjustment has been applied to each satellite dataset in an effort to calibrate all the instruments to a common standard. All data in the present version of the merged dataset have been derived using the TOMS version 8 and SBUV version 8 algorithms. A recent manuscript (Stolarski and Frith, 2006) evaluates the instrument record uncertainty for one of these datasets and shows that the variations among them are within the uncertainties. For this Assessment, SBUV total ozone data are also included in the merged dataset without any adjustments. There are inherent uncertainties in the possible drift of each instrument and in the offset of overlapping instruments. For the merged dataset, Stolarski and Frith (2006) estimated an overall drift uncertainty of a little more than 1%/decade due to instrument effects. This corresponds to about 8 DU over the 25-year period of the measurements. The data, and information about how they were constructed, can be found at http://hyperion.gsfc.nasa.gov/Data_services/merged/mod_data.public.html.

National Institute of Water and Atmospheric Research (NIWA) Assimilated Dataset

The assimilated database combines satellite-based ozone measurements from 4 Total Ozone Mapping Spectrometer (TOMS) instruments, 3 different retrievals from the Global Ozone Monitoring Experiment (GOME), and data from 4 Solar Backscatter Ultraviolet (SBUV) instruments (Bodeker et al., 2005). The dataset used in this analysis is an update and extension of the homogenized total column ozone dataset developed by Bodeker et al. (2001). Specific changes include: version 8 Nimbus 7 and Earth Probe TOMS data are used rather than version 7 (<http://toms.gsfc.nasa.gov/>). GOME data from the European Space Agency (ESA) are updated from version 2.4 (used in Bodeker et al., 2001) to version 3.1. Assimilated total column ozone fields from the Royal Netherlands Meteorological Institute (KNMI) (<http://www.knmi.nl/goa>) based on GOME measurements are included. Total column ozone fields from the KNMI total ozone algorithm from GOME using the Ozone Monitoring Instrument algorithm (<http://www.temis.nl/protocols/O3total.html>) are included. Version 8 SBUV (Solar Backscatter Ultraviolet) data from the NASA Nimbus 7, NOAA 9, NOAA 11, and NOAA 16 satellites (<http://www.cpc.ncep.noaa.gov/products/stratosphere/sbuv2to/>) are included. The analysis period is extended to the end of 2004.

3A.2 Ozone Profile Measurements

Stratospheric Aerosol and Gas Experiment (SAGE)

The SAGE measurement technique (McCormick et al., 1989) is based on solar occultation, with ozone profile measurements obtained at sunrise and sunset on each of 14 orbits per day. This technique provides high vertical resolution (~1 km) and very small long-term drifts resulting from instrument calibration. However, spatial sampling is limited, and it takes approximately one month to sample the latitude range 60°N to 60°S. SAGE I ozone profile data cover the time period February 1979 to November 1981. A difficulty in combining the SAGE I and SAGE II data for trend studies arises from an apparent error in the reference altitude for SAGE I. An empirical altitude correction has been applied to the SAGE I data in an attempt to remove this bias (Wang et al., 1996). SAGE II ozone profile data commenced in November 1984 and the science mission ended in August 2005. The analysis here used SAGE II version 6.2 (v6.2), which was released in its entirety in September 2005. In mid-2000, SAGE II experienced a failure of the azimuth gimbal in the pointing system. After an approximate two-month interruption in science data gathering, normal science operation resumed at a reduced duty-cycle. The failure precluded the ability to take both sunrise and sunset observations on each orbit. Events of only one type occur in blocks of approximately 35 days. The event type switched from one type to the other after each spacecraft yaw-maneuver (performed in order to maintain proper illumination of the spacecraft's fixed solar panels). The spatial and temporal sampling in the reduced mode of operation does not introduce any new significant gaps or biases in the latitudinal and seasonal coverage. The species profiles have a vertical resolution of 1 km or better and are placed on a 0.5 km altitude grid. The species separation and inversion in v6.2 is similar to that used in v6.1 (the basis for the SAGE II ozone data in WMO (2003)), but v6.2 incorporates an improved spectral characterization of the 940 nm channel optical properties that results in significantly improved water vapor retrievals. In general, the ozone results are of good quality down to the tropopause. As in previous Assessments, the data analyzed here exclude time periods of enhanced aerosol extinction following the eruption of Mt. Pinatubo in June 1991. A small percentage of SAGE II data is affected by errors caused by interference from aerosol (including stratospheric aerosol from major volcanic eruptions), clouds, and other, not always known, factors and should be removed (Rind et al., 2005). The data are available from <http://eosweb.larc.nasa.gov/>.

Solar Backscatter Ultraviolet (SBUV, SBUV/2)

The SBUV/2 instrument is a scanning double monochromator measuring backscattered solar radiation in 12 discrete wavelength bands ranging from 252.0 to 339.8 nm. In previous SBUV algorithms, total column ozone was retrieved using the longest 4 wavelengths, and then a profile was retrieved using the shortest 8 wavelengths. In the version 8 algorithm released in 2004, an ozone profile is retrieved using all 12 wavelengths, and total column ozone is the integral of the profile (Bhartia et al., 2004). The version 8 algorithm is optimized to provide a self-consistent long-term ozone record. The SBUV(2) satellite data used here are reprocessed with the version 8 algorithm and are available at <http://daac.gsfc.nasa.gov/data/dataset/TOMS/DVD-ROMs> and from <http://www.cpc.ncep.noaa.gov/products/stratosphere/sbuv2to>. The data are available as column ozone in Dobson units (DU) for 13 layers, each 3.2 km thick except for Layer 1, which is about 18 km in depth, and as ozone mixing ratios at 15 levels. To avoid errors related to volcanic aerosols, it is recommended to exclude from the analysis data between 40°S and 40°N for the 1-year periods following the major volcanic eruptions in 1982 and 1991 (SPARC, 1998). Results of SBUV(2) ozone profile comparisons with other data sources are discussed by Petropavlovskikh, et al. (2005a), Nazaryan and McCormick (2005), Fioletov et al. (2006), and Terao and Logan (2006). Combined datasets are now becoming available for profile data. Stolarski and Frith have put together the SBUV series from the version 8 results (http://hyperion.gsfc.nasa.gov/Data_services/merged/mod_data.public.html). Brunner et al. (2006) reconstructed the vertical ozone distribution in equivalent latitude coordinates.

Ozonesonde Data

A network of stations provides ozone profile information from balloonborne sondes, which measure ozone from the ground to about 33 km, with a vertical resolution of ~150 m. Details of ozonesonde measurements and data processing are discussed in SPARC (1998). Data are available from the WMO World Ozone and UV Data Centre (WOUDC) (<http://www.woudc.org>). Data from many sonde stations are normalized to the overhead ozone column measured on the same day by a Dobson or Brewer instrument. The normalizing factor (called the correction factor) is commonly used to screen the data, as described in Logan et al. (1999). Data are available from about 1970 for stations in North America, Europe, and Japan. The European stations make measurements 2-3 times a week, while other stations make weekly

GLOBAL OZONE

measurements. The long-term records from Payerne and Uccle have been reprocessed since the SPARC (1998) assessment, and the Japanese sonde data since 1994 are now available with much higher vertical resolution than previously.

Umkehr Data

The Umkehr technique is used to derive the vertical distribution of ozone from ground-based measurements of zenith sky radiation. The method is based on principles of differential absorption of solar UV light by atmospheric ozone and molecular scattering. The ratio of zenith blue sky radiation at two UV wavelengths is measured over a range of solar zenith angles between 60° and 90°. A representative total ozone measurement is required as part of the data input. The resulting profile is reported as mean partial pressure values for ten pressure layers, where the pressure at the top of the layer is half of the pressure at the bottom of the layer, and layer 10 contains ozone integrated above the ~1 hPa pressure level. The analysis is based on a climatological first guess and an iterative solution is reached. The dependence of Umkehr retrievals on a priori information becomes a serious issue for trend analysis. (Dütsch and Staehelin, 1992; Mateer et al., 1996). In the presently used operational UMK92 algorithm, the a priori profiles are constructed using total ozone column measured by the same instrument. This makes it difficult to ascertain whether the retrieved long-term changes are forced by a priori or whether they reflect information contained in the measurements. The new UMK04 algorithm includes revised a priori profiles based on the new ozone climatology (McPeters et al., 2003) that vary with season and latitude, but have no day-to-day or long-term variability. It also uses new look-up tables and an improved forward model. In addition, the impacts of both algorithm smoothing and measurement errors on the retrieved ozone profiles have been further optimized (Petrovavlovskikh et al., 2005a, b). The overall accuracy of the Umkehr method (1σ) is estimated to be $\pm 25\%$ for the troposphere (layers 0 and 1), $\pm 15\%$ for low stratosphere (layers 3 and 2), less than $\pm 10\%$ for the middle stratosphere (layers 4 to 6), less than $\pm 10\%$ for the upper stratosphere (layers 7 and 8), and errors slightly increase in ozone integrated above layer 7. The algorithm description and the data are available at <http://www.srrb.noaa.gov/research/umkehr/>. Zanis et al. (2006) described re-evaluation of the 1956-2003 Umkehr series from Arosa, Switzerland. The vertical profiles of ozone trends from Umkehr data shown in Figure 3-8 are the average of trends derived from measurements at Arosa (1979-2004), Haute-Provence (1984-2004), Boulder (1979-2004), and Belsk (1979-2004), processed with the new UMK04 algorithm.

Lidar Data

The Differential Absorption Lidar (DIAL) ozone measurement technique retrieves the vertical profile of ozone absorption by comparing atmospheric return at two UV wavelengths, one absorbed by ozone (usually 308 nm) and one much less absorbed (353 or 355 nm) (Donovan et al., 1997; Guirlet et al., 2000; Leblanc and McDermid, 2000, 2001; Godin et al., 2001, 2002). The DIAL method is differential in wavelength and altitude, which makes it self-calibrating and ideally suitable for long-term routine measurements. Altitude resolution of the measurements ranges from 1 km (below 30 km) to 5 km (at 45-50 km), and the altitude range is typically from 15 to 45-50 km, with accuracies of approximately 3% below 35 km and 10% above 40 km. Observations are made during clear nights. High quality, continuous time series are available since the late 1980s (Keckhut et al., 2005b). The data are available from the Network for the Detection of Atmospheric Composition Change (NDACC) site at <http://www.ndacc.org/>.

Microwave Ozone Measurements

The method is based on measurements of microwave thermal radiation in the ~100-200 GHz range, emitted by ozone and measured at high spectral resolution. As the observed emission line is broadened by pressure, information about the vertical distribution of ozone in the atmosphere can be retrieved from the measured spectra by means of an inversion algorithm. Individual rotational spectral lines with frequencies most often either 100 or 142 GHz, are used. A review of the methodology and instrumentation used for ozone observations in the microwave frequency range is given, for example, in Parrish (1994) and Clancy and Muhleman (1993). Ground-based microwave radiometers allow unattended, continuous observations of the atmosphere that are nearly independent of weather conditions. A vertical resolution is typically ~10 km and the temporal resolution is 1-2 hours. The altitude range is typically 20-70 km, with accuracies of ~5%. High quality, continuous time series are available since 1992 (Tsou et al., 2000; Klein et al., 2002; Calisesi et al., 2003; Nagahama et al., 2003; Ricaud et al., 2004). The data are available from the NDACC site at <http://www.ndacc.org/>.